Dynamic behavior of collective and reduced Quantum dots system.

By:

M. C. Sergio Sánchez Sánchez

INAOE

A dissertation Submitted to the program in Optics.

Optics Department.

In partial fulfillment of the requirements for the degree of

DOCTOR IN SCIENCES WITH SPECIALITY OF OPTICS

At

National Institute for Astrophysics Optics and Electronics

November 2011

Tonantzintla, Puebla.

Advisor:

Dr. José Javier Sánchez Mondragón

INAOE researcher

ABSTRACT

In this dissertation we show a theoretical study on quantum nanostructures of 3D confinement better known as Quantum Dots (QDs). We explore the collective and cooperative potential of such systems under a quantum scheme that is all quantum i.e. radiation-matter quantization (QDs and EM field), also we make a semi-classical approach for solve the collective system derived of the Heisenberg picture. We make use of Excited Atomic Coherent States in order to facilitate the theoretical study of nonlinear Hamiltonian. Subsequently we reduce our system to a simple system of two QDs in its own cavity for research the quantum entanglement necessary for producing qubits (bits of quantum information processing) for quantum computing and information.

Looking for ways of light the essence of the beings and things (Lola Álvarez Bravo, 1913-1993 mexican-Photographer)

RESUMEN

En esta tesis se presenta un estudio teórico sobre nano-estructuras cuánticas de confinamiento tridimensional mejor conocidas como Puntos Cuánticos. Se exploran las potencialidades colectivas y cooperativas de dichos sistemas bajo un esquema todo cuántico es decir cuantización de la materia-radiación (Puntos y Campo EM), además hacemos una aproximación semi-clásica para la solución del sistema colectivo derivada de la imagen de Heisenberg. Hacemos uso de Estados Atómicos Coherentes Excitados para facilitar el estudio teórico no lineal del Hamiltoniano. Posteriormente reducimos nuestro sistema a un sistema simple de dos puntos en su propia cavidad para estudiar el entrelazamiento cuántico necesario para producir qubits (bits para procesamiento de información cuántica) para computación e información cuántica.

Busco por los caminos de la luz la esencia de los seres y de las cosas (Lola Álvarez Bravo, 1913-1993- Fotógrafa mexicana)

DEDICATORIAS-DEDICATED TO

A Isis y Schaddaí mis preciados hijos – My precious children

A Yolanda Amelia mi amorosa madre – My loving mother

A EVA LUCIA. Por compartir una época con la luz de tu vida. Aunque fue un breve suspiro en la eternidad efímera, pero lleno de amor y esperanza. Una vida no basta para agradecerte. **In Memorian †**

By sharing a season with the light of your life. Although a brief breath in ephemeral eternity, but full of love and hope. A life is not enough to thank you. **†**

Vuelve a vivir una vez más tus sueños en el horizonte de la luz, en el resurgimiento del infinito manantial de vida donde los más altos poderes te guían bajo su protección hacia un nuevo principio, a una razón por vivir, y un significado más profundo… Vuelve a vivir súbitamente, que tu luz es real,… la luz eres tú.

Relive your dreams once again on the horizon of light in the revival of the infinite source of life where the highest powers under its protection guide you toward a new beginning, a reason for living, and a deeper meaning ... relive suddenly, your light is real ... the light are you.

AGRADECIMIENTOS-ACKNOWLEDGEMENTS

A las instituciones y Dependencias:

Mi profundo y sincero agradecimiento al Consejo Nacional de Ciencia y Tecnología (CONACyT) por el apoyo económico durante mis estudios de posgrado en el Instituto Nacional de Astrofísica Óptica y Electrónica (INAOE-Puebla).

Al INAOE por el apoyo académico e institucional brindado durante mis estudios de posgrado y estancias de investigación, en especial a todos mis profesores, personal administrativo y directivos que sin su dedicación no sería posible una estancia de enorme desarrollo profesional.

A la Universidad del Istmo (UNISTMO-Tehuantepec Oaxaca) no solo por emplearme como profesor investigador, sino por proporcionarme los medios económicos durante mi año sabático para la conclusión satisfactoria de este trabajo de tesis doctoral.

A las personas:

Mi más profundo Agradecimiento

A mi asesor y mentor el Dr. José Javier Sánchez Mondragón que durante muchos años he recibido su guía y enseñanzas en las buenas y en las malas.

A mis sinodales de tesis y examen doctoral por su comprensión, paciencia y pronta revisión: Dr. Sergio Vázquez y Montiel, Dr. Francisco Javier Renero Carrillo, Dr. Ponciano Rodríguez Montero, Dr. Esteban Tlelo Cuautle y al Dr. Daniel Alberto May Arrioja.

A mis profesores y asesores pasados en INAOE y otras instituciones por formarme profesionalmente.

Quiero enfatizar mi profundo agradecimiento a los Drs. Sergio Vázquez (ex coordinador de óptica) y Francisco Renero (ex representante docente), por su paciencia y comprensión todos los años que estuve trabajando fuera de INAOE, a pesar de las dificultades provocadas a la coordinación de óptica no me negaron su apoyo institucional.

También al actual coordinador de óptica Dr. Víctor Arrizón Peña y al representante docente Dr. Baldemar Ibarra Escamilla por su apoyo durante mi estancia sabática en INAOE para la conclusión de mi tesis. Así mismo al Dr. Roberto Stack Murphy Arteaga director de Formación Académica de INAOE y a la Lic. Martha Olmos y Flores jefa del mismo departamento por su comprensión y paciencia.

También gracias a mis papás (Yola y Benja (†)), hermanos (Pili, Sinaí, Gus e Iván), hijos (Isis, Schada y su mamá Meyalli gracias por cuidarlos y enriquecer mi vida con esas dos luces), y demás familiares, amigos, compañeros, colegas y estudiantes que han sido parte de mi vida y que de alguna manera pequeña, grande o enorme han contribuido a mi formación personal y profesional de toda mi vida.

Potius sero quam nunquam

Gracias infinitas Padre Eterno.

Deus dedit, Deus abstulid

Memento mori

Fatum Fatis ego perea

PREFACE

"I know that when I was in my late teen and early twenties the world was just a Roman candle –rockets all the time… You lose that sort of thing as time goes on… physics is an otherworld thing. It requires a taste for things unseen, even unheard of- a high degree of abstraction… These faculties die off somehow when you grow up… profound curiosity happens when children are young. I think physicists are the Peter Pans of the human race… Once you are sophisticate, you know too much – far too much. Pauli once said to me 'I know a great deal. I know too much. I Am a quantum ancient." (Isidor Rabi-Nobel Laureate)

For several decades since the last century have been studied by different researchers worldwide individual and collective dynamics of atoms interacting with other atoms or with electromagnetic field, called Radiation-Matter Interaction, either in free space or in structured environments, such as micro-cavities, crystalline molecules or micro and nano-electronic devices including solid state and condensed matter environments. Not only as an aspect of disinterested pursuit and curiosity about the mystery of quantum world, but because it allows performing experiments and technological development results to provide science and technology for human consumption. On other hand there have been developed a wide variety of theoretical models for their description and understanding, creating complete theories in order to insight the deeper meaning of their behavior in isolation from one or two atoms as far as a lot of atoms systems as a collective dynamic. The most famous contributions are, in the case of single two-level atom interacting with a cavity mode, the famous Jaynes-Cummings Model (JCM) with the phenomenon of quantum revivals. In addition to the collective issue is the Dicke model (DM) dealing with systems of many atoms of two-levels, with no mutual interaction between them, but in interaction with EM field, it is a phenomena similar to the JCM. This model is also known as the Tavis-Cummings model, which has especially the phenomenon of cooperative Superradiance. The importance of studying theses systems is because they provide an understanding almost exactly at the theoretical level of quantum behavior in structured environments, allowing perform experiments and implementation of technology support with reduced systems of the few atoms as far as a large number of them, i.e. collectively.

These atomic models have helped to develop other models for more complex structures such as quantum wells and quantum wires as far as quantum

dots (QDs) or artificial atoms, which have similar features to natural atoms, although not identical, by the quantization their energy levels and the confinement of charge carriers. The models have been very different for distinct approaches and applications. But all models based on the JCM and DM. Some are extensions of these and some more by adding other dynamic features. Whose Hamiltonian have a variety of solutions. From traditional solutions using Schrödinger (picture) equation, the Heisenberg picture with equation operator systems, Dirac picture, which is a hybrid of two previous pictures as far as solutions complex with stochastic equations, density matrix, quantum trajectories, and so on. In the midst of complexity we choose a Hamiltonian with complete features [Quiroga et. al. and Surendra et. al.] yet synthesized which contains the physical information of radiation-mater interaction (atoms, quantum structures, so on) and included the property of Förster interaction better known as Förster Resonant Energy Transfer (FRET) which is an important feature not only for quantum molecular structures but also of type chemical and biological. In these latter areas has been quite results significant in explaining the energy transfer phenomena in biochemical reactions between biological molecules, such as the photosynthesis. We will use it as a way of understanding the mechanisms of energy and information transfer between quantum dots, which by its dimensions seen tiny molecules of the order of a few to several hundred nanometers.

The virtue of this Hamiltonian is done by the algebra of the angular momentum operators which synthesizes the collective characteristics of the charge carriers (excitons, electron-hole) into these quantum dots. This allows one to treat the number of dots needed under study. In particular our system for the collective issue in chapter 2 through 4 is to research the dynamic behavior of a few QDs using the algebraic operator technique including the Hamiltonian diagonalization to find their eigenvalues (eigenenergys) and eigenvectors (wave functions). In this way, we may understand the collective and cooperative behavior, especially for cases in resonance. On other hand we use the Heisenberg picture which given us a differential equation system of the operators involved in the Hamiltonian (chapter 4), considering the complex conjugate simplifications as well as the constants of motion. Systems of this kind is not easy to solve because it is nonlinear, then we resourse the so-called Atomic Coherent States (ACS), and Excited Atomic Coherent States (EACS) [Obada, et.al.] that allows us to factor out the angular momentum operators as a non-commutative algebra. Considering a classical EM field interaction which leads us to make the analysis of the evolution in semiclassical

way and thus understand the dynamic behavior in time of this system. The solutions are given as functions of the values of expectation in the appropriate basis and numerically solved, since it is not feasible analytically.

Furthermore we analyzed in chapter 5 for a pair of quantum dots (bipartite system) implemented as a pair of quantum bits (qubits) to measure the degree of quantum entanglement. With the peculiarity of these QDs previously was entangled (under some special mechanism, we do not know) and embedded in a cavity Jaynes-Cummins type. It is for this reason that our study is in the context of cavity Quantum Electrodynamics (CQED). Based upon previous studies with only two-level atoms (TLA) [Yonac, et.al.] and QDs [Loss, Di Vincenzo; Mitra et. al.] but not immersed in CQED. There are other proposes with CQED [Imamoglu, et. al.] but with configurations more complicate that our proposed.

In the case of our qubits comes into play not only the interaction with the field but also the Förster energy transfer (interaction), which makes them have a greater interdependence between themselves, but the benefit is to preserve entanglement longer. With our analysis allows us to observe that there are few areas of the so-called Entanglement Sudden Death, at least lower that in order to the atomic case of Yu-Eberly-Yonac. In our system remain open many possibilities for analysis of initial states with different combinations with the field (i.e. change of conditions for the initial entanglement state), which provides dynamics to evolve very different behavior each.

Our interest in researching the dynamics of bipartite quantum dots as qubits is not just a fashion forward, but rather we are interested in fundamental aspects that arise as a possibility of new physics and not only as an implementation of the so dreamed quantum computer, it is a race behind the theoretical and experimental quantum technology now where there are large groups of experts sponsored by the best wide world universities and large computer companies (hardware) and programming (software) in around of the globe. Making it very challenging compete with these groups, however our theoretical contribution with new fundamental physics aspects of the behavior of quantum dots as qubits leaves a better chance to further research these quantum systems in parallel to other developments including technological and experimental. Such as production of more efficient solar cells, light emitting diodes lasers and physics technologies yet to be explored, as far as biology and medicine applications.

PREFACIO

Sé que cuando era adolecente y mis primeros años de juventud el mundo era solo como un velero romano – cohetes todo el tiempo-… Pero se pierden ese tipo de cosas con el paso del tiempo… la física es una cosa de otro mundo. Esta requiere el gusto por las cosas invisibles, incluso inauditas- inclusive un alto grado de abstracción… Estas facultades mueren de alguna manera cuando creces… sucede una profunda curiosidad cuando eres un niño pequeño. Creo que los físicos somos los Peter Pan de la raza humana… una vez que son sofisticados, que sabes tanto, demasiado. "Pauli una vez me dijo: Yo sé demasiado, yo sé tanto, que Yo Soy un Ancestro Cuántico". (Isidor Rabi- Nobel Laureado)

Durante varias décadas desde el siglo pasado se han venido estudiando por distintos investigadores a nivel global la dinámica individual y colectiva de átomos en interacción con otros átomos o bien con la radiación electromagnética, la llamada *Interacción Radiación-Materia*, ya sea en espacio libre o bien en entornos estructurados, como pueden ser micro-cavidades, moléculas cristalinas, o dispositivos de micro y nano-electrónica entre otros entornos de estado sólido y materia condensada. No solo como un aspecto de búsqueda desinteresada y curiosidad por el misterio del mundo cuántico, sino porque permite ejecutar experimentos y desarrollo tecnológico con resultados que aporten ciencia y tecnología para el consumo humano. Por otra parte se han desarrollado una gran variedad de modelos teóricos para su descripción y comprensión, creando teorías completas que permitan entender el significado más profundo de su comportamiento aislado de uno o dos átomos, o bien de sistemas de muchos átomos como una dinámica colectiva. Los estudios más celebres son, para el caso de un solo átomo de dos niveles en interacción con un modo de la cavidad, el famoso Modelo de Jaynes-Cummings (JCM) con el fenómeno de los resurgimientos cuánticos. Por otro lado para el caso colectivo está el Modelo de Dicke (DM) que trata con sistemas de muchos átomos de dos niveles, sin interacción mutua entre ellos, pero sí en interacción con el campo EM y con fenómenos similares al de JCM. A este modelo también se le conoce como el Modelo de Tavis-Cummings, el cual trata en especial el fenómeno de la Superradiancia como fenómeno cooperativo.

La importancia de estudiar estos sistemas es porque nos proporcionan un entendimiento casi exacto a nivel teórico del comportamiento cuántico en entornos estructurados, lo cual permite la ejecución de experimentos y la implementación de tecnología con ayuda de sistemas reducidos de uno a unos cuantos átomos

hasta un gran número de ellos, i.e. colectivamente. Estos modelos atómicos han permitido desarrollar otros modelos para objetos más complejos de estructuras cuánticas como pozos y alambres hasta los Puntos Cuánticos (QDs) o Átomos Artificiales, que tienen características, si bien no iguales, pero si similares a los átomos *naturales,* por la cuantización de sus niveles de energía y el confinamiento de los portadores de carga*.* Estos modelos han sido muy variados, para distintos enfoques y aplicaciones. Pero todos basados en los modelos de JCM y de Dicke. Algunos como extensiones de estos, y algunos más añadiéndoles características dinámicas adicionales. Cuyas soluciones a partir del Hamiltoniano es también muy variada. Desde las tradicionales soluciones, usando la ecuación de (imagen) Schrödinger, pasando por la imagen de Heisenberg con sistemas de ecuaciones de operadores, la imagen de interacción de Dirac, que son un hibrido de las dos anteriores, hasta complejas soluciones de tipo estocástica con matriz de densidad, trayectorias cuánticas, etc. En medio de tanta complejidad nosotros elegimos un Hamiltoniano de características muy completas [Quiroga, et. al. And Surendra et. al.] y a la vez sintetizadas en el cual contiene la información física de la interacción radiación-materia (átomos, estructuras cuánticas, etc.) así como la propiedad de incluir la llamada interacción de Förster mejor conocida como Transferencia Resonante de Energía de Förster (*FRET,* por sus siglas en inglés) la cual es una importante característica de moléculas no solo de tipo cuántico sino químico y biológico. En estas últimas áreas ha dado bastantes resultados importantes al explicar fenómenos de transferencia de energía en reacciones bioquímicas entre moléculas biológicas, como la fotosíntesis. Por nuestra parte la usaremos como una forma de entender los mecanismos de transferencia de energía e *información* entre puntos cuánticos, los cuales por sus dimensiones suelen parecer diminutas moléculas del orden de unos pocos a unos cientos de nanómetros.

La virtud de este Hamiltoniano se hace gracias a los operadores del algebra de momento angular con los cuales se sintetizan las características colectivas de los portadores de carga (excitones: electrón-hueco) dentro de estos puntos cuánticos. Esto permite tratar de uno hasta el número que se necesite de puntos bajo estudio. En particular nuestro sistema para el caso colectivo en capítulos 2 a 4 consiste en investigar el comportamiento dinámico de unos cuantos puntos usando la técnica algebraica de operadores incluyendo la diagonalización del Hamiltoniano para encontrar sus eingenvalores (eigen-energías) y eigenvectores (funciones de onda). De tal manera que podamos comprender el comportamiento colectivo y cooperativo, en especial para casos en resonancia. Por otra parte usamos la

imagen de Heisenberg para obtener un sistema de ecuaciones diferenciales acopladas de los operadores involucrados en el Hamiltoniano (capitulo 4), considerando simplificaciones con los complejos conjugados así como las constantes de movimiento. Sistemas de esta clase no son fácil de resolver debido a que es no lineal, entonces recurrimos e los llamados estados atómicos coherentes excitados [Obada, et. al] que nos permiten factorizar los operadores de momento angular como un algebra no conmutativa. Considerando un campo electromagnético de interacción clásico lo que nos lleva a hacer el análisis de la evolución de un sistema semi-clásico y así entender el comportamiento dinámico en el tiempo de este sistema. Para la solución se hacen con funciones que contienen los valores de expectación en la base adecuada y se resuelven numéricamente, ya que analíticamente es poco factible.

Por otra parte analizamos en el capítulo 5 el caso de un par de puntos cuánticos (sistema bipartita) implementados como un par de quantum bits (qubits) para medir su grado de entrelazamiento cuántico (quantum entanglement). Con la peculiaridad de que estos puntos previamente entrelazados (bajo algún mecanismo especial, que desconocemos), son inmersos dentro de una cavidad del tipo Jynes-Cummings. Es por esta razón que nuestro estudio es en el contexto de la electrodinámica cuántica de cavidades (CQED, por sus siglas en inglés). Basándonos en estudios previos solo con átomos de dos niveles [Yonac, et. al.] y con puntos [Loss, Di Vincenzo; Mitra, et. al] pero sin estar inmersos en cavidades QED. Hay otras propuestas usando CQED [Imamoglu, et. al.] pero en configuraciones más complicadas que la de nuestra propuesta.

Para el caso de nuestros qubits entra en juego no solo la interacción con el campo sino también la transferencia de energía (interacción) de Förster, la cual los hace tener una mayor interdependencia entres sí mismos, pero que resulta en beneficio para conservar el entrelazamiento por mayor tiempo. Lo cual con el análisis que hacemos nos permite observar que hay pocas zonas de la llamada *muerte súbita del entrelazamiento* (*Entanglement Sudden Death*), al menos menores que para el caso atómico de Yonac-Yu-Eberly. En nuestro sistema quedan abiertas muchas posibilidades de análisis de combinaciones con distintos estados iniciales con el campo (es decir cambiar las condiciones para el estado inicial de entrelazamiento) que al evolucionar proporcionan dinámicas de comportamiento muy diferentes cada una.

Nuestro interés al investigar la dinámica bipartita de puntos cuánticos como qubits no es solo por una moda de vanguardia, sino más bien nos interesan los aspectos fundamentales que surgen como una posibilidad de obtener nueva física y no solo como una implementación del tan soñado computador cuántico, que es una carrera teórica y experimental tras la tecnológica cuántica de actualidad en la que hay grandes grupos de expertos patrocinados por las mejores universidades del mundo y las grandes compañías de computación (hardware) y programación (software) alrededor del globo. Con lo cual es un desafío muy grande competir con esos grupos, más sin embargo nuestra aportación teórica con nuevos aspectos físicos fundamentales del comportamiento de puntos cuánticos como qubits deja una mejor posibilidad para seguir investigando paralelamente estos sistemas cuánticos inclusive para otros desarrollos tecnológicos y experimentales. Tales como producción de celdas solares más eficientes, emisores de luz, diodos láseres, como otras tecnologías aún por explorar, hasta aplicaciones en biología y medicina.

CONTENTS

CHAPTER 1

INTRODUCTION

The many-particle systems are a topic that has been studied since the beginning of classical physics. Many efforts have been devoted to trying to understand the laws governing these systems under a collective scheme in which their behavior is not as simple as a single particle. This is because the collective behavior produces a dynamic that can be either cooperative or chaotic, in this case by itself is very interesting study, but has its own problems in ordered chaos theory even at the level of classical physics. However their study was not limited only to classical mechanics but also to thermodynamics, as well as statistical mechanics, which study the collective behavior of many particles based on statistical averages. Upon entering the realm of quantum mechanics the situation is further complicated because their feature is not only random but also indeterministic of the systems of many particles and quantum. Speaking specifically to study atomic systems from a few to many particles interacting with electromagnetic radiation field, the interest arises not only at the fundamental level but also by the novel experimental and technological applications. The technological development of micro and nano-technology has brought new challenges at a fundamental level in quantum theory, especially in the Quantum Optics and Cavity quantum electrodynamics (CQED). These systems are studied phenomena of interaction radiation with matter as well as quantum confinement. Taking into account its quantum properties thus how it can be studied in semiclassical level (quantization particles only) or fully quantum (quantization both particles of matter and radiation).The model for excellence has been used is the Jaynes-Cummings (JCM), widely studied and applied to various phenomena in these areas. In this model we study in a little more detail in Chapter 3. JCM basically shows the effects of quantized radiation and as to affect an atom with

two levels. Despite its physical simplicity, but not mathematical gives us a lot of information at a fundamental level to insight the phenomenon of interaction which in turn is the basis for collective systems of many atoms or many particles at the atomic scale. Collective systems are based on atomic Dicke model (DM) which studies systems of several particles, nevertheless can be solved only for a few atoms. In our research we have implemented approximate methods [1], where we explore various perspectives of research and application in this dissertation. Here we review various methods of distinct kinds, especially algebraic and differential methods in the respective images of Schrodinger, Heisenberg and Interaction obviously. The understanding and revelation of the fundamental aspects are of our interest in this thesis to propose experimental applications and technology implementations. Within the last two or three decades, a great deal of attention has grown in semiconductor nanostructures for the wide range of possible technological applications and for the simplicity with which basic principles of quantum mechanics can be studied experimentally. Among these semiconductor nanostructures are quantum dots (QDs), which are sought after for their optoelectronic properties. In particular the study of so-called *artificial atoms* [3], also known as *quantum dots* (QDs). Due to quantum nature, the three-dimensional confinement leads to discrete energy levels much like the ones found in atoms, thus giving them the common-known name of artificial atoms [2,3,4]. QDs are semiconductor heterostructures (quantum wires, wells, and dots) whose size is on the order of nanometers, where charge carriers are confined in all three spatial directions to lengths which are smaller than their de Broglie wavelengths [5-8]. These structures of micro and nano-metric size serve for the confinement of atomic and subatomic entities that allow a more detailed understand of quantum behavior that otherwise would be impossible to perceive or detect without this confinement. Thus we seek a deeper meaning within these research fields, which serve not only for applications, as mentioned above, but as more fundamental contributions in quantum physics, especially quantum optics and CQED. Quantum dots have been widely studied under traditional theoretical frameworks (3D potential at Schrödinger equation, for instance). Mean field theories like Hartree, Hartree-Fock and density-functional theories, being the simplest approach, are used to describe QDs by assuming the charge carriers to be moving independently within an average field created by particle interactions and external confinement. Empirically, the mean field is approximated by an effective potential [9]. But mainly experimental [3, 11, 12] since they have implemented works that has allowed the design of technology to small, medium and large scale. However there

are still without understanding fundamental aspects, such as quantum entanglement that serves as a cornerstone of quantum computing and quantum information. Because is into our interest to study under the scheme of QDs. The coupling of several QDs interacting with the electromagnetic field modes brings a lot of valuable information that helps to understand these systems collectively and cooperatively. As a result of coupling two of more quantum dots to a common electromagnetic environment (quantum electromagnetic field), the dynamics of spontaneous emission from these system is different than that observed for a single dot. This effect is well known in atomic systems (superradiance) In the case of quantum dots, it is essential to take into account the inhomogneity of their parameters (in particular, of the energy of radiative transition) as well as the possible strong coupling (of dipole or tunneling origin) between the dots. Due to these couplings collective emission effects can appear for these systems in spite of considerable differences between their energetic parameters, which is manifested, e.g., by the enhanced rate of spontaneous emission (exciton recombination).

Another aspect of great interesting in the study of collective QDS systems is the interaction between two dots, i.e. the interaction in pairs. It is type Coulombian interaction, this interaction has been little studied, until the work of [Quiroga, Surendra] where the collective Hamiltonian of type Dicke acquires a nonlinear characteristic due to this interaction non radiative. That is reflected in the nonlinear terms into collective atomic operator of angular momentum. This feature distinguishes the QDs systems and its Hamiltonian of the multi-atomic Dicke model. In the latter model the study of groups of atoms is in the context of Cavity Quantum Electrodynamics (CQED). This explores the phenomena of cooperative spontaneous emission, known as Superradiancia. So we will seek to insight the meaning of these phenomena in QDs by analyzing the complete Hamiltonian with nonlinear characteristic, which extends the use of these quantum objects for more impacting innovative technology applications.

On class challenges in this dissertation comes from the field of quantum computation and quantum information due to the key strengthening for insight the quantum entanglement and the so called quantum bit implementation in real systems how it to be best efficient performance.

Not only are the energy levels of the charge carriers in the mean field potential of the QD atomic-like in their being discrete; but they also present a *shell* structure analogous to atoms, where degenerate or nearly-degenerate levels

bunch up together and are separated from other bunches by energy gaps. This level bunching is a result of dimensionality and symmetry of the mean field potential, and is not exclusive to QD systems, but can be found in the properties of other finite quantum, many-fermion systems, such as conductance, ionization energies, etc. A high degree of symmetry, hence high degeneracy, results in a pronounced level bunching.

Another important feature for the development of technologies for quantum computing is to understand the transfer of quantum entanglement without the loss of this characteristic, which is lost by the Decoherence phenomena. In this dissertation [chapter 5] is in our interest to research a system (Bipartite) of two quantum dots embedded in its own cavity have previously been entangled, to measured the degree of Entanglement based on the measures established for the quantification of entanglement: *Entanglement of Formation and Concurrence* [13-15] It is among several reasons why we study this bipartite system, where entanglement plays a key role. What is perhaps the most basic question in entanglement dynamics is considered: what resources are necessary in order to create entanglement between distant particles? The answer is surprising: sending separable states between the parties is sufficient; entanglement can be created without it being carried by a *messenger* particle.

So that in this thesis we deal with two essential problems: i. e. first one study collective and cooperative phenomena in quantum dot (QDs) systems [chapters 3, 4 and 5] together with the Hamiltonian that includes the Förster's interaction (FRET) [1, 17, 18], which provides significant information on these phenomena that are not otherwise apparent. On the other hand we study a simple system of two QDs in its own cavity [Chapters 2 and 5], where we assume that are entangled, and therefore we are able to measure the degree of entanglement [13, 15] transfer without loss of coherence.

In following we explain how the distribution of this thesis. *In Chapter 2* we collect into particular way the theoretical foundations necessary for the development and insight of this work, under which we develop our theoretical, purpose in quantum mechanics framework and especially the Quantum Optics, we focus into quantum entanglement. We studied the fundaments of deeper meaning as quantum entanglement, i.e. entangled states as fundamental states of quantum information processing. We also study the Rabi oscillations, and implications for Quantum Information Theory, where it is used to measure the Quantum

Entanglement Degree. *In Chapter 3*, we study concisely the so called Quantum Dots (QDs), we reviewing the state of art, as well as introducing the theoretical concepts necessary to model out and implement different ways of QDs systems, because we used to generate the results of our research. We get early developments grounded in mathematical models of Jaynes-Cummings and Dicke atomic collective model. We present the nonlinear QDs Hamiltonian, which includes the Förster interaction to non radiative transfer energy between dots (nonlinear part). We diagonalized this Hamiltonian at the QDs excitons basis that is very useful in the description and implementation of Quantum-bits (qbits). It is also introduced the so-called Coherent Atomic States (ACS) or Angular Momentum States and its generalization consistent as Excited Atomic Coherent States (EACS) which we will use in our work in the next chapter. For *Chapter 4*, more results are obtained by applying the theoretical concepts studied in previous chapters. It shows the collective effects of QDs systems relaying on the Hamiltonian model of QDs, as well as the use of EACS in the general case, and for sake of simplicity we study a particular soluble case into the semiclassical regime. Ok, so now we are getting somewhere, digging a bit deeper to introduce into *Chapter 5* the application to Theory of Quantum Information and Computation. In this we study the effects to apply and implement QDs systems for Quantum Computing, where we get results when we diagonalized the Hamiltonian to obtain the necessary ingredients for Quantum Entanglement Measure for a pair of entangled QDs. Because the collective effects of nonlinearity are evident in the QDs system. Finally in *Chapter 6* we give the general conclusions of this work and future prospects of our proposed by use and implementation of QDs systems.

REFERENCES

[1] (a) J. Sanchez-Mondragon, A. Alejo-Molina, S. Sanchez-Sanchez and M. Torres-Cisneros, "Comparison of the Dicke Model and the Hamiltonianfor *L* Quantum Dots", *Quantum Dots, Nanoparticles, and Nanoclusters II*, edited by Diana L. Huffaker, Pallab K. Bhattacharya, *Proceedings of SPIE* Vol. 5734 (SPIE, Bellingham, WA, 2005) (b) A. Alejo-Molina, J. J. Sánchez-Mondragón, S. Sánchez-Sánchez, *DETUNING COLECTIVO DEL MODELO DE L PUNTOS CUÁNTICOS,* XLVIII CONGRESO NACIONAL SMF / XVIII REUNION ANUAL AMO GUADALAJARA JALISCO 2005.

[2] Kastner, M. A. Artificial Atoms. *Phys. Today* **46**, 24 (1993).

[3] Ashoori, R. C. Electrons in Artificial Atoms. *Nature* **379**, 413 (1996).

[4] Gammon, D. Semiconductor Physics: Electrons in Artificial Atoms *Nature* **405**, 899 (2000).

[5] Reed, M. A., Randall, J. N., Aggarwal, R. J., Matyi, R. J., Moore, T. M. & Wetsel, A. E. Observation of Discrete Electronic States in a Zero-Dimensional Semiconductor Nanostructure. *Phys. Rev. Lett.* **60**, 535 (1988).

[6] Brunner, K., Bockelmann, U., Abstreiter, G., Walther, M. & Weimann, G. Photoluminescence from a Single GaAs/AlGaAs Quantum Dot. *Phys. Rev. Lett.* **69**, 3216 (1992).

[7] Brunner, K., Abstreiter, G., Bohm, G., Trankle, G. & Weimann, G. Sharp-Line Photoluminescence and Two-Photon Absorption of Zero-Dimensional Biexcitons in a GaAs/AlGaAs Structure. *Phys. Rev. Lett.* **73**, 1138 (1994).

[8] Snyder, C. W., Orr, B. G., Kessler, D. & Sander, L. M. Effect of Strain on Surface Morphology in Highly Strained InGaAs Films. *Phys. Rev. Lett.* **66**, 3032 (1991).

[9] Reimann, S. M. & Manninen, M. Electronic Structure of Quantum Dots. *Rev. Mod. Phys.* **74**, 1283 (2002).

[10] Kastner, M. A. Artificial Atoms. *Phys. Today* **46**, 24 (1993).

[11] Gammon, D. Semiconductor Physics: Electrons in Artificial Atoms *Nature* **405**, 899 (2000).

[12] Brack, M., Damgaard, J., Jensen, A. S., Pauli, H. C., Strutinsky, V. M. & Wong, C. Y. Funny Hills: The Shell-Correction Approach to Nuclear Shell Effects and its Applications to the Fission Process. *Rev. Mod. Phys.* **44**, 320.

[13] M. A. Neilsen and I. L. Chuang, *Quantum Computation and Quantum Information*, Cambridge University Press (2000).

[14] S. Hill and W. K. Wootters, Phys. Rev. Lett. **78**, 5022 (1997).

[15] W. K. Wootters, Phys. Rev. Lett. **80**, 2245 (1998). Quantum Inf. Comput. **1**, 27 (2001).

[17] L. Quiroga and N. F. Johnson, Phys. Rev. Lett. 83, 2270 (1999).

[18] J. H. Reina, L. Quiroga, and N. F. Johnson, Phys. Rev. A. 62, 012305 (2000).

CHAPTER 2

QUANTUM ENTANGLEMENT FUNDAMENTS

2.1 Introduction

In this chapter reviews and introduces concepts and tools of the theory of Quantum Entanglement (QE) and quantum theory. We rely on classical texts [1-4, 25] and in some with more modern focus in matter [23, 24, 26]. We describe the QE not only because it is hot topic in modern quantum theory, despite having been already proposed by E. Schrödinger since the time of beginning of the theory in the 20's years with his famous Schrödinger's Cat. Since 30 years ago, the QE has acquired a great interest not only for its theoretical aspect, but by its potential applications to the development of Quantum Computation and Quantum Information, among other branches of quantum physics. It is very important to understand the quantum concepts in order to develop our proposal to use of Quantum Dots (QDs) in cavity QED as a system of quantum bits entangled in chapter 5. Further that these quantum fundaments are fully general and help us to develop in this chapter and next the topics that we need to following developments to our proposals of the thesis. There are many aspects into quantum theory that is our interests: namely those special topics as quantum

theory of Radiation together to Cavity Quantum Electrodynamics (CQED), which are the foundations in Quantum Optics. Because quantum optics to perform a service into this work. So we study specific subjects necessary in order to develop our theoretical system proposal.

The interaction of matter with radiation has been one of the driving forces of modern physics. The problem of blackbody radiation led Planck to reluctantly introduce the idea of quantization at the turn of the previous century. In describing the photoelectric effect Einstein, in one of his seminal papers of 1905, introduced the concept of the photon. The problems of spectral radiation from atoms culminated in the development of Quantum Mechanics during of 1920s. Physics' most accurate theory, Quantum Electrodynamics (QED) describes the interaction of electrons and other leptons with the electromagnetic field. The advent of the laser has not only opened up new vistas in physics research, but also revolutionized communications. In more recent years the advent of atom trapping and optical microcavities has opened new opportunities to test fundamental physics and possible links to future technologies, for example Quantum Computing. One of the areas of Quantum Optics that relates to this is known as Cavity Quantum Electrodynamics (CQED). CQED is an area of considerable theoretical and experimental interest. The core system of Cavity QED is that of cold atoms held inside an optical resonator interacting with external laser light fields. In this report we examine a model of this system. The Jaynes Cummings Model describes a two level atom in the radiation field. Much of the initial work on two level systems was undertaken in the context of magnetic resonance of spin-1/2 particles. In an optics context this two level model was put forward in 1963 by Jaynes and Cummings [1]. The Jaynes Cummings Model is the one of the simplest systems in quantum optics. Not only can it be solved exactly but it also displays interesting phenomena of more general interest, e.g. collapse-revival phenomena. This means that the Jaynes-Cummings Model serves as a useful approximation to more complicated systems. Hence it is still a research topic some 40 years after its introduction.

2.2 Quantum Spin and Pauli Matrices

For beginning this review [23, 25], we study a class the interest operators (matrix representation) that appears at quantum theory are the Pauli Matrices. These are introducing in Quantum Angular Momentum in the study of *Electron-*

Spin. Furthermore these matrices are very use at Quantum Optics and Quantum Computation Theory.

The *Pauli matrices*, also known as the spin matrices, are defined (three forms due to use in quantum optics and quantum computation) by

$$\sigma_1 = \sigma_x = X = \begin{pmatrix} 0 & 1 \\ 1 & 0 \end{pmatrix}; \quad \sigma_2 = \sigma_y = Y = \begin{pmatrix} 0 & -i \\ i & 0 \end{pmatrix};$$
$$\sigma_3 = \sigma_z = Z = \begin{pmatrix} 1 & 0 \\ 0 & -1 \end{pmatrix}; \quad \sigma_0 = I = \begin{pmatrix} 1 & 0 \\ 0 & 1 \end{pmatrix}; \tag{2.1}$$

Let us consider spin 1/2 particles, such as an electron or a proton. These particles have an internal degree of freedom: the spin-up and spin-down states. (To be more precise, these are expressions that are relevant when the *z*-component of an angular momentum S_z is diagonalized. If S_x is diagonalized, for example, these two quantum states can be either *spin-right* or *spin-left*. Moreover we must remember that $\vec{\sigma} = 2\vec{S}$). Since the spin-up and spin-down states are orthogonal, we can take their components to be

$$|e\rangle = |\uparrow\rangle = \begin{pmatrix} 1 \\ 0 \end{pmatrix}; \quad |g\rangle = |\downarrow\rangle = \begin{pmatrix} 0 \\ 1 \end{pmatrix} \tag{2.2}$$

Verify that they are eigenvectors of σ_z satisfying $\sigma_z|\uparrow\rangle = |\uparrow\rangle$ and $\sigma_z|\downarrow\rangle = -|\downarrow\rangle$ .In quantum information, we often use the notations $|1\rangle = |\uparrow\rangle$ and $|0\rangle = |\downarrow\rangle$ (Some authors use convention: $|0\rangle = |\uparrow\rangle$ and $|1\rangle = |\downarrow\rangle$). Moreover, the states $|0\rangle$ and $|1\rangle$ are not necessarily associated with spins. They may represent any two mutually orthogonal states, such as horizontally and vertically polarized photons. Thus we are free from any physical system, even though the terminology of spin algebra may be employed.

For electrons and protons, the spin angular momentum operator is conveniently expressed in terms of the Pauli matrices σ_k as $S_k = (\hbar/2)\sigma_k$. We often employ

natural units in which $\hbar \equiv 1$. Note the tracelessness property $tr(\sigma_k) = 0$ and the Hermiticity $\sigma_k^\dagger = \sigma_k$ (Mathematically speaking, these two properties imply that $i\sigma_k$ are generators of the $su(2)$ Lie algebra associated with the Lie group $SU(2)$). In addition to the Pauli matrices, we introduce the unit matrix I in the algebra, which amounts to expanding the Lie algebra $su(2)$ to $u(2)$. The Pauli matrices satisfy the anticommutation relations

$$\{\sigma_i, \sigma_j\} = \sigma_i\sigma_j + \sigma_j\sigma_i = 2\delta_{ij} I \tag{2.3}$$

Therefore, the eigenvalues of σ_k are found to be ±1. The commutation relations between the Pauli matrices are

$$[\sigma_i, \sigma_j] = \sigma_i\sigma_j - \sigma_j\sigma_i = 2i\sum_k \varepsilon_{ijk}\sigma_k \tag{2.4}$$

where ε_{ijk} is the totally antisymmetric tensor of rank 3, also known as the *Levi-Civita symbol*, with value +1 if ε_{ijk} even permutation, -1 if ε_{ijk} odd permutation, and 0 in otherwise.

The commutation relations, together with the anticommutation relations, yield

$$\sigma_i\sigma_j = i\sum_{k=1}^{3} \varepsilon_{ijk}\sigma_k + \delta_{ij} I \tag{2.5}$$

The *spin-flip* ("ladder") operators are defined by

$$\sigma_+ = \frac{1}{2}(\sigma_x + i\sigma_y) = \begin{pmatrix} 0 & 1 \\ 0 & 0 \end{pmatrix}; \quad \sigma_- = \frac{1}{2}(\sigma_x - i\sigma_y) = \begin{pmatrix} 0 & 0 \\ 1 & 0 \end{pmatrix} \tag{2.6}$$

We can verify that eigenvectors are $\sigma_+ |\uparrow\rangle = \sigma_- |\downarrow\rangle = 0$, $\sigma_+ |\downarrow\rangle = |\uparrow\rangle$ and $\sigma_- |\uparrow\rangle = |\downarrow\rangle$. The projection operators to the eigenspaces of σ_z with the eigenvalues ±1 are

$$\mathrm{P}_+ = |\uparrow\rangle\langle\uparrow| = 1/2(\mathrm{I} + \sigma_z) = \begin{pmatrix} 1 & 0 \\ 0 & 0 \end{pmatrix}, \ \mathrm{P}_- = |\downarrow\rangle\langle\downarrow| = 1/2(\mathrm{I} - \sigma_z) = \begin{pmatrix} 0 & 0 \\ 0 & 1 \end{pmatrix} \tag{2.7}$$

In fact, it is straightforward to show $\mathrm{P}_+\left|\uparrow\right\rangle=\left|\uparrow\right\rangle,\ \mathrm{P}_+\left|\downarrow\right\rangle=0,\ \mathrm{P}_-\left|\uparrow\right\rangle=0,\ \mathrm{P}_-\left|\downarrow\right\rangle=\left|\downarrow\right\rangle$.

Finally, we note the following identities:

$$\sigma_\pm^2=0,\ \ \mathrm{P}_\pm^2=\mathrm{P}_\pm,\ \ \mathrm{P}_+\mathrm{P}_-=0 \tag{2.8}$$

Other interesting identities that we obtained independent of the above are as follows

$$\left(\sigma_+\pm\sigma_-\right)^2=\sigma_+^2\pm\left(\sigma_+\sigma_-+\sigma_-\sigma_+\right)+\sigma_-^2 \tag{2.9}$$

And

$$\begin{aligned}\left(\hat{n}\cdot\vec{\sigma}\right)^2&=\sum_{i=1}^{3}n_i\sigma_i\sum_{j=1}^{3}n_j\sigma_j=\sum_{i,j=1}^{3}n_in_j\sigma_i\sigma_j=\sum_{i,j=1}^{3}n_in_j\left(i\sum_{k=1}^{3}\varepsilon_{ijk}\sigma_k+\delta_{ij}I\right)\\&=i\sum_{k=1}^{3}\sum_{i,j=1}^{3}n_in_j\varepsilon_{ijk}\sigma_k+I\sum_{i,j=1}^{3}n_in_j\delta_{ij}=n\bullet nI+i\sum_{k=1}^{3}\left(\sum_{i,j=1}^{3}n_in_j\varepsilon_{ijk}\right)\sigma_k=I\end{aligned} \tag{2.10}$$

$$\exp\left(i\varsigma\sigma_3\right)=\cos\left(\varsigma\sigma_3\right)+i\frac{\sigma_3}{\sqrt{\sigma_3{}^2}}\sin\left(\varsigma\sigma_3\right)=\cos\left(\varsigma\right)+i\frac{\sigma_3}{\sqrt{\sigma_3{}^2}}\sin\left(\varsigma\right),$$

$$\exp\left(i\varsigma\sigma_3\right)\exp\left(-i\varsigma\sigma_3\right)=\left(\cos\left(\varsigma\right)+i\frac{\sigma_3}{\sqrt{\sigma_3{}^2}}\sin\left(\varsigma\right)\right)\left(\cos\left(\varsigma\right)-i\frac{\sigma_3}{\sqrt{\sigma_3{}^2}}\sin\left(\varsigma\right)\right),$$

$$\exp\left(i\varsigma\sigma_\pm\right)=1+i\varsigma\sigma_\pm+\sum_{n=1}^{\infty}\frac{\left(i\varsigma\sigma_\pm\right)^{2n}}{\left(2n\right)_¡}+i\varsigma\sigma_\pm\sum_{n=1}^{\infty}\frac{\left(i\varsigma\sigma_\pm\right)^{2n}}{\left(2n+1\right)_¡}=1+i\varsigma\sigma_\pm \tag{2.11}$$

$$\exp\left(i\varsigma\sigma_\pm\right)\exp\left(-i\varsigma\sigma_\pm\right)=\left(1+i\varsigma\sigma_\pm\right)\left(1-i\varsigma\sigma_\pm\right)=1$$

$$\begin{aligned}\exp\left(i\varsigma\hat{n}\cdot\vec{\sigma}\right)&=\sum_{n=0}^{\infty}\frac{\left(i\varsigma\hat{n}\cdot\vec{\sigma}\right)^{2n}}{\left(2n\right)_¡}+i\varsigma\sigma_\pm\sum_{n=0}^{\infty}\frac{\left(i\varsigma\hat{n}\cdot\vec{\sigma}\right)^{2n}}{\left(2n+1\right)_¡}=\sum_{n=0}^{\infty}\frac{\left(-1\right)^n\varsigma^{2n}}{\left(2n\right)_¡}+i\sigma_\pm\sum_{n=0}^{\infty}\frac{\left(-1\right)^n\varsigma^{2n+1}}{\left(2n+1\right)_¡}\\&=\cos\varsigma+i\sigma_\pm\sin\varsigma\end{aligned}$$

2.3 Applications: Rabi Oscillations

A of the most interesting cases in the quantum theory of radiation is understand the phenomena of dynamic interaction of light with atoms, it is so-called *Rabi problem.* The original Rabi problem is of magnetic origin, but in the optic case consists do it comparison with the system of the two-level atom (TLA) and radiation electromagnetic field in interaction. A TLA is formally similar to a spin-1/2 system with two possible states. We can do an approximation, i.e. in the dipole approximation; when the field wavelength is larger than the atomic size, the atom-field interaction problem is mathematically equivalent to a spin-1/2 particle interacting with a time dependent magnetic field. Just as this system undergoes the so-called *Rabi Oscillation* between the spin-up and spin-down states under the action of an oscillating magnetic field, the TLA also undergoes *optical Rabi oscillations* under the action of the driving electromagnetic field. These oscillations are damped if the atomic levels decay. An insight of this simple model of the atom-field interaction enables us to consider more complicated problems involving an ensemble of atoms or other quantum structures system interacting with the field. There are two approximations to investigate this problem (which we study completely in next sections and chapters): namely Semi-classical and totally quantum approximations. The first one is when the field is it consider as only classically, i.e. without quantization, so only matter (atoms or atomic structures) must be quantized. Another one both field and matter must be quantized. This has many implications, not only mathematically but physically. Since in many instances where a classical field fails to explain experimentally observed results and quantized description of the field is required. This is true of spontaneous emission of the atomic system. It is need to quantized the field for understand this phenomenon. By mean a rigorous treatment of the atomic level decay in free space, we need to consider the interaction of the atom with the vacuum modes of the space.

Even in the simplest system involving interaction of a single mode radiation field with a single TLA, the predictions for the dynamics of the atom are quite distinct in the semi-classical theory and fully quantum theory. In the absence of the decay process, the semi-classical theory predicts Rabi oscillations for the atomic inversion whereas the quantum theory predicts a interesting phenomena known as Collapse and Revival due to the quantum aspects of the field. These interesting theoretical predictions have been experimentally verified. In reality this problem (Rabi) originally is most complicate, due to that their energy potential

characteristic depends of the time, which we must solve with help of Time dependent Perturbation theory besides the interaction picture. Thus, Let us consider a spin-1/2 particle in a magnetic field along the *z*-axis, whose Hamiltonian is given by

$$H_0 = -\frac{\omega_0}{2}\sigma_z \tag{2.12}$$

It is assume the particle is irradiated by an oscillating magnetic field of angular frequency ω, which introduces transitions between two energy eigenstates of H_0 (We will take the natural unit $\hbar \equiv 1$ to simplify our notation throughout this example). Then the perturbed Hamiltonian ($H = H_0 + \gamma V(t)$), is modeled as

$$\begin{aligned} H &= -\frac{\omega_0}{2}\sigma_z + \frac{g}{2}\begin{pmatrix} 0 & e^{i\omega t} \\ e^{-i\omega t} & 0 \end{pmatrix} \\ H &= -\frac{\omega_0}{2}\sigma_z + \frac{g}{2}\left[e^{-i\omega t}\sigma_- + e^{i\omega t}\sigma_+ \right] \end{aligned} \tag{2.13}$$

where $g > 0$ is a parameter proportional to the amplitude of the oscillating field. Let us evaluate the wave function $|\psi(t)\rangle$ at time $t > 0$ assuming that the system is in the ground state of the unperturbed Hamiltonian

$$|\psi(0)\rangle = \begin{pmatrix} 1 \\ 0 \end{pmatrix} \tag{2.14}$$

At $t = 0$. Do not use directly the solution equation (2.2) to Hamiltonian, since note that we cannot simply exponentiate the Hamiltonian since it is time-dependent. Surprisingly, however, the following trick makes it time independent. Let us consider the following "gauge transformation":

$$|\varphi(t)\rangle = e^{-i\omega\sigma_z t/2}|\psi(t)\rangle \tag{2.15}$$

What must satisfiers the Schrodinger equation for the interaction Hamiltonian, i.e. a straightforward calculation shows that $|\varphi(t)\rangle$ satisfies

$$-i\frac{d}{dt}|\varphi(t)\rangle = \tilde{H}|\varphi(t)\rangle \tag{2.16}$$

Because with $V(t) \neq 0$ we are no longer dealing with *stationary* case; the time evolution operator is no longer as simple as $e^{-iHt/\hbar}$ when H itself involves time. We can show that $\tilde{H}$ is given for,

$$\begin{aligned}\tilde{H} &= e^{-i\omega\sigma_z t/2} H e^{+i\omega\sigma_z t/2} - i e^{-i\omega\sigma_z t/2} \frac{d}{dt}\left(e^{+i\omega\sigma_z t/2}\right) \\ &= -\frac{\omega_0}{2}\sigma_z + \frac{g}{2}\frac{1}{2}\left(\sigma_- + \sigma_+\right) + \frac{\omega}{2}\sigma_z = -\frac{\omega_0}{2}\sigma_z + \frac{g}{2}\sigma_x + \frac{\omega}{2}\sigma_z \qquad (2.17) \\ \tilde{H} &= \frac{1}{2}\begin{pmatrix} -\omega_0 + \omega & g \\ g & \omega_0 - \omega \end{pmatrix} = -\frac{\Delta}{2}\sigma_z + \frac{g}{2}\sigma_x\end{aligned}$$

If we attempt to diagonalize this Hamiltonian we find the corresponding eigenvalues

$$\begin{aligned}\begin{vmatrix} -\Delta - \lambda & g \\ g & \Delta - \lambda \end{vmatrix} &= -\left(\Delta + \lambda\right)\left(\Delta - \lambda\right) - g^2 = -\Delta^2 + \lambda^2 - g^2 \\ &= -\left(\Delta^2 + g^2\right) + \lambda^2 = 0 \qquad (2.18) \\ \Rightarrow \quad \Omega(\Delta) &= \sqrt{\Delta^2 + g^2}\end{aligned}$$

Where $\Delta = \omega_0 - \omega$; is the *detuning* in this case between ω and ω_0. In fact $\tilde{H}$ is time independent. We do the algebraic change as $\Omega(\Delta) = \sqrt{\Delta^2 + g^2}$, multiply and dividing, so [see reference 23],

$$\tilde{H} = \frac{1}{\Omega}\left[-\frac{1}{\Omega}\frac{\Delta}{2}\sigma_z + \frac{1}{\Omega}\frac{g}{2}\sigma_x\right] = \frac{\Omega}{2}\left(\frac{g}{\Omega}\sigma_x - \frac{\Delta}{\Omega}\sigma_z\right) \qquad (2.19)$$

Also the operator $\tilde{H}$ can be put into the form

$$H = -\frac{\hbar}{2}\omega\hat{n}\cdot\vec{\sigma} \qquad (2.20)$$

Where $\hat{n}$ is a unit vector in $\mathbb{R}^3$. The time-evolution operator is readily obtained, by making use of the result of (remember that for our purpose $\hbar \equiv 1$),

$$U(t) = \exp(-iHt/2) = \cos(\omega t/2)\mathrm{I} + i(\hat{n}\cdot\vec{\sigma})\sin(\omega t/2) \tag{2.21}$$

Thus the Hamiltonian time independent is ($\omega \to \Omega$),

$$\begin{aligned}\tilde{U}(t) &= \exp(-iHt/2) = \cos(\Omega t/2)\mathrm{I} + i(\hat{n}\cdot\vec{\sigma})\sin(\Omega t/2) \\ &= \cos(\Omega t/2)\mathrm{I} + i\left(\frac{g}{\Omega}\sigma_x - \frac{\Delta}{\Omega}\sigma_z\right)\sin(\Omega t/2)\end{aligned} \tag{2.22}$$

$$\tilde{U}(t) = \begin{pmatrix} \cos(\Omega t/2) + i\frac{\Delta}{\Omega}\sin(\Omega t/2) & i\frac{g}{\Omega}\sin(\Omega t/2) \\ -i\frac{g}{\Omega}\sin(\Omega t/2) & \cos(\Omega t/2) - i\frac{\Delta}{\Omega}\sin(\Omega t/2) \end{pmatrix}$$

The wave function $|\varphi(t)\rangle$ with the initial condition $|\varphi(0)\rangle = \begin{pmatrix}1\\0\end{pmatrix}$ is

$$\begin{aligned}|\varphi(t)\rangle &= \tilde{U}(t)|\varphi(0)\rangle \\ &= \begin{pmatrix} \cos(\Omega t/2) + i\frac{\Delta}{\Omega}\sin(\Omega t/2) & i\frac{g}{\Omega}\sin(\Omega t/2) \\ -i\frac{g}{\Omega}\sin(\Omega t/2) & \cos(\Omega t/2) - i\frac{\Delta}{\Omega}\sin(\Omega t/2) \end{pmatrix}\begin{pmatrix}1\\0\end{pmatrix}\end{aligned} \tag{2.23}$$

$$|\varphi(t)\rangle = \begin{bmatrix} \cos(\Omega t/2) + i\frac{\Delta}{\Omega}\sin(\Omega t/2) \\ -i\frac{g}{\Omega}\sin(\Omega t/2) \end{bmatrix}$$

We find $|\psi(t)\rangle$ from Eq. (2.15) as

$$\left|\psi(t)\right\rangle = e^{+i\omega\sigma_z t/2}\left|\varphi(t)\right\rangle = e^{i\omega\sigma_z t/2}\begin{pmatrix}\cos(\Omega t/2)+i\dfrac{\Delta}{\Omega}\sin(\Omega t/2)\\ -i\dfrac{g}{\Omega}\sin(\Omega t/2)\end{pmatrix} \tag{2.24}$$

Let us assume the applied field is in resonance with the energy difference of two levels, namely $\omega = \omega_0$. We obtain $\Delta = 0$ and $\Omega = g$ in this case. The wave function $\left|\psi(t)\right\rangle$ at later time $t > 0$ is,

$$\begin{aligned}\left|\psi(t)\right\rangle &= e^{+i\omega\sigma_z t/2}\left|\varphi(t)\right\rangle = e^{i\omega_0\sigma_z t/2}\begin{pmatrix}\cos(gt/2)\\ -i\sin(gt/2)\end{pmatrix}\\ \left|\psi(t)\right\rangle &= \begin{pmatrix}e^{i\omega_0\sigma_z t/2}\cos(gt/2)\\ -ie^{i\omega_0\sigma_z t/2}\sin(gt/2)\end{pmatrix}\end{aligned} \tag{2.25}$$

Where, we made a spectral decomposition of the operator, or we can regard it operator as a rotation operator $\hat{R}(\theta)$, ($\theta = \omega t = \omega_0 t$) which is expanded in Taylor series as

$$R(\omega t) = e^{+i\omega\sigma_z t/2} = \begin{pmatrix}e^{+i\omega t/2} & 0\\ 0 & e^{-i\omega t/2}\end{pmatrix}$$

Thus, we obtain the wave function with an additional phase, but it does not affect the outcome final, of the probabilistic interpretation (atomic inversion, etc.). The probability with which the system is found in the ground (excited) state of H_0 is given by

$$\begin{cases}\mathrm{P}_1 = \cos^2(gt/2), & \text{ground state}\\ \mathrm{P}_2 = \sin^2(gt/2), & \text{excited state}\end{cases} \tag{2.26}$$

This oscillatory behavior is called the *Rabi oscillation*. The frequency g is called the *Rabi frequency*, while Ω in Eq. (2.18) and (2.19) is called the *generalized Rabi frequency* [23]. In the graphics we show the Rabi Oscillations for both states,

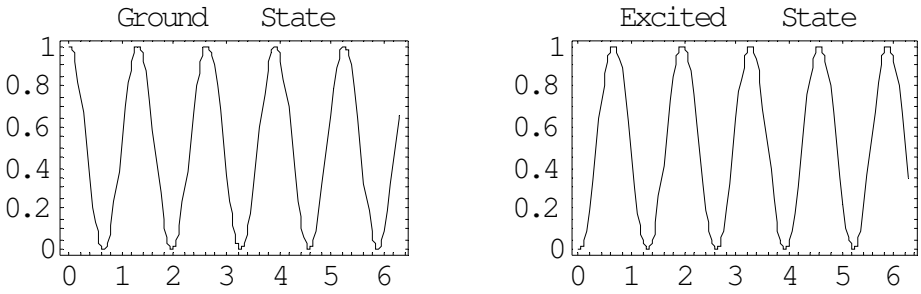

Figure 2.1 Plots of the Rabi Oscillations in Ground and Excited States

2.4 Quantum Entanglement and Multipartite Systems

It is possible for a particle to interact with another particle in such a way that the quantum states of the two particles form a single *entangled* state. The definition of an entangled state is that it is not entirely independent of other states [see reference 23, 25, 24, 26]: its state is dependent on another state in some way. Because of this dependency it is a mistake to consider either state in isolation from the other. Rather we should combine the states and treat the result as a single, entangled state.

First recognized by Einstein, Podolsky and Rosen [7] and Schrodinger [8], it is one of the most astonishing features of the quantum formalism. The main problem in Entanglement Theory is that we do not fully understand what entanglement is. More precisely, we only know is its mathematical definition and its manifestations [4, 5, 9]. Entanglement appears as the consequence of the combination of two of the quantum postulates [26]:

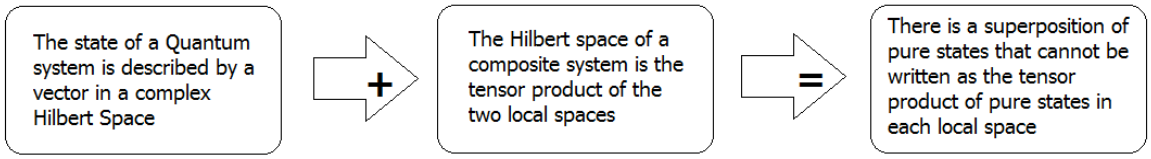

Contrary to the entangled states are the separable states, i.e., a state is entangled if and only if it is not separable. Whether a given state is entangled or just classically correlated is easy to determine for pure states. However, for arbitrary mixed states it is a hard problem [9]. We will see this later.

2.4.1 Multipartite Systems and Tensor Product

So far, we have assumed implicitly that the system is made of a single component. Suppose a system is made of two components; one lives in a Hilbert space H_1 and the other in another Hilbert space H_2. A system composed of two separate components is called *bipartite.* Then the system as a whole lives in a Hilbert space $H = H_1 \otimes H_2$, whose general vector is written as

$$|\psi\rangle = \sum_{i,j} c_{i,j} |v_{1,i}\rangle \otimes |v_{2,j}\rangle \tag{2.27}$$

Where $\{v_{k,j}\}$, (k=1.2) is a orthonormal basis in H_k and $\sum_{i,j} |c_{i,j}|^2 = 1$. A state $|\psi\rangle \in H$ written as a tensor product of two vectors as $|\psi\rangle = |\psi_1\rangle \otimes |\psi_2\rangle$, ($|\psi_a\rangle \in H_a$) is called a *separable state or a tensor product state.* A separable state admits a classical interpretation such as "The first system is in the state $|\psi_1\rangle$, while the second system is in $|\psi_2\rangle$."It is clear that the set of separable states has dimension $\dim(H) = \dim(H_1) + \dim(H_2)$. Note however that the total space *H* has different dimensions since we find, by counting the number of coefficients in (2.26), that $\dim(H) = \dim(H_1)\dim(H_2)$. This number is considerably larger than the dimension of the separable states when $\dim(H_a)$ (*a* = 1, 2) are large. What are the missing states then? Let us consider a spin state

$$|\psi\rangle = \frac{1}{\sqrt{2}}\left[|\uparrow\rangle \otimes |\uparrow\rangle + |\downarrow\rangle \otimes |\downarrow\rangle\right] \tag{2.28}$$

Of two separated electrons. Let us assume that $|\psi\rangle$ may be decomposed as

$$|\psi\rangle = \left[c_1|\uparrow\rangle + c_2|\downarrow\rangle\right] \otimes \left[d_1|\uparrow\rangle + d_2|\downarrow\rangle\right]$$
$$= \left[c_1 d_1|\uparrow\rangle \otimes |\uparrow\rangle + c_1 d_2|\uparrow\rangle \otimes |\downarrow\rangle + c_2 d_1|\downarrow\rangle \otimes |\uparrow\rangle + c_2 d_2|\downarrow\rangle \otimes |\downarrow\rangle\right]$$

However this decomposition is impossible because the constants cross should be nullified in order to this system to maintain consistency, since we must have

$$c_1 d_2 = c_2 d_1 = 0, \quad c_1 d_1 = c_2 d_2 = 1/\sqrt{2}$$

Simultaneously, and it is clear that the above equations have no common solution. Therefore the state $|\psi\rangle$ is not separable. Such non-separable states are called *entangled* in quantum theory [10]. The fact

$$\dim(H_1)\dim(H_2) \gg \dim(H_1) + \dim(H_2)$$

Tells us that most states in a Hilbert space of a bipartite system are entangled when the constituent Hilbert spaces are higher dimensional. These entangled states refuse classical descriptions. Entanglement will be used extensively as a powerful computational resource in quantum information processing and quantum computation.

Let to assume a bipartite state (2.28) is given. We are interested in when the state is separable and when entangled. The criterion is given by the Schmidt decomposition of $|\psi\rangle$.

2.4.2 Separability and Entanglement

Deciding whether several systems are entangled or whether they are just classically correlated is known as the separability problem [24, 26]. In this section we present the separability condition for pure and mixed states, i.e., the definition of entangled states. We will be referring to bipartite systems in a Hilbert space $H = H_A \otimes H_B$, as mentioned above.

Pure States A pure state $|\psi\rangle$ is entangled if and only if it is not separable, i.e., it cannot be written as a tensor product

$$|\psi\rangle = |\psi_A\rangle \otimes |\psi_B\rangle \quad \text{or} \quad |\psi\rangle = |\psi_1\rangle \otimes |\psi_2\rangle \tag{2.29}$$

THEOREM 2.1 (*Schmidt decomposition*). Let to we assume $|\psi\rangle$ is a pure state of a composite system, AB. Then there are orthonormal states $\{|i_A\rangle\}$ for system A, and orthonormal states $\{|i_B\rangle\}$ of system B such that

$$|\psi\rangle = \sum_i \lambda_i |i_A\rangle \otimes |i_B\rangle \tag{2.30}$$

where λ_i are non-negative real numbers satisfying $\sum_i \lambda_i^2 = 1$ known as Schmidt coefficients. If there is no degeneracy, this decomposition is unique up to arbitrary opposite phases in $|i_A\rangle$ and $|i_B\rangle$.

The *Schmidt rank* is defined as the number of non-vanishing Schmidt coefficients. Then, the criterion for pure states is

$|\psi\rangle$ *is pure* $\Leftrightarrow$ $|\psi\rangle$ *has Schmidt rank one.*

Mixed States: A mixed state ρ is entangled if and only if it is not separable, i.e., it cannot be written as [11]

$$\rho = \sum_{i=1}^{N} p_i \left[\left|\psi_A^i\right\rangle \left\langle\psi_A^i\right| \otimes \left|\psi_B^i\right\rangle \left\langle\psi_B^i\right| \right] \tag{2.31}$$

That is, a separable state can be prepared by two distant observers who receive instructions from a common classical source and prepare the different pure states $\left|\psi_A^i\right\rangle$ and $\left|\psi_B^i\right\rangle$ with probability p_i (Fig. 2.1). So, entangled states are those that cannot be created using local operations and classical communication.

The criteria for entanglement of mixed state are many and diverse. Here we start introducing two of them [12, 13]. The symbol T_i indicates the transposition of subsystem i, i.e., partial transposition of the entire system with respect to i (see section 2.4).

THEOREM 2.2 (Peres) If ρ is separable then

$$\rho^{\mathrm{T}_A} \geq 0 \text{ and } \rho^{\mathrm{T}_B} = \left(\rho^{\mathrm{T}_A}\right)^{\mathrm{T}} \geq 0 \tag{2.32}$$

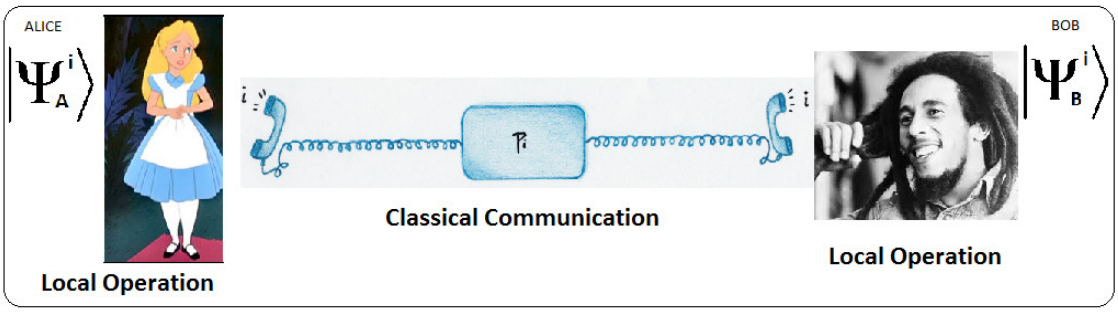

Figure 2.2: Separable-states factory. A classical source gives with probability p_i the output i, indicating far away partners which state to prepare. (Alice and Bob)

Generalization to a system with more components, i.e., a *multipartite system*, should be obvious. A system composed of N components has a Hilbert space

$$\mathrm{H} = \mathrm{H}_1 \otimes \mathrm{H}_2 \otimes \cdots\cdots \otimes \mathrm{H}_i \otimes \cdots \otimes \mathrm{H}_N \tag{2.33}$$

Where H_a is the Hilbert space to which the $a\mathrm{th}$ component belongs. Classification of entanglement in a multipartite system is far from obvious, and an analogue of the Schmidt decomposition is not known to date for $N \geq 3$.

2.4.3 Density Operator (Matrix) and Mixed States

It might happen in some cases that a quantum system under consideration is in the state $|\psi_i\rangle$ with a probability p_i. In other words, we cannot say definitely which state the system is in. Therefore some random nature comes into the description of the system. This random nature should not be confused with a probabilistic behavior of a quantum system. Such a system is said to be in a *mixed state,* while a system whose vector is uniquely specified is in a *pure state.* A pure state is a special case of a mixed state in which $p_i = 1$ for some i and $p_j = 0$, ($j \neq i$). Mixed states may happen in the following cases, for example:

- Let us assume we observe a beam of totally unpolarized light and measure whether photons are polarized vertically or horizontally. The measurement outcome of a particular photon is *either* horizontal *or* vertical. Therefore when the beam passes through a linear polarizer, the intensity is halved.

The beam is a mixture of horizontally polarized photons and vertically polarized photons.

- A particle source emits a particle in a state $|\psi_i\rangle$ with a probability p_i ($1 \le i \le N$).
- Let us consider a canonical ensemble. If we pick up one of the members in the ensemble, it is in a state $|\psi_i\rangle$ with energy E_i, and probability $p_i = \exp(E_i / k_B T) / Z(T)$, where $Z(T) = Tr\left(e^{-H/k_B T}\right)$ is the partition function.

In each of these examples, a particular state $|\psi_i\rangle \in \mathrm{H}$ appears with probability p_i, in which case the expectation value of the observable *a* is $\langle\psi_i|A|\psi_i\rangle$, where we assume $|\psi_i\rangle$ is normalized; $\langle\psi_i|\psi_i\rangle = 1$. The mean value of *a* is then given by

$$\langle A\rangle = \sum_{i=1}^{N} p_i \langle\psi_i|A|\psi_i\rangle \tag{2.34}$$

where *N* is the number of available states. Let us introduce the *density matrix* by

$$\rho = \sum_{i=1}^{N} p_i |\psi_i\rangle\langle\psi_i| \tag{2.35}$$

Then the equation (2.33) is rewritten in a compact form as

$$\langle A\rangle = Tr(\rho A) \tag{2.36}$$

Properties which a density matrix ρ satisfies are very much like axioms for pure states.

A1. A physical state of a system, whose Hilbert space is *H*, is completely specified by its associated density matrix $\rho : H \to H$. A density matrix is a positive semi-definite Hermitian operator with $Tr(\rho) = 1$.

A2. The mean value of an observable *a* is given by

$$\langle A\rangle = Tr(\rho A) \tag{2.37}$$

A3. The temporal evolution of the density matrix is given by the *Liouville von Neumann equation,*

$$i\hbar \frac{d}{dt}\rho = [H, \rho] \tag{2.38}$$

Where the *H* is the Hamiltonian of system.

THEOREM 2.4 A state ρ is pure if and only if $\rho^2 = \rho$.

DEFINITION 2.1 A state ρ is called *uncorrelated* if it is written as

$$\rho = \rho_1 \otimes \rho_2 \tag{2.39}$$

It is called *separable* if it is written in the form

$$\rho = \sum_i p_i \left(\rho_{1,i} \otimes \rho_{2,i} \right) \tag{2.40}$$

Where $0 \leq pi \leq 1$ and $\sum_i p_i = 1$. It is called *inseparable* if ρ does not admit the decomposition (2.39). It is important to realize that only inseparable states have quantum correlations analogous to that of an entangled pure state. However, it does not necessarily imply separable states have no non-classical correlation. It was pointed out that useful non-classical correlation exists in the subset of separable states [14].

2.4.4 Entanglement Measures

Perhaps the most remarkable feature of quantum mechanics, a feature that clearly distinguishes it from classical physics, is this: for any composite system, there exist pure states of the system in which the parts of the system do not have pure states of their own. Such states are called entangled.

One can also define the concept of entanglement for mixed quantum states: a mixed state is entangled if it cannot be represented as a mixture of unentangled pure states. For both pure and mixed quantum states, there are good measures of the degree of entanglement. In the case of pure states of a bipartite system there is a single widely accepted measure of entanglement, whereas for mixed states of such systems there are three measures that have been extensively studied.

Quantifying quantum entanglement is one of the main challenges in quantum theory and more specifically in the quantum computation theory. Thus the questions that arise:

- ✓ How can entanglement be *measured* or quantified,
- ✓ how can entanglement be classified, i.e., what physically different types of entanglement exist, and
- ✓ Finally how does entanglement behave as a physical resource for quantum communication, quantum computation, etc.?

To begin, we must know how to quantify entanglement [15, 26] and what do such a measure. We answer this important question by stating the conditions that every measure of entanglement E has to satisfy:

- Entanglement is non-negative. It is zero if and only if the state is separable

$$E(\psi) \geq 0 \ \ \forall \psi, \ \ E(\psi) = 0 \Leftrightarrow \psi \ \text{ is separable}$$

- Entanglement of independent systems is additive

$$E\left(\psi^{\otimes n}\right) = nE(\psi)$$

- Entanglement is conserved under local unitary operations

$$\psi \to U\psi, \quad U = U_A \otimes U_B : E(\psi) = E(U\psi)$$

$\mapsto$ a local change of basis has no effect on E

- Its expectation value cannot be increased by local non-unitary operations

$$\psi - \text{local non-unitary} \to \{p_j, \psi_j\} : \sum_j p_j E(\psi_j) \leq E(\psi)$$

For more on this see the pioneering paper on entanglement measures [15].

A *pure state's* entanglement is measured by its *entropy of entanglement* $E(\psi)$

$$|\psi\rangle = \sum_i p_i |\psi_A^i\rangle \otimes |\psi_B^i\rangle : \quad E(\psi) = S(\rho_A) = S(\rho_B) \tag{2.41}$$

i.e., the apparent entropy of any of the systems considered alone, where

$$S(\rho) = Tr(\rho \log \rho) \tag{2.42}$$

is the *von Neumann entropy*, $\rho_A = Tr_B |\psi\rangle\langle\psi|$ is the reduced density matrix of A, obtained after tracing over B's degrees of freedom, and the logarithm is to base two (the information is stored in *qubits*). The entropy measures how much uncertainty there is in the state of the physical system. For example, if ρ_A and ρ_B describe pure states (there is no uncertainty in the individual systems), then $E(\psi) = 0$ (there are no quantum correlations between them).

We define an *ebit* as the amount of entanglement in a maximally entangled state of two qubits, for which $E = 1$.

Another possibility is to use the *rank of the Schmidt decomposition* (SD) as a measure. If *A* is a subset of n qubits and *B* the rest of them, the SD of $|\psi\rangle$ with respect to the partition *A*: *B* reads

$$|\psi\rangle = \sum_{\beta=1}^{\chi_A} p_\beta |\psi[A]_\beta\rangle \otimes |\psi[B]_\beta\rangle$$

The rank χ_A of ρ_A (the reduced density matrix for block *A*) is a natural measure [16] of the entanglement between the qubits in *A* and those in *B*. Therefore, a good measure to quantify the entanglement of state $|\psi\rangle$ would be the maximal value of χ_A over all possible bipartite splits *A*: *B* of the *n* qubits, namely

$$\chi := \max_A (\chi_A)$$

or the related entanglement measure E_χ, then $E_\chi := \log_2(\chi)$.

In the bipartite setting, E_χ upper bounds the more standard measure entropy of entanglement.

For mixed states we have a lot of measures, there is not a unique measure of entanglement. The choice of one measure or another depends on what you need. We will see some examples in what follows. In principle, there are two approaches to quantify entanglement [17, 18]:

Abstract approach. A state function can be used to quantify entanglement if it satisfies the natural properties stated before as definition of a measure.

1. *Von Neumann entropy S*: already introduced in (2.3.4).
2. *Relative Entropy of Entanglement* E_R: it is based on the idea of distance; the closer the state is to the set of separable states, the less entangled it is.
3. Other measures: Squashed Entanglement E_{sq}, Rényi Entropy E_α, Logarithm of the Negativity E_{N}, Concurrence *C*, etc.

Operational approach. The system is more entangled if it allows for better performance of some task impossible without entanglement.

1. *Entanglement of Formation* EoF : having a large number *n* of Bell states, we want to produce as many (high-fidelity) copies $|\psi\rangle$ using LOCC, getting finally *m* copies, therefore 's E of formation is the limiting ratio *n/m*.
2. *Distillable entanglement* E_D: performing the reverse process, it is the limiting ratio *m/n*, when having a large number m of copies of $|\psi\rangle$ and we want to distill as many Bell states using LOCC (local operations and classical communications), getting finally *n* EPR pairs.
3. Other measures: *Entanglement Cost* E_C, *Entanglement of Assistance* EoA, etc.

All these measures are equivalent in certain limits, e.g. [19]. We have so many definitions not only due to the diverse interpretations, but because calculating some of they are of the Big Open Problems of QIT.

REFERENCES

[1] P. A. M. Dirac, *Principles of Quantum Mechanics* (4th ed.), Clarendon Press (1981).

[2] L. I. Shiff, *Quantum Mechanics* (3rd ed.), McGraw-Hill (1968).

[3] A. Messiah, *Quantum Mechanics*, Dover (2000).

[4] J. J. Sakurai, *Modern Quantum Mechanics* (2nd Ed.), Addison Wesley, Boston (1994).

[5] L. E. Ballentine, *Quantum Mechanics*, World Scientific, Singapore (1998).

[6] A. Peres, *Quantum Theory: Concepts and Methods*, Springer (2006).

[7] A. Einstein, B. Podolsky and N. Rosen, Phys. Rev. 47, 777 (1935).

[8] E. Schrödinger, Naturwissenschaften 23, 807 (1935).

[9] L. Gurvits, quant-ph/0303055 (2003).

[10] R. Horodecki *et al.*, eprint, quant-ph/0702225 (2007).

[11] R. F. Werner, Phys. Rev. A 40, 4277 (1989).

[12] M. Horodecki, P. Horodecki and R. Horodecki, Phys. Lett. A 223, 1 (1996).

[13] A. Peres, Phys. Rev. Lett. 76, 1413 (1997).

[14] C. H. Bennett *et al.*, Phys.Rev.A**59**, 1070 (1999) and D. P. DiVincenzo, D. W. Leung and B. M. Terhal, IEEE Trans. Info. Theory **48**, 580 (2002). See also A. SaiToh, R. Rahimi and M. Nakahara, e-print quantph/0703133.

[15] C. H. Bennett, D. P. DiVincenzo, J. A. Smolin and W. K. Wootters, Phys. Rev. A 54, 3824 (1996). C. Bennett, G. Brassard, C. Crepeau, R. Jozsa, A. Peres and W. K. Wootters, Phys.

[16] G. Vidal, Phys. Rev. Lett. 91, 147902 (2003).

[17] C. H. Bennett, D. P. DiVincenzo, J. A. Smolin and W. K. Wootters, Phys. Rev. A 54, 3824 (1996).

[18] M. Horodecki, Quant. Inf. Comp. 1, No 1, 3-26 (2001).

[19] P. Hayden, M. Horodecki and B. M. Terhal, J. Phys. A, 34(35), 6891-6898 (2001).

[20] A. Barenco, D. Deutsch, A. Ekert and R. Jozsa, Phys. Rev. Lett. 74, 4083 (1995).

[21] J. S. Bell, Physics 1, 194 (1964).

[22] C. H. Bennett, H. J. Bernstein, S. Popescu and B. Schumacher, Phys. Rev. A 53, 2046 (1996). Rev. Lett. 70, 1895 (1993).

[23] M. Nakahara, T. Ohmi, *Quantum Computing: From Linear Algebra to Physical Realizations*, CRC Press Taylor and Francis Group (2008)

[24] M. A. Neilsen and I. L. Chuang, *Quantum Computation and Quantum Information*, Cambridge University Press (2000).

[25] S. M. Barnett and P. M. Radmore, *Methods in Theoretical Quantum Optics* (Oxford: Clarendon Press, 1997).

[26] María G. Eckholt Perotti, *Master Thesis: Matrix Product Formalism*, (Chapter 2) Technische Universität München und am Max-Planck-Institut für Quantenoptik Garching, September 2005

CHAPTER 3

PHYSICAL PRINCIPLES OF QUANTUM DOTS SYSTEMS

In this chapter introduced many concepts and tools referents to quantum structures but especially the quantum dots, because are these items which we research in this dissertation theoretically. However we are interesting in a focus experimental and technological application. The firsts sections 3.1 and 3.2 we review the art state about quantum structures, mainly QDs. The following sections 3.3 and 3.4 present a series of theoretical calculations related to physical processes in atomic systems for quantum structures, especially the modelling of QDs, the concept CQED of the Jaynes-Cummings Model, and so on. In sections 3.5 and 3.6 we study and review the Förster interaction (*Förster Resonance Energy Transfer*), the QD-Hamiltonian and we diagonalized this Hamiltonian. Later in section 3.7 we review the collective systems from the Dicke model and in section 3.8 we introduce the Atomic Coherent States (ACS) and Excited Atomic Coherent states (EACs) as generalized collective states.

3.1 Introduction

Theoretical research on electronic properties of mesoscopic systems in condensed matter has focused primarily on the degrees of freedom of the electron charge, while the degrees of freedom of spin had not yet received the same attention. However, an increase in the number of experiments [1-6] in connection with the spin, show that the spin of the electron offers unique possibilities to find new mechanisms for processing and transmission of information as most remarkable quantum-confined nanostructures usually with long dephasing [2, 3, 4] about microseconds, as well as long distances above 10 microns [2] on which the spin can be transported coherently in phase. Behind the intrinsic interest in the spin-related phenomena, mainly there are two promising areas for future applications: conventional devices based on the spin [1] as well as quantum computer hardware [7]. In conventional computers, the electron can be expected to increase the performance of quantum electronic devices; examples include spin transistors (based on spin currents and spin injection), non-volatile memories, single spin as the ultimate limit of information storage, etc. [1]. On the other hand, none of these devices already exist, and progress experimental and theoretical research are needed to provide guidance and support in the search for feasible implementations. On the other hand the emerging field of quantum computing [8,9] and quantum communication [9, 10] require a radically new approach to the appointment of the necessary hardware. As noted in reference [7, 11] principle, the electron spin is the natural candidate for quantum bit (quantum-bit: qbit) the fundamental unit of quantum information. We [7] observed that qbits spin, when located in quantum confinement structures such as semiconductor quantum dots or atoms or molecules; satisfy all the requirements for a scalable quantum computer. Moreover, such qbits spin are attached to an electron with orbital degrees of freedom, and can be transported along the conducting wires between different subunits in a quantum network [9]. In particular, can be created entangled electron spin (spin-entangled) quantum dots - as pairs mobile Einstein-Podolsky-Rosen (EPR) [9] - and then provide the necessary resources for quantum communication. In both areas related to the spin - conventional computers and quantum computers-needed physical tools and concepts similar and sometimes identical, the immediate goal is to find common ways of controlling the coherent dynamics of electron spin confined in nanostructures. This is the common goal to do research

on electron-spin in nanostructures-spinotronics - a highly attractive area. While advances in our understanding of the physics of spin in many-body systems, we will gain meaning that promises to be useful for future technologies. As first highlighted [11] have been many proposals for solid state implementations of quantum computers along with all other proposals. One very clear reason is that the solid-state physics is a branch of physics more versatile in almost any possible phenomenon in physics can be covered in a properly designed system of condensed matter. A related reason is that the solid-state physics has been closely allied with computer technology and has exhibited great versatility in creating artificial structures and devices. This is being exploited to produce more capable computing devices. Seem natural to expect that this versatility is also extended to the creation of solid state quantum computers, the proposals indicate that indeed this is true, but only time will tell if any of these proposals actually provide a successful path to quantum computer . In the following will review the current status found in our theoretical efforts towards the goal of implementing quantum computation and communication with the electron spin in quantum confined nanostructures. Much of the results presented here have been discussed in several places in the literature, (for an excellent review see for example [25] and references therein), for which we refer for details to reader's interested want.

Quantum dots have become a system of study in a broad range of disciplines in a relatively short time. The incredible progress in synthesis, growth and fabrication quality fed further the advances in optical investigations in physics, biology and chemistry. Particular to quantum physics, quantum dots allow optical studies of confined charge and spin systems and in parallel studies on engineering light–matter interaction and even the suppression of spontaneous emission. We star below with an introduction about quantum structures, defining the concept of different quantum structures based on their degrees of freedom. The following sections develop the atomic theory needed to understand the meaning of the interaction of radiation-matter, ie from the first principles of the interaction of a single mode within the cavity with a single atom (Jaynes-Cummings Model [24]). Also review the basic models of QDs and their similar and difference features with purely atomic systems.

3.2 Quantum Structures

Essentially there are three types of quantum structures studied in the literature, from basic textbooks to books and papers on advanced research, namely: Quantum Wells (QW), Quantum Wires (QWI), and Quantum Dots (QD). Their difference lies mainly in its attributes to confine or trap atomic and subatomic particles (electrons, protons, ions, etc.), i.e. the degrees of freedom that allows each quantum structure. To be more precise, the reduction in dimensionality produced by confining electrons (or holes) to a thin semiconductor layer leads to a dramatic change in their behavior. This principle can be developed by further reducing the dimensionality of the environment electrons from two-dimensional QW to a dimensional one-dimensional QWI and eventually to a zero-dimensional QD. In this context, of course, the dimensionality refers to the degrees of freedom in the electron momentum; in fact, within a quantum wire, the electron is confined across two directions, rather the just the one in a quantum well, and so on, therefore, reducing the degrees of freedom to one. In quantum dot, the electron is confined in all three-dimensions, thus reducing the degrees of freedom to zero. If the number of degrees of freedom is labeled as D_f and the number of directions of confinement is labeled as D_c, then we have clearly,

$$D_f + D_c = 3 \tag{3.1}$$

For all solid state systems. These values are highlighted for the four possibilities shown in Table 3.1. Tradition has determined that the reduced dimensionality systems are labeled by the remaining degrees of freedom in the electron motion, i.e. D_f, rather that the number of directions with confinement D_c.

System	D_c	D_f
Bulk	0	3
Quantum Well (QW)	1	2
Quantum Wire (QWI)	2	1
Quantum Dot (QD)	3	0

Table 3.1 The number of degrees of freedom D_f in the electron motion, together with the extent of the confinement D_c, for the four basic dimensionality systems.

The systems studied in this work are semiconductor quantum dots embedded in an optical microcavity. In this Chapter, we set the stage for the detailed discussions in the main part of the thesis. To facilitate the understanding of the physical system, basic principles of quantum dots and optical transitions in quantum dots shall be introduced in Section 3.2.1.

The aim of this thesis is to achieve faithful storage of the state of an optical microcavity in the nuclear spins of a quantum dot. The interaction between light and nuclear spins is mediated by the hyperfine interaction between the singly charged quantum dot electron and the nuclear spins. Section 3.2.1, introduces basic concepts used in this work to describe the hyperfine interaction between the electron and the nuclear spin ensemble. In the present work, high polarization of the nuclear spins is assumed. Thus, state of the art techniques for polarizing nuclear spins in quantum dots shall be discussed. Next, assuming high polarization of the nuclei, an approximation enabling the description of collective spin operators in terms of bosonic operators will be reviewed.

The main objective of quantum electrodynamics (QED) is to describe the interaction between light and matter; indeed it is regarded as one of the (if not the) most precise theories of physics in its agreement with experimental results. Despite its exceptional explanatory power, QED still has unexplored areas; one of these concerns systems with many particles – a rich field of research even in

classical mechanics. For example, the subtle limit between microscopic (quantum) and macroscopic (classical) systems is a fundamental problem in many-body quantum mechanics, yet to be fully understood. One of the main difficulties in dealing with many-body problems in quantum mechanics is computational. For a number N of two level atoms, $2N$ states are needed to fully describe the state of the system, and one must seek approximation methods. In the quantum optics context the main tool to deal with macroscopic problems is the quantum-to-classical correspondence, which maps a discrete many-body system onto a description in terms of a continuous probability distribution, generating partial differential equations to be solved or simulated.

3.2.1 Quantum Dots characteristics: from the growth to energy levels

The quantum heterostructures has been provided in the progress of the so called material science that have allowed its growth to exhibit inhomogeneities at atomic and subatomic scales that alter the spectrum of excitons into these materials [25]. As mentioned above the quantum dot (QD) heterostructures are designed to provide three-dimensional spatial confinement for excitons (electron-hole pairs). In QDs yields a discrete energy spectrum similar to that of atoms, so it is no coincidence that they refer to as artificial atoms. A series of quantum confined systems for physical applications that display a discrete energy spectrum, for example there exist fluctuations in the QDs interface formed in gallium arsenide/ aluminum gallium arsenide (GaAs/ AlGaAs) barrier boundary in quantum well, core-shell cadmium selenide/zinc sulfide nanocrystals (CdSe/ZnS) formed by both methods and colloidal QDs grown by metal organic vapor phase epitaxy (MOVPE), electrically defined QDs through gate electrodes patterned on the two-dimensional electron gas giving precise control over the local electrostatic potential and self-assembled QDs grown by molecular beam epitaxy (MBE).

The process of epitaxial growth is where a new crystal is grown over a host crystal surface via layer-by-layer atomic deposition [12]. These techniques are capable of depositing high quality semiconductors with a sudden change in material composition having monolayer (~ 3 Å) accuracy. The formation of InAs/GaAs QDs is a natural process and is the manifestation of a strain-driven phase transition that occurs when combining two materials of different lattice constants during one material growth cycle. All materials have its own lattice constant and this commonly leads to formation of strain on two layers constituting

an abrupt interface. Figure 3.1(a) illustrates the two typical cases of strain release: a monolayer-thick material embraces a lattice constant dictated by the host material or a sufficiently thick material recovers its own lattice constant resulting in strain release via dislocations and defects at the interface. The formation occurs exactly during the transitional period linking the two regimes of strain release. If the lattice constants are significantly different (e.g. 7% mismatch between l_a and l_b, as is the case for GaAs and InAs lattices), the epitaxial growth of InAs with the GaAs lattice cannot be sustained for more than two monolayers of growth. At one point, the newly formed layer goes through a phase transition forming miniature islands, very much like mercury droplets do on a smooth flat surface. Further growth with the same material as the handle wafer, in this case GaAs, caps the QDs and protects them from the surrounding environment. After growth, the height of the QDs is typically 4–5 nm, as determined by cross-sectional scanning tunnelling microscopy image of Figure 3.1(b) [13]. It should be noted that, although the self-assembled QDs exhibit pristine optical properties, the in-plane QD distribution is chaotic and great efforts are still made today in this field in order to achieve better control over the island size distribution and location of nucleation.

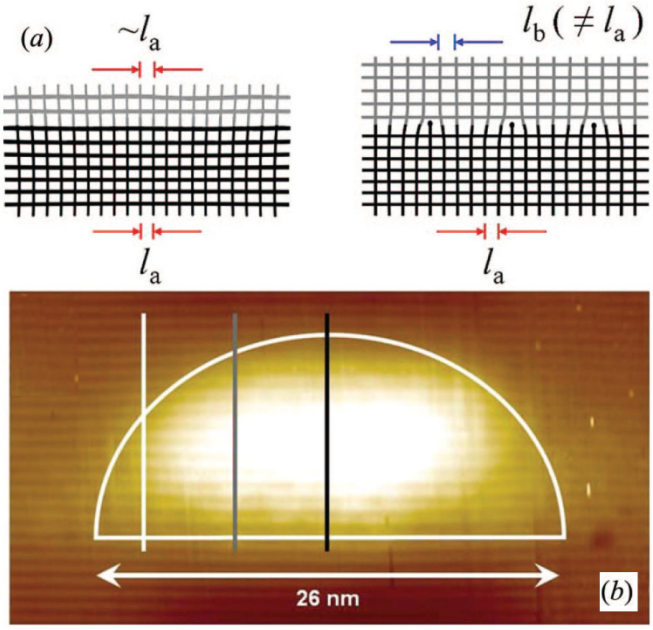

Figure 3.1 (a) An illustration of lattice constant mismatch for two materials grown by MBE for strained thin layers and dislocated thick layers. (b) Cross-sectional scanning tunnelling microscopy of a self-assembled InAs QD grown by MBE [13].

In the case of MBE growth process results in strong three-dimensional carrier confinement for electrons in QDs resulting in quantization of energy states. Nevertheless, QDs are composed of around 105 atoms, and thus form a mesoscopic system with arbitrary shape and composition which differ from QD to QD. The distribution in shape and composition combined with the strain profile experienced by the QD all influence the single particle QD energy levels in the form of inhomogeneous broadening. In addition to material properties, if multiple charges are confined in the QD the Coulomb interaction between the quantum confined carriers has to be taken into account when calculating the multiparticle energy levels. All the previous complications make an analytical determination of QD properties practically impossible and modelling typically relies on perturbative or numerical methods. Even with all these complications it is striking that the roughly 10^5 InAs atoms in the GaAs matrix conspire to exhibit a discrete atomic-like energy spectrum. The QDs of InAs/GaAs are semiconductors in bulk (three-dimensional) form. Therefore, to solve for the energy levels of QDs, it is natural to begin from the bulk material properties and determine the consequences of reducing the system's dimensionality. For bulk semiconductor band structures is necessary to make a phenomenological approach satisfactory enough to resort to a perturbative $\vec{k}\bullet\vec{p}$ model. In $\vec{k}\bullet\vec{p}$ single-particle wavefunctions and energy eigenvalues are assumed to be known at $\vec{k}=0$ and the band dispersion is obtained in the small $\vec{k}$ approximation around the Γ-point [14]. In order to QDs can also be applied perturbative methods because the $\vec{k}$-vector distribution of confined charges is concentrated around $\vec{k}=0$. In figure 3.2 is showed a schematic of the band structure of bulk GaAs with relevant parameter values at room temperature. The band structure of InAs looks essentially identical, but, the values of the indicated parameters differ significantly from GaAs. Excitation of an electron across the bandgap leaves an empty electronic state in the otherwise electron filled valence band. These holes can equally be treated as positively charged particles with modified mass and g-factor. The lowest conduction band has to a very good approximation parabolic dispersion around the Γ-point, as indicated by the red curve in Figure 3.2. The wavefunctions for this band have s-wave character sustaining a twofold spin-degeneracy with $\left[S\|S_z\right]=\left[1/2\|\pm 1/2\right]$. The valence band wavefunctions have p-wave character that would normally sustain a six-fold spin-degeneracy forming a $\left[3/2\|\pm 3/2,\pm 1/2\right]$ quadruplet and $\left[1/2\|\pm 1/2\right]$ doublet. However, spin orbit coupling in these semiconductors causes the $\left[1/2\|\pm 1/2\right]$

doublet to be separated in energy forming what is referred to as the split-off band (Figure). Further, upon including the influence of other bands, even the fourfold degeneracy of the $\left[3/2\|\pm 3/2,\pm 1/2\right]$ states is lifted for $\vec{k}\neq 0$ forming the heavy hole and the light-hole bands with near-parabolic negative curvature dispersion as seen in Figure 3.2. When the dimensionality of the system is reduced such that the effective Bohr radius becomes comparable to the physical extent of the confining material, quantum confinement strongly influences the density of states, band dispersion and degeneracies. In the case of QDs, the dimensionality is zero resulting in motional confinement along all three directions. Therefore, a set of discrete energy levels arise with level spacing's determined by the, not necessarily equal, confinement strength along each direction. In fact, due to their particular lens-like topology (see Figure 3.1(b)), the QDs considered here display strongest motional confinement along the growth (z) axis. Therefore, the main features of the energy levels of these QDs can be seen by simply considering a strong confinement along the z direction with a two-dimensional quasi-parabolic confinement in the two remaining directions. A generally accepted approach to quantifying the QD energy levels and the corresponding wavefunctions relies on pseudopotential theory [15, 16].

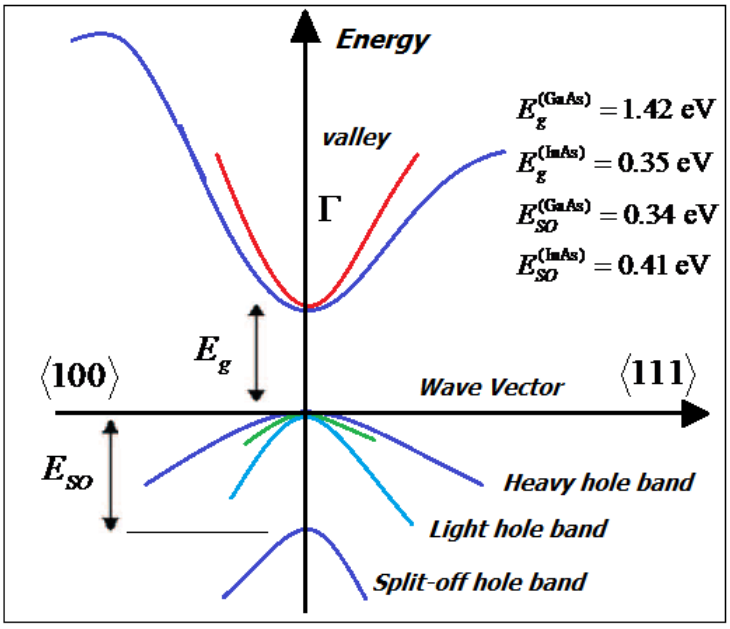

Figure 3.2 A simplified band structure scheme for III–V semiconductors such as GaAs and InAs with the typically accepted values for key energy scales.

From the optics point of the view an important trait of the quantum confinement is that despite the energy spectrum of the QD is modified when compared to the bulk semiconductor, the electrons and holes that become trapped in the QD inherit the spin structure of the bulk semiconductor. This determines the optical (polarization) selection rules for transitions between QD electron and hole states mediated by a photon. Explicitly, focusing on the conduction band and heavy hole valence band, we can specify the QD electron and hole spin. The QD levels derived from the conduction band levels sustain their twofold spin degeneracy, while the QD levels derived from the valence band states display a confinement-induced splitting into heavy-hole and light-hole doublets. We qualitatively established the energy levels of electrons and holes confined in all three dimensions in semiconductor QDs. We now identify the energy scales of common InAs/GaAs QD charge configurations that are probed optically. The simplest charge configuration linked to an optical emission is the neutral exciton X^0 (see Figure 3.3), i.e. a single electron–hole pair occupying the lowest discretised energy levels within the original conduction and valence bands. The electron in the conduction band can have spin quantum number $\left[S \| S_z\right] = \left[1/2 \| \pm 1/2\right]$.The heavy hole in the valence band has spin $\left[J \| J_z\right] = \left[3/2 \| \pm 3/2\right]$. Using the angular momentum theory, specifically addition of angular momentum, a single electron–hole pair in the QD can end up in any one of four spin-state combinations. The total angular momentum of these combinations being $\Delta J = \pm 1$ or $\Delta J = \pm 2$, but each doublet is degenerate. The angular momentum must be conserved into of an optical transition, and this is evidence in the polarization of the emitted photons. Recombination via a single-photon emission process can only occur for the $\Delta J = \pm 1$ exciton doublet, since single photons carry angular momentum ± 1.

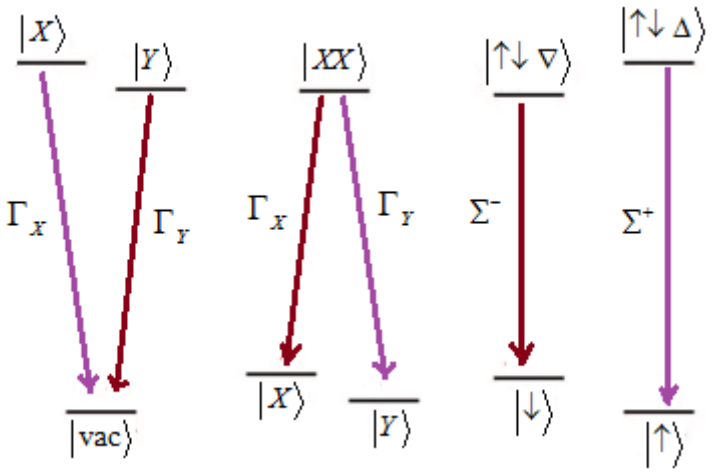

Figure3.3. Neutral exciton (X^0), biexciton (XX) transitions under excitonic level splitting and negatively charged trion (X^{1-}) transitions under magnetic field along the growth axis for a typical quantum dot. The wavy arrows indicate photon mediated transitions between the states. For the negatively charged trion (right illustration) the up (down) arrow represents the electron spin projection of +1/2 (-1/2) along the growth direction and the up (down) triangle is the hole projection of +3/2 (-3/2). The ground state of the trion transition is a single electron with its spin projection up or down. Each transition is decorated with a symbol indicating the emitted photons polarization $-\Gamma_X$ (Γ_Y) for horizontal (vertical) and Σ^+ (Σ^-) for right (left) circularly polarized photons. The direction of linear polarization (horizontal and vertical) is defined with respect to the major and minor axis of the elliptical QD base (as opposed to circular) due to strain-induced anisotropy of the dot geometry.

We can see the angular momentum conservation in the polarization emitted photon. Specifically, photons carrying +1 (-1) angular momentum are left (right) hand circularly polarized and are denoted with the symbol Σ^+ (Σ^-). The exciton doublet $\Delta J = \pm 1$ that is linked to photon emission is called *bright*, while the remaining optically inactive doublet is called *dark* (the $\Delta J = \pm 2$ excitons). The polarization selection rules also constrain the set of excitons that may be created optically to the $\Delta J = \pm 1$ doublet. Of course, in the practice is not simple! The previously mentioned shape non-uniformity and strain act to coherently mix the bright $\Delta J = \pm 1$ exciton doublet via the electron–hole exchange interaction. This interaction couples the spins of the electron and hole confined in the QD and depends sensitively on the structural symmetry of the QD. The electron–hole exchange serves to both break the $\Delta J = \pm 1$ exciton doublet's degeneracy and alter the polarization of the emitted photons from circular to linear, indicated by π_X / π_Y in Figure 3.3. Therefore the new polarization basis, which is defined along the major and minor axis of the elliptical QD base, led to the phrase X – Y splitting to denote this effect. Because to exchange interaction, an electron–hole pair once created in $\Delta J = +1$ state will precess coherently between $\Delta J = \pm 1$ spin configurations. This are diagonalized Hamiltonian after including this interaction leads to new eigenstates with the degeneracy of their energies lifted in proportion

to the interaction strength. Typical energy scale for the $\Delta J = \pm 1$ exciton doublet fine structure splitting is $\sim 10\ \mu\mathrm{meV}$ for self-assembled InAs/GaAs QDs. The interested in a more complete discussion of the exchange interaction between electrons and holes we refer them to the reference [17]. Another QD charge complex that we discuss is two electrons and one hole. We call this singly charged excitonic QD excited state a trion, see Figure 3.3 (right diagram), and label it as X^{1-}. In forming the trion complex, Pauli's principle forces the electron pair to form a spin singlet state where the closest triplet state has energy much higher than typical ambient temperature (4 K). Since the resident hole can have either spin up or spin down, each QD has two trionic transitions that are energetically degenerate. Due to Coulomb interactions in this three-body problem, the recombination energy is modified with respect to the original neutral X^0 excitonic transition energy (ignoring fine structure) by $\Delta E = E_{ee} - E_{eh}$ the direct energy due to electron–electron and electron–hole Coulomb interaction [18] as dictated by the wavefunctions via the form

$$E_{mn} \propto \frac{(-1)^{(1-\delta_{m,n})} e^2}{4\pi\varepsilon_0\varepsilon_r} \iint dr dr' \frac{|\psi_m(r)||\psi_n(r')|}{|r - r'|} \tag{3.2}$$

In the InAs/GaAs QDs considered here the result is a total shift of $\Delta E = 6\ \mathrm{meV}$ to lower energy for the trionic transitions. In contrast to the neutral exciton where the electron–hole spin exchange breaks the twofold degeneracy, the electronic spin singlet is immune to electron–hole exchange and the two trion states remain degenerate. In this case, the polarization of the emitted photon is in the circular basis and using the right hand rule is determined the direction of the resident hole spin. Conceptually this situation is similar when there are two electron–hole pairs present in the QD referred to as the biexciton (XX) shown in Figure 3.3 (middle diagram). The shift in the transition energy for a biexcitonic transition can once more be determined by the energy difference between the initial and final states, $\Delta E = 2E_{ee} + 2E_{hh} - E_{eh}$, and is on the order of $2\ \mathrm{meV}$ for InAs QDs. Ultimately, every charge combination results in a distinct spectral signature due to the Coulomb interaction, and for more detailed explanation the reader can see reference [18] of this approach for direct and exchange type interactions.

We must note that here the energy scales for each mechanism considered are well defined. The optical transitions occur at eV range while direct Coulomb interactions within a QD are at tens of meV. The fine structure such as X–Y splitting is on the order of tens of $\mu\mathrm{eV}$, which is still much larger than the characteristic transition linewidth of $1\ \mu\mathrm{eV}$. While each quantum dot can have enormous different emission energies due to inhomogeneity characteristics in the quantum dot ensemble, the relative energy shifts are conveniently rather robust. With an insight of common QD charge complexes, we can begin to address how the tools of Quantum Optics and specially Cavity Quantum Electrodynamics reveal physical properties of the QD systems.

3.3 QDs with Cavity Quantum Electrodynamics

The dynamics of an optical and/or photonic emitter changes drastically when it is placed in a cavity. The cavity alters the density of states of optical modes, and therefore increases or inhibits interactions with the emitter. The effect was first put to use by Purcell in nuclear magnetic resonance for the practical purpose of thermalizing spins at radio frequencies, by bringing down their relaxation time from $\approx 10^{-21}$s to a few minutes [19]. Kleppner applied the same idea in the opposite way, to increase the relaxation time of an excited atom, i.e., to inhibit its spontaneous emission (SE) [20]. The emitter, that in the case of Purcell was sought to be resonant with the cavity mode to increase the photon density of states with respect to the vacuum, was in the case of Kleppner put out of resonance, namely in a photonic gap, where the photon density of states is smaller than in vacuum. This tuning of the relaxation time of an emitter placed in a cavity, now known as the Purcell effect, has many potential technological applications, one of the most compelling being the decrease of the lasing threshold. The effect, which had first been actively looked for with atoms in cavities [21], was therefore also intensively (and more recently) pursued in the solid state, more prone for massive technological implementations. Semiconductor heterostructures are the state of the art arena for this purpose. They allow to engineer, with an ever rising control, the solid state counterpart of the atomic system to match or isolate their excitation spectra and thus control their behaviour. Typical examples are quantum dots (QDs) placed in cavities made in micropillars, microdisks or photonic crystals, where Purcell inhibition has been distinctly demonstrated [22, 23]. In the description of the Purcell effect, the possible reabsorption of the photon by the emitter is so weak that it can be neglected. It is responsible for the energy shift known as the Lamb shift that, in

quantum electrodynamics, is interpreted as the perturbative influence of virtual photons emitted and re-absorbed by the emitter. In the case of inhibition of the spontaneous emission, this shift is indeed orders of magnitude smaller than the radiative broadening. In the case where emission is enhanced, and the linewidth narrowed, the probability of reabsorption of a photon by the emitter becomes closer to that of escaping the cavity, until the perturbative—so-called weak-coupling (WC)—regime breaks down and instead *strong coupling* (*SC*) takes place. In this case, photons emitted are then reflected by the mirrors and there is a higher probability for their reabsorption by the atom than for their leaking out of the cavity. A whole sequence of absorptions and emissions can therefore take place, known as *Rabi oscillations* (already studied at section 2.2.3). This regime is of greater interest, as it gives rise to new quantum states of the light-matter coupled system, usually referred to as *dressed states* in atomic physics and as *polaritons* in solid-state physics. Experimentally, SC is more difficult to reach, as it requires a fine control of the quantum coupling between the *bare* modes and in particular to reduce as much as possible all the sources of dissipation. Theoretically, it is better dealt with by first getting rid of the dissipation, and starting with the strong-coupling Hamiltonian. Throughout this work we will consider systems of one or many atoms inter-acting with a single cavity mode. In this chapter we derive the theoretical model for such a system and consider the case of one two-level atom as a representative example. The coupling between the atomic transition and the quantized cavity field is described by the Jaynes-Cummings model introduced in section 3.3.1.

3.3.1 Jaynes-Cummings model

The interaction between a single cavity mode and a two-level atom is described by the Jaynes-Cummings model [24]. In the following we will introduce it in a similar way as in [25]. We denote the frequency of the transition between the ground state $|g\rangle = |\downarrow\rangle$ and the excited state $|e\rangle = |\uparrow\rangle$ of the atom by $\omega_a = \omega_2 - \omega_1$. This transition couples to a cavity mode with frequency ω_c. The complete time-independent Hamiltonian of the system is

$$H = \frac{\hbar}{2}(\omega_2 + \omega_1)\mathrm{I} + \frac{\hbar}{2}(\omega_2 - \omega_1)\sigma_z + \hbar\omega\left(a^\dagger a + 1\right) - i\hbar g\left(\sigma_+ - \sigma_-\right)\left(a - a^\dagger\right) \qquad (3.3)$$

Where $\hbar\omega_1$ and $\hbar\omega_2$ are the energies the uncoupled states $|g\rangle$ and $|e\rangle$, respectively, and ω is the frequency of the field mode. With the atomic operators $\sigma_+ = |e\rangle\langle g|$, $\sigma_- = |g\rangle\langle e|$ and $\sigma_z = |e\rangle\langle e| - |g\rangle\langle g|$. $a^\dagger$ and a are the creation and annihilation operator of the cavity mode. The photon operator is a Bose annihilation operator, satisfying the usual commutation rule $\left[a, a^\dagger\right] = 1$. Applying the unitary transformation, with $\Delta = \omega_2 - \omega_1 - \omega = \omega_a - \omega$ and $\delta = \Delta/2$. We find the Hamiltonian in the interaction picture is

$$H = \frac{\Delta}{2}\sigma_z - ig\left(\sigma_+ e^{i\omega t} - \sigma_- e^{-i\omega t}\right)\left(ae^{-i\omega t} - a^\dagger e^{i\omega t}\right) \tag{3.4}$$

Making the rotanting-wave approximation removes the explicit time dependence and gives the Jaynes-Cummings Hamiltonian ($\hbar$ is taken as 1 along the thesis),

$$H_{JC} = \frac{\Delta}{2}\sigma_z - ig\left(\sigma_+ a - \sigma_- a^\dagger\right) \tag{3.5}$$

Where introduce the detuning $\Delta = \omega_a - \omega$. The omitted interaction terms $\sigma_- a$ and $\sigma_+ a^\dagger$ and correspond to downward transition in the atom accompanied by absorption of a photon and to an upward transition with the emission of a photon. These processes do not preserve the total number of quanta and are strongly suppressed. This is the so-called rotating-wave approximation. We also neglected the coupling of the system to the environment. This is justified if the spontaneous emission rate of the atom γ and the cavity decay rate κ obey:

$$\begin{aligned} \gamma &\ll g\sqrt{\bar{n}} \\ \kappa &\ll \frac{g}{\sqrt{\bar{n}}} \end{aligned} \tag{3.6}$$

With $\bar{n}$ being the average photon number in the cavity. We consider an initial state of the system in which atom is in the lower state $|g\rangle = |\downarrow\rangle$, while the field is in a

superposition of photon number states. Thus we will now calculate the time evolution of the system for an initial state

$$\left|\psi_I(0)\right\rangle = \sum_{n=0}^{\infty} a_n \left|g\right\rangle \otimes \left|n\right\rangle = \sum_{n=0}^{\infty} a_n \left|g,n\right\rangle \tag{3.7}$$

Where $|g\rangle\otimes|n\rangle = |g\rangle|n\rangle$ is the product of states with $|g\rangle$ and *n* photons in the cavity mode. H_{JC} is block-diagonal in the basis $\{|e,n\rangle,|g,n+1\rangle\}$, with *n* being the number of photons in the cavity. In other words, the total number of quanta is conserved and $|e,n\rangle$ only couples to $|g,n+1\rangle$ while $|g,0\rangle$ are uncoupled. So at subsequent times, the state evolves into a superposition

$$\left|\psi_I(t)\right\rangle = \sum_{n=0}^{\infty}\left[c_{g,n}(t)\left|g\right\rangle\left|n\right\rangle + c_{e,n}(t)\left|e\right\rangle\left|n\right\rangle\right] \tag{3.8}$$

In general, this state is entangled in the sense that it cannot be expressed as a product of an atom state and a field state. The solution for the dynamics of this model is simplified by the fact that the operator

$$\hat{N} = \hat{a}^{\dagger}\hat{a} + \hat{\sigma}_{+}\hat{\sigma}_{-} \tag{3.9}$$

Representing the total number of quanta, commutes with the Hamiltonian (3.4) and hence that the number of quanta is conserved. Each coupled pair of states evolves as a distinct two-state system. Substituting (3.7) into the Schrödinger equation (2.1), with the Hamiltonian (3.4), we obtain the *equations of motion*

$$\begin{aligned}
\frac{d}{dt}c_{g,n}(t) = \dot{c}_{g,n}(t) &= \frac{i\Delta}{2}c_{g,n}(t) + g\sqrt{n}c_{e,n-1}(t) \\
\frac{d}{dt}c_{e,n-1}(t) = \dot{c}_{e,n-1}(t) &= -\frac{i\Delta}{2}c_{e,n-1}(t) - g\sqrt{n}c_{g,n}(t)
\end{aligned} \tag{3.10}$$

for the probability amplitudes with initial conditions $c_{g,n}(t=0)=a_n$ and $c_{e,n-1}(t=0)=0$. The solution of Eqs. (3.9) is given by

$$\begin{aligned} c_{g,n}(t) &= a_n\left[\cos\left(\Omega_R\frac{t}{2}\right)+i\frac{\Delta}{\Omega_R}\sin\left(\Omega_R\frac{t}{2}\right)\right] \\ c_{e,n-1}(t) &= -a_n\frac{2g\sqrt{n}}{\Omega_R}\sin\left(\Omega_R\frac{t}{2}\right) \end{aligned} \tag{3.11}$$

Where $\Omega_R=\sqrt{\Delta^2+4g^2n}$ is the photon-number dependent Rabi frequency. For the resonant case, we set $\Delta=0$ and obtain for the probability to find the system in the atomic ground state

$$P_g(t)=\sum_{n=0}^{\infty}\left|c_{g,n}(t)\right|^2=\frac{1}{2}\sum_{n=0}^{\infty}\left|a_n\right|^2\left(1+\cos\left[2g\sqrt{n}t\right]\right) \tag{3.12}$$

As an example, we consider the field to be initially in a coherent state, the mean photon number $\bar{n}$ for which

$$\left|a_n\right|^2=\frac{\bar{n}^n e^{-\bar{n}}}{n!} \tag{3.13}$$

and plot $P_g(t)$ in Fig. 3.4 for $\bar{n}=10$.

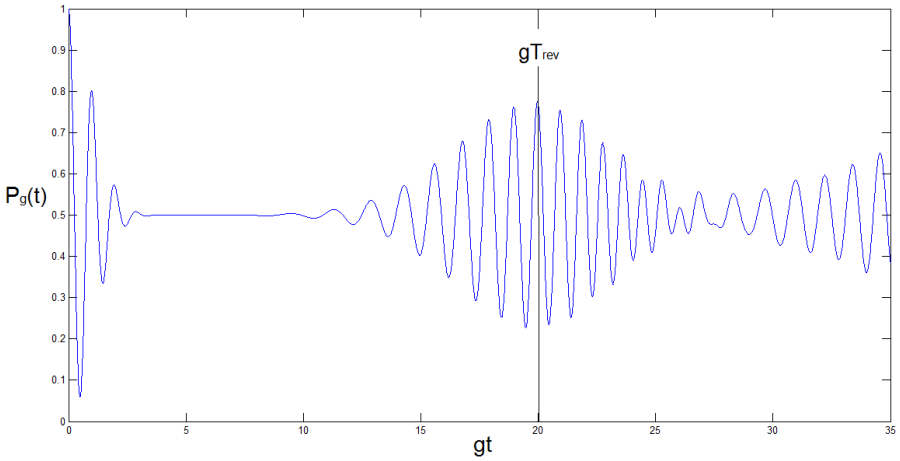

Figure 3.4: The plot shows the probability $P_g(t)$ to find the atom in its ground state $|g\rangle$. Initially we assumed a coherent state with mean photon number $\bar{n}=10$. One observes Rabi oscillations at a frequency of approximately $2g\sqrt{\bar{n}}$ under an envelope that periodically collapses and revives. The first revival appears at approximately $T_{rev} \simeq 2\pi\sqrt{\bar{n}}\,/\,g$.

It oscillates at a frequency approximately equal to $2g\sqrt{\bar{n}}$ under an envelope that periodically collapses and revives. The reason for this behavior is the interference between the individual oscillatory terms with different incommensurate frequencies $2g\sqrt{n}$ in eq. (3.11). So the collapse is a consequence of the initial spread of different photon numbers in the field. The peak of the revival appears at time T_{rev} when a significant number of oscillating terms are in phase. For the first revival we find

$$2g\sqrt{\bar{n}}T_{rev} - 2g\sqrt{\bar{n}-1}T_{rev} = 2\pi \tag{3.14}$$

With approximate solution

$$T_{rev} \simeq 2\pi\sqrt{\bar{n}}\,/\,g \tag{3.15}$$

Also other initial field states lead to the phenomenon of collapses and revivals. Their form depends on the initial probability distribution of the photon numbers.

A different behavior of the system arises if the cavity mode is initially prepared in a Fock state. Then the initial state is

$$|\psi_I(0)\rangle = |g,n\rangle \tag{3.16}$$

It couples only to $|e,n-1\rangle$ and the system remains in the corresponding subspace. The time evolution is then governed by the Hamiltonian

$$H_n = -\frac{\Delta}{2}\sigma_z - ig\sqrt{n}\left(|e,n-1\rangle\langle g,n| - |g,n\rangle\langle e,n-1|\right) \tag{3.17}$$

which is diagonal in the basis of the so-called dressed states

$$\begin{pmatrix} |+,n\rangle \\ |-,n\rangle \end{pmatrix} = \begin{pmatrix} \sin\theta_n & \cos\theta_n \\ \cos\theta_n & -\sin\theta_n \end{pmatrix} \begin{pmatrix} |g,n\rangle \\ |e,n-1\rangle \end{pmatrix} \tag{3.18}$$

Here $\tan(2\theta_n) = -2g\sqrt{n}/\Delta$ and $0 \le 2\theta_n \le 2\pi$. Together with $|g,0\rangle$ the dressed states form the eigen subspaces of H_I. The corresponding eigenvalues are

$$\begin{aligned} E_0 &= \Delta/2 \\ E_{\pm}^n &= \pm\sqrt{\Delta^2/4 + g^2 n} \end{aligned} \tag{3.19}$$

This result shows that the permanent exchange of excitation between the atom and the cavity mode due to the Jaynes-Cummings interaction leads to a shift of the original eigenvalues of the system. In the resonant case ($\Delta = 0$) the original eigen frequencies are shifted by $\pm\sqrt{n}g$. For *n* = 1 one speaks of "vacuum Rabi oscillations" and in the Schrödinger picture for *n* = 1 the original resonance frequency $\omega_a = \omega$ is then shifted by $\pm g$. The effect can be verified experimentally by measuring the transmission spectrum of the cavity and identifying the shifted resonance peaks. Since dissipation (due to atom and cavity decay) suppresses the effect, observing it, as reported in [26], is a clear evidence for the strong-coupling regime ($g \gg \kappa, \gamma$).

3.4 Modeling Quantum Dots Systems

Many parameters, characteristics and behavior of the QDs were discovered experimentally but there are some classic and semiclassic models based on local perturbation of the electric field, the effective mass approximation, variational calculus approaches to configuration interaction techniques and Monte Carlo methods, among others. For an excellent review of these methods, see reference [27, 28, 29]. However, these methods are only applicable to a quantum dot containing a small number of charge carriers, as electrons or excitons either in the presence of magnetic field or without it. On the other hand, there are studies using quantum electrodynamics cavities (CQED), it have been developed only for one, two and three QDs [30-32]. So is the goal and purpose of this dissertation investigate the behavior of a system of QDs, each containing an exciton, in the presence of an electric field and a quantum singled-mode QD to through models completely quantum into pictures as Schrödinger, Heisenberg, and Dirac (Interaction) pictures. In the previous sections has been revised that a quantum dot is the general term ascribed to a small semiconductor region that can trap a few electrons and holes. The dimensions of quantum dots can vary between just a few nanometers and a few microns and it can be defined artificially with electrodes or through a growth technique such as self-assembly. The term "*quantum*" in quantum dot arises from the discrete energy levels that electrons and holes can occupy. The discretization can arise from the Coulombic interaction among the small number of electrons and holes within the dot or from the physical confinement of these particles in a small space. The Coulombic interaction varies as $1/r$ and dominates for larger dots while the quantum confinement varies as a $1/r^2$ and dominates for smaller dots, such as the ones considered in this thesis. There are many effects to consider which affect the energy state of bound exciton within a dot. An overview of the energy perturbations on a quantum dot-bound exciton is shown in Figure 3.5. Each of these effects is discussed below and the associated parameters are defined.

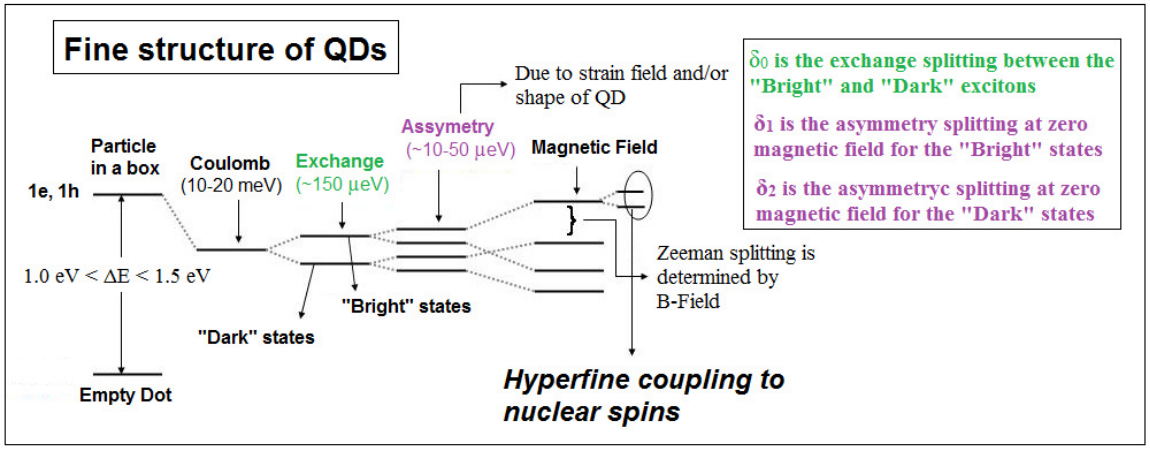

Figure 3.5. This picture shows the various effects on the fine structure of the excitons energy levels. The exciton itself is created by exciting an electron from the valence band into the conduction band. This energy difference, or the band-gap, is 1.52eV for GaAs and between 1.3 and 1.44eV for InAs. The first effect diagrammed is the quantum confinement of a particle in a box. Then, the first correction is electrostatic attraction between the electron and hole which reduces the energy of the lowest occupied excitonic level by $\sim 10-20\ \mathrm{meV}$. An exchange interaction, $\delta_0 \sim 100\ \mu\mathrm{eV}$, splits the excitonic levels into bright and dark excitons. In addition, due to dot asymmetry, these states split further. Finally, the application of magnetic field further moves the levels. Interaction between the trapped electron spin and the nuclear spin can be considered a manifestation of magnetic field, but in the diagram here it is given the label of hyperfine coupling.

3.4.1 Quantum Confinement and Wavefunction Approach

There are different approaches for modeling quantum dots systems, based on different images of the quantum theory (Schrödinger, Heisenberg, and Dirac). In this dissertation, our main contribution we make in the images of Heisenberg and Dirac. But before continuing it is worth reviewing other approaches in the traditional Schrödinger picture, based on solving wave equation in this image, in order to find the wavefunction of system.

To a first approximation we consider the quantum dot to be an attractive potential where an exciton (or electron-hole pair) can become localized. We can then solve either a particle in a box or a parabolic potential from which discrete energy levels arise. Both approaches have been used to describe the energy levels within a quantum dot. The actual envelope wavefunction can be calculated more precisely if the exact structure of the quantum dot is known [33, 34, 35, 36]. For a single particle (electron or hole) in a semiconductor the wavefunction is not just the envelope wavefunction which gives the distribution of where the electron is localized but also includes a periodic component $u(\vec{r})$, where $e^{i\vec{k}\cdot\vec{r}}u(\vec{r})$ is a Bloch wavefunction. The overall wavefunction of a particle with $\vec{k}=0$ is given by

$$\psi(\vec{r}) = \varphi_i(\vec{r})u_i(\vec{r}) \tag{3.20}$$

There are many approaches to calculate the states of excitons (electron and hole) into quantum dots, in references [37, 38], [39-42] can see different ways to calculate, but it depends on the ultimate goal of each particular system in which to use. The aim here is to provide a simple illustration of how to observe resonant energy transfer between quantum dots experimentally, and how to exploit this inter-dot interaction to perform quantum logic. Therefore, we shall consider the most basic models [37, 38] [43] that can provide us with analytical expressions for the energies of the single particle states and for the dipole-dipole interaction between two dots.

In the effective mass and envelope function approximations [44, 45] the Schrödinger equation for single particles may be written as:

$$H_i(\vec{r})\varphi_i(\vec{r}) = \left[-\frac{\hbar^2}{2m}\nabla\left(\frac{1}{m_i^*}\right)\nabla + V_i(\vec{r}) \right]\varphi_i(\vec{r}) = E_i\varphi_i(\vec{r}) \tag{3.21}$$

where $i = e,h$ for electron or hole, $V_i(\vec{r})$ is the dot confinement potential which accounts for the difference in band-gaps across the heterostructure, and m_i^* is the effective mass of particle i. Here, $\varphi_i(\vec{r})$ is the envelope function part of the total wavefunction $\psi(\vec{r})$, defined in (3.20). The envelope function describes the slowly varying contribution to the change in wave-function amplitude over the dot region and the physical properties of the single particle states can be derived purely from this contribution. $u_i(\vec{r})$ is as mentioned above called the Bloch function and has the periodicity of the atomic lattice. Its consideration is vital when describing the interactions between two or more particles. In the simple analytical model, a separable potential comprising infinite parabolic wells in all three dimensions represents the quantum dot, (With this choice of potential we are able to model both the convenient situation of a spherically symmetric quantum dot, and the more common situation in self-assembled dots of stronger confinement in the growth (*z*) direction than in the *x, y* plane.)

$$V(x,y,z) = \frac{1}{2}c_{i,x}x^2 + \frac{1}{2}c_{i,y}y^2 + \frac{1}{2}c_{i,z}z^2 \tag{3.22}$$

where the frequency $\omega_{i,j} = \sqrt{c_{i,j}/m^*}$ for *j = x, y, z*. Hence, the Schrödinger equation (3.21) is also separable and provides simple product solutions for the electron and hole states. The envelope functions are therefore given by

$$\varphi_i(\vec{r}) = f_{i,x}(x)\, g_{i,y}(y) h_{i,z}(z) \tag{3.23}$$

for the parabolic confinement ($\vec{r} = (x, y, z)$). We now drop the subscript *i* but remember that due to their differing effective masses electrons and holes may take different values for the constants defined throughout this thesis. The solutions to the one-dimensional Schrödinger equation for the potential form (3.22) are given by

$$\xi^n(x) = \left(\frac{1}{n! 2^n d_x \sqrt{\pi}}\right)^{1/2} H_n\left(\frac{x}{d_x}\right) \exp\left(-\frac{x^2}{2d_x^2}\right) \tag{3.24}$$

in the *x*- direction with analogous expressions for *y* and *z*. The constant $n = (0, 1, 2, 3, \ldots)$ labels the quantum state, with energy $E_n = (n + 1/2)\hbar\omega_x$, the H_n are Hermite polynomials, and $d_x = \left(\hbar/\sqrt{m^* c_x}\right)^{1/2} = \left(\hbar/(m^*\omega_x)\right)^{1/2}$. We are only interested in the ground state solutions of each well so our envelope function is given by

$$\varphi(x, y, z) = \left(\frac{1}{d_x d_y d_z \pi^{3/2}}\right)^{1/2} \exp\left(-\frac{x^2}{2d_x^2}\right) \exp\left(-\frac{y^2}{2d_y^2}\right) \exp\left(-\frac{x^2}{2d_z^2}\right) \tag{3.25}$$

with energy $E_0 = 1/2\hbar(\omega_x + \omega_y + \omega_z)$. The choice of constants c_i and hence d_j will be different for changing confinement potentials and particle masses, and so will depend upon the energies of the system under consideration and whether the particle is an electron or hole.

3.4.2 Excitons and Confinement

The excitation of an electron from a valence band state to a conduction band state leaves a hole in the valence band. The electron and hole are oppositely charged and may form a bound state, the exciton, and as stated earlier we consider the absence or presence of a ground state exciton within a dot to form our qubit basis ($|0\rangle$ and $|1\rangle$ respectively). Therefore, for excitons, we must consider an electron-hole pair Hamiltonian

$$H = H_e + H_h - \frac{e^2}{4\pi\varepsilon(r_e - r_h)\left|\vec{r}_e - \vec{r}_h\right|} + E_{\text{gap}} \tag{3.26}$$

Where H_e and H_h are given by (3.21) with the appropriate effective masses and potentials; E_{gap} is the semiconductor band-gap energy, and $\varepsilon(r_e - r_h)$ is the background dielectric constant of the semiconductor. We shall consider the simplest case of $\varepsilon(r_e - r_h) = \varepsilon_0\varepsilon_r$, i.e. the relative permittivity ε_r is independent of $(r_e - r_h)$. The intra-dot energy shift due to the Coulomb term $H_{eh} = e^2 / 4\pi\varepsilon_0\varepsilon_r \left|\vec{r}_e - \vec{r}_h\right|$ is a small contribution to the total energy and we treat it as a first-order perturbation. We construct an antisymmetric wavefunction representing a single exciton state given by

$$\Psi_I = A\left[\psi'_n(\vec{r}_1, \sigma_1), \psi_m(\vec{r}_2, \sigma_2)\right] \tag{3.27}$$

Where $\vec{r}$ and σ are position (from the centre of the dot) and spin variables respectively, *n* and *m* label the quantum states, and *A* denotes overall antisymmetry. Here, one electron $\psi'_n(\vec{r}_1, \sigma_1)$ has been promoted from the valence band into a conduction band state whilst $\psi_m(\vec{r}_2, \sigma_2)$ represents a state in the valence band. Taking the Coulomb matrix element between the initial state Ψ_I above and an identical state Ψ_F (in effect coupling an electron and hole via the Coulomb operator) leads to two terms [46, 47], the direct term

$$M_{IF}^{\text{Direct}} = \frac{e^2}{4\pi\varepsilon_0\varepsilon_r}\iint \psi'^{*}_{n}(\vec{r}_1)\psi'_{n}(\vec{r}_1)\frac{\psi'^{*}_{m}(\vec{r}_2)\psi'_{m}(\vec{r}_2)}{\left|\vec{r}_1-\vec{r}_2\right|}d\vec{r}_1 d\vec{r}_2 \qquad (3.28)$$

And the exchange term

$$M_{IF}^{\text{Exch}} = \pm\frac{e^2}{4\pi\varepsilon_0\varepsilon_r}\iint \psi'^{*}_{n}(\vec{r}_1)\psi_{m}(\vec{r}_1)\frac{\psi'_{n}(\vec{r}_2)\psi^{*}_{m}(\vec{r}_2)}{\left|\vec{r}_1-\vec{r}_2\right|}d\vec{r}_1 d\vec{r}_2 \qquad (3.29)$$

The sign of the exchange term is determined by the symmetry of the spin state of the two particles; triplet spin states give positive exchange elements whereas singlet spin states give negative values. We shall now show how to calculate the direct electron-hole Coulomb matrix element on a single dot where *n* and *m* are both taken as ground states. The exchange interaction is much smaller [46] and we shall not consider it here. If we consider identical potential wells in all three directions then we can use the spherical symmetry of the system to derive an analytical expression for the direct Coulomb matrix element which we call M_{eh}. For identical wells in all three dimensions $\left(d = d_x = d_y = d_z\right)$, (3.25) may be written in spherical polar coordinates as

$$\varphi(r) = \left(\frac{1}{d\sqrt{\pi}}\right)^{3/2}\exp\left(-\frac{r^2}{2d^2}\right) \qquad (3.30)$$

Substituting into equation (3.28) leads to

$$M_{eh} = \frac{e^2}{4\pi\varepsilon_0\varepsilon_r}\left(\frac{1}{d_e\sqrt{\pi}}\right)^3\left(\frac{1}{d_h\sqrt{\pi}}\right)^3\iint\exp\left(-\frac{r_1^2}{d_e^2}\right)\exp\left(-\frac{r_2^2}{d_h^2}\right)\frac{1}{\left|\vec{r}_1-\vec{r}_2\right|}d\vec{r}_1 d\vec{r}_2 \qquad (3.31)$$

Where we have assumed that the contribution of the Bloch functions $u(\vec{r})$ may be neglected. We now express $1/\left|\vec{r}_1-\vec{r}_2\right|$ in terms of Legendre polynomials as [48]

$$\frac{1}{|\vec{r}_1-\vec{r}_2|}=\begin{cases}\dfrac{1}{r_1}\sum_{k=0}^{\infty}\left(\dfrac{r_2}{r_1}\right)^k P_k(\cos\theta), & \text{for } r_1>r_2\\ \dfrac{1}{r_2}\sum_{k=0}^{\infty}\left(\dfrac{r_1}{r_2}\right)^k P_k(\cos\theta), & \text{for } r_1<r_2\end{cases} \tag{3.32}$$

Substituting this into equation (3.31) and integrating over polar angles, leads to

$$\begin{aligned}M_{eh}=\frac{4\pi e^2}{\varepsilon_0\varepsilon_r}\left(\frac{1}{d_e\sqrt{\pi}}\right)^3\left(\frac{1}{d_h\sqrt{\pi}}\right)^3\int_0^{\infty}\exp\left(-\frac{r_1^2}{d_e^2}\right)r_1^2dr_1\\ \times\left[\int_0^{r_1}\frac{1}{r_1}\exp\left(-\frac{r_2^2}{d_h^2}\right)r_2^2dr_2+\int_{r_1}^{\infty}\frac{1}{r_2}\exp\left(-\frac{r_2^2}{d_h^2}\right)r_2^2dr_2\right]\end{aligned} \tag{3.33}$$

where use has been made of the orthogonality relations of Legendre polynomials. The integrations are now simple and give us the following expression for M_{eh},

$$M_{eh}=\frac{1}{2}\frac{e^2}{\pi^{3/2}\varepsilon_0\varepsilon_r}\frac{1}{\sqrt{d_e^2+d_h^2}} \tag{3.34}$$

In a similar manner, we may also approximate the behavior of M_{eh} in the presence of an external electric field. For a constant field applied to the dot, the potential in the field direction (for simplicity says *z*, although the spherical symmetry we assume means all three directions are equivalent) becomes

$$V(z)\mapsto V(z)+qFz \tag{3.35}$$

Where $q = -e$ for conduction band electrons, $q = +e$ for holes, and F is the electric field strength. Substituting this into the Schrödinger equation for the *z*-

component leads us to a new Schrödinger equation that has the same parabolic potential form

$$\left[-\frac{\hbar^2}{2m*}\frac{\partial^2}{\partial^2 z'^2}+\frac{1}{2}c_z z'^2\right]\varphi(z')=E'\varphi(z') \tag{3.36}$$

With

$$\begin{aligned} z'_e &= z - eF/c_{e,z} \quad \text{for electrons} \\ z'_h &= z + eF/c_{h,z} \quad \text{for holes} \\ E'_i &= E + (eF)^2/2c_{i,z} \quad i = e,h \end{aligned} \tag{3.37}$$

Therefore, electrons and holes are displaced in opposite directions and their envelope functions are the same as (3.25) with z replaced by z'. The simplicity of the change in envelope function with applied electric field is a great advantage of the parabolic well model, although it should be pointed out that this same simplicity implies that the charges can continue separating indefinitely with applied field strength and is therefore unrealistic at very high fields. Again, in spherical polar coordinates, the envelope functions in the presence of a field may be written as

$$\varphi_e(\vec{r})=\left(\frac{1}{d_e\sqrt{\pi}}\right)^{3/2}\exp\left(-\frac{(\vec{r}-\hat{k}eF/c_e)^2}{2d_e^2}\right) \tag{3.38}$$

For electrons, and

$$\varphi_h(\vec{r})=\left(\frac{1}{d_h\sqrt{\pi}}\right)^{3/2}\exp\left(-\frac{(\vec{r}+\hat{k}eF/c_h)^2}{2d_h^2}\right) \tag{3.39}$$

For holes, where $\hat{k}$ is the unit vector in the *z*-direction. This time substituting into equation (3.28), leads to

$$M_{eh} = C\iint \exp\left(-\frac{r_1^2}{d_e^2}\right)\exp\left(-\frac{r_2^2}{d_h^2}\right)\frac{\exp(r_1\alpha\cos\theta)}{\left|\vec{r}_1-\vec{r}_2\right|}d\vec{r}_1 d\vec{r}_2 \qquad (3.40)$$

Where

$$C = \frac{e^2}{4\pi\varepsilon_0\varepsilon_r}\left(\frac{1}{d_e\sqrt{\pi}}\right)^3\left(\frac{1}{d_h\sqrt{\pi}}\right)^3\exp\left[-\frac{(eF)^2}{d_e^2}\left(\frac{1}{c_e}+\frac{1}{c_h}\right)^2\right] \qquad (3.41)$$

And

$$\alpha = \frac{2eF}{d_e^2}\left(\frac{1}{c_e}+\frac{1}{c_h}\right) \qquad (3.42)$$

We proceed as before, again making use of Legendre polynomials and their orthogonality relations, and integrate over $\vec{r}_2$ to leave

$$M_{eh} = \frac{2\pi^{5/2}Cd_h^3}{\alpha}\int \exp\left(-\frac{r_1^2}{d_e^2}\right)\mathrm{erf}\left(-\frac{r_1}{d_h}\right)\left[\exp(r_1\alpha)-\exp(-r_1\alpha)\right]dr_1 \qquad (3.43)$$

For $\alpha < 1/d_e$ (valid up to fields of order 10^7 V/m for $c_e = c_h = 0.00641$ J/m^2, $d_e = 2.627 \times 10^{-9}$ m), we expand the exponentials in α up to the term in α^3 and integrate over r_1. Keeping only the terms up to F^2 order in the resultant expressions gives us an estimate for the suppression of the electron-hole binding energy as an external field is applied

$$M_{eh} = \frac{e^2}{2\pi^{3/2}\varepsilon_0\varepsilon_r\sqrt{d_e^2 + d_h^2}}\left[1 - \frac{(eF)^2}{3\left(d_e^2 + d_h^2\right)}\left(\frac{1}{c_e} + \frac{1}{c_h}\right)^2\right] \qquad (3.44)$$

Which reduce to (3.34) at *F=0*.

3.5 Förster Interaction in Coupled QDs

We have now characterized the single particle electron and hole states within a simple quantum dot model, as well as accounting for the binding energy due to electron-hole coupling within a dot when estimating the ground state exciton energy. In this section we shall consider excitons in two coupled quantum dots and the Coulomb interactions between them. More specifically, we shall derive an analytical expression for the strength of the inter-dot Förster coupling. We shall show that this coupling is, under certain conditions, of dipole-dipole type [49, 50] and that it is responsible for resonant exciton exchange between adjacent quantum dots. This is a transfer of energy only, not a tunnelling effect (If the electron and hole are strongly bound, so that they do not tunnel separately, a tunnelling between the two dots will simply add a small correction to the off-diagonal elements in the interaction Hamiltonian). In the next section we describe the phenomenon known as *Förster Resonance Energy Transfer: FRET (or Fluorescent Resonance Energy Transfer).*

3.5.1 Förster Resonance Energy Transfer (FRET)

In 1946, Theodor Förster published a paper in *Naturwissenschaften* [60, 61] outlining the quantum-mechanical behavior of the transfer of electronic excitation energy between two molecules in a solution. His breakthrough work in spectroscopy was built upon the earlier theories of J. and F. Perrin, and explained the transfer of energy between two molecules nonradiatively. His contribution, FRET, is an acronym for Förster resonance energy transfer or fluorescence resonance energy transfer. His equations were the basis to interpret FRET results quantitatively in terms of parameters than can be derived experimentally [60]. Originally, fluorescence spectroscopy and time-resolved fluorescence were primarily used for research in biochemistry and biophysics to determine molecular

distances (FRET is an excellent spectroscopic ruler) and conformational changes; however, fluorescence is now used in environmental monitoring, clinical chemistry, DNA sequencing, and genetic analysis by fluorescence *in situ* hybridization (FISH) among other applications [61]. Therefore, FRET is an important topic of discussion and knowledge of the subject is vital to Biology, Chemistry and Physics. This section will detail Förster Resonance Energy Transfer in order to quantitatively describe FRET, from the labor of the Perrin's and Förster to modern day experimental methods and analysis. Förster grew interested in the energy transfer because of the efficient photosynthetic process. He was aware from previous experiments, that leaves capture and use light energy much more effectively than would be expected, even if photons hit the reaction centers precisely [60]. The efficient transfer of energy between the closely spaced chlorophyll molecules must be responsible, allowing the absorbed energy to diffuse into the relatively sparse reaction centers by hopping rapidly between molecules. He knew of the earlier work of the Perrin's, suggesting that energy could be transferred over distances longer than the molecular diameters.

Förster developed a correct theoretical basis of FRET in first paper in 1946. He assumed that the oscillators were identical and the interaction energy is small compared to the energies of the spectral transitions [62]. From these assumptions, he knew that the excited molecules will experience complete relaxation to their equilibrium states. Therefore, probability arguments could be used in the calculations! With that information, he defined the probability of a resonance condition between two narrow band oscillators. Since the frequencies of the donor and the acceptor are independently spread over a wide frequency range, this probability will be low, and the time for transfer will be shortened considerably. Förster was well aware of quantum theory describing the electronic structure of molecules. He knew that the atomic vibrations in complex molecules and interactions with the solvent in condense media considerably broaden absorption and emission spectra [60]. The quantum theories of spectroscopic transitions had shown the need to take into account the effect of broadened energy distributions when calculating the rate of a kinetic proves between two quantum states. He also realized that the classical theory of the interaction of oscillating dipoles was very similar to the theoretical description of absorption and fluorescence spectroscopic transitions that occur when a single molecular transition dipole interacts with the

oscillating electric field of light [60]. The similarities between these two theories contributed to his development of a quantitative theory of the rate of transfer in terms of the overlap integral, which is the integral of the product of the acceptor absorption spectrum and the donor fluorescence spectrum over the entire frequency range. This integral represents the probability that the two molecular transition dipoles will have the same frequency. He could then show how R_0 could be calculated, resulting in an expression for the distance dependence of FRET efficiency. Although the quantum theories he used are complicated, his procedures for determining E from fluorescence spectral measurements are fairly easy to understand. With the explicit expression for the fluorescence intensity, including direct excitation of the donor and acceptor and the energy transfer, he was able to take into account any pair for the excitation and emission frequency. Depending on the donor-acceptor pair, he needed to find a possible wavelength where only the donor or only the acceptor, is either excited or emits [62]. Since some of fluorescence spectra (excitation and emission) of the donor and acceptor he used were already known, it became possible to extract the individual contributions of the donor or acceptor from the fluorescence spectra containing emissions from both species. Then by using this data, he combined fluorescence with absorbance data, to determine E in terms of known absorption constants and quantum yields.

The Förster theory of intermolecular energy transfer, an expression for the quantum yield of the donor fluorescence resulting from intermolecular transfers was confirmed with the experimental results for many different donor-acceptor pairs, such as fluorescence quenching by Rhodamine B in glycerol and for 2,5-diphenyloxazole quenched by 9,10-dibromoanthracene in cyclohexane [63]. Additionally, experiments have been conducted duplicating his original papers, using Fluorescein and Rhodamine B in glycerol, +4% water with 0.25 mol/L NaOH, as well as Fluorescein and Rhodamine 6G in glycerol, +4% water with 0.25 mol/L NaOH. From these experiments, Förster was able to experimentally confirm his theory [62].

3.6 QDs Hamiltonian with Förster Interaction

We consider L identical semiconductor quantum dots that are equally coupled to each other via coulombic interaction. The QDs interact with a quantized field (dipole interaction) in a high-Q cavity. Then the coupled QD-field system is described by the Hamiltonian [30-32, 51],

$$H/\hbar = \omega a^{\dagger}a + \frac{\varepsilon}{2}\sum_{k=1}^{L}\left(e_k^{\dagger}e_k - h_k h_k^{\dagger}\right) + g\sum_{k=1}^{L}\left(e_k^{\dagger}h_k^{\dagger}a - a^{\dagger}h_k e_k\right) + \frac{W}{2}\sum_{k,l=1}^{L}\left(e_k^{\dagger}h_l e_l h_k^{\dagger} - h_k e_l^{\dagger}h_l^{\dagger}e_k\right) \tag{3.45}$$

where $e_k^{\dagger}\left(h_k^{\dagger}\right)$ is the electron (hole) fermionic creation operator in the nth QD and $a^{\dagger}(a)$ is the bosonic creation (aniquilation) operator for the quantized cavity field, ε is the QD band gap, g is the coupling strength between the field and the QDs, ω is the field frequency, and W represents the interdot coulomb interaction. The coulomb interaction process known as Forster process exchanges energy, but does not require the physical transfer of the electrons and holes. For equal coupling these QDs are equidistant from each other so that the dots lie on a line for *N = 2*, at the vertices of an equilateral triangle for *N = 3*, and at the vertices of a regular pyramid for *N = 4*. The Hamiltonian (1) can be rewritten in a much more suitable in the representation of angular momentum, with the following changes [20, 27]

$$J_{+} = \sum_{k=1}^{L}\left(e_k^{\dagger}h_k^{\dagger}\right); \quad J_{-} = \sum_{k=1}^{L}\left(h_k e_k\right); \quad J_z = \frac{1}{2}\sum_{k=1}^{L}\left(e_k^{\dagger}e_k - h_k h_k^{\dagger}\right). \tag{3.46}$$

which satisfy the usual angular momentum commutation relations: $[J_{+}, J_{-}] = 2J_z$ and $[J_z, J_{\pm}] = \pm J_{\pm}$ Using these quasi-spin operators the Hamiltonian of Eq. (3.45) can be written as ($\hbar = 1$),

$$H = \omega a^{\dagger}a + \varepsilon J_z + g\left(J_{+}a + a^{\dagger}J_{-}\right) + W\left(J^2 - J_z^2\right) \tag{3.47}$$

In reference [51] we obtained that may consist of two parts, one with the Dicke H_{Dk} Hamiltonian itself and the other is the interaction Hamiltonian Förster H_F, defined as

$$H_{Dk} = \Delta J_z + g\left(J_+ a + a^\dagger J_-\right), \qquad \Delta = \varepsilon - \omega; \qquad \mathrm{H}_F = W\left(J^2 - J_z^2\right), \tag{3.48}$$

Where Δ is the detuning between the electromagnetic field and the band gap. The Hamiltonian of L QDs can be rewritten in the form: $H = \omega N + H_L$, with $N = a^\dagger a + J_z + L/2$ is the number of atoms and photons and $H_L = H_{Dk} + H_F$ are constants of motion. However there is another way to rewrite the Hamiltonian (3.47), using the relations of the algebra of angular momentum given as follows

$$H = \omega a^\dagger a + \varepsilon' J_z + g\left(J_+ a + a^\dagger J_-\right) + W J_+ J_-; \qquad \varepsilon' = \varepsilon - W \tag{3.49}$$

Here we see the term of Förster WJ_+J_- ($\mathrm{H}_F = W\left(J^2 - J_z^2\right)$) as a non-linearity and we has introduced a new constant ε', as defined above. Again we rewrite the Hamiltonian to include explicitly the detuning (Δ) which now call *Förster Detuning* (Δ'), so we get

$$H = \omega\left(a^\dagger a + J_z\right) + \Delta' J_z + g\left(J_+ a + a^\dagger J_-\right) + W J_+ J_-; \qquad \Delta' = \Delta + \mathrm{W} = \varepsilon - \omega + W \tag{3.50}$$

In a frame rotating with the field frequency ω, Eq. (3.50) takes the form

$$H_r = \Delta' J_z + g\left(J_+ a + a^\dagger J_-\right) + W J_+ J_- \tag{3.51}$$

In this Hamiltonian appear the Förster detuning Δ' in which we can make W=0, so that only stay the typical detuning Δ, which represent the old acquaintance excited Dicke Hamiltonian off-diagonal, i.e.

$$H_{Dk} = \Delta J_z + g\left(J_+ a + a^\dagger J_-\right) \tag{3.52}$$

3.6.1. QDs Hamiltonian Diagonalization

Using the Hamiltonian (3.51) we determine the state vectors describing the coupled QD-field system for two QDs. This will simplify the task of studying the time evolution of the coupled QD-field system. Starting with the initial condition representing the vacuum of excitons, $|j=1,m=-1\rangle$, only the $j=1$ subspace is optically active while the $j=0$ subspace remains dark. We choose the basis of eigenstates of J^2 and J_z , $|0\rangle=|j=1,m=-1\rangle$, $|1\rangle=|j=1,m=0\rangle$, $|2\rangle=|j=1,m=1\rangle$, as an appropriate representation for this problem $|0\rangle$ represents the vacuum for excitons, $|1\rangle$ denotes a symmetric delocalized single-exciton state, while $|2\rangle$ represents the bi-exciton state. If we represent the field state by the Fock state $|n\rangle$ and consider the QDs in the entangled state involving the vacuum and bi-exciton states $(1/\sqrt{2})[|0\rangle\pm|2\rangle]$, then we will have an invariant subspace spanned by $|0,n+2\rangle=|0\rangle\otimes|n+2\rangle$, $|1,n+1\rangle=|1\rangle\otimes|n+1\rangle$, $|2,n\rangle=|2\rangle\otimes|n\rangle$, $|0,n\rangle=|0\rangle\otimes|n\rangle$, $|1,n-1\rangle=|1\rangle\otimes|n-1\rangle$ and $|2,n-2\rangle=|2\rangle\otimes|n-2\rangle$. With these basis vectors we determine the matrix elements of the Hamiltonian in Eq. (7) and obtain the eigenvalues, and the eigenvectors. Thus the explicit matrix is,

$$H_F=\begin{pmatrix} \Delta' & \sqrt{2(n+2)} & 0 & 0 & 0 & 0 \\ \sqrt{2(n+2)}g & 2W & \sqrt{2(n+2)}g & 0 & 0 & 0 \\ 0 & \sqrt{2(n+1)}g & 2W-\Delta' & 0 & 0 & 0 \\ 0 & 0 & 0 & \Delta' & \sqrt{2n}g & 0 \\ 0 & 0 & 0 & \sqrt{2n}g & 2W & \sqrt{2(n-1)}g \\ 0 & 0 & 0 & 0 & \sqrt{2(n-1)}g & 2W-\Delta' \end{pmatrix} \quad (3.53)$$

The characteristic polynomial is

$$P(\lambda)=\left[\lambda(\lambda-2W)^2+2g(2nW+\lambda-2n\lambda)-2[g^2+W(2W-\lambda)]\Delta'+(2W-\lambda)(\Delta')^2\right]\times$$
$$\left[\lambda(\lambda-2W)^2+g^2[4(n+2)W-2(2n+3)\lambda]-2[g^2+W(2W-\lambda)]\Delta'+(2W-\lambda)(\Delta')^2\right]$$

At resonance ($\Delta = 0$) and with the field frequency ω, and we define the constants for simplicity as $\delta_1 = \left[8g^2(2n-1)+W^2\right]^{1/2}$; $\delta_2 = \left[8g^2(2n+3)+W^2\right]^{1/2}$, the eigenvalues, take the form,

$$\begin{gathered}\lambda_{E1} = W,\ \lambda_{E2} = W,\ \lambda_{E3} = (1/2)\left(3W - \delta_1\right),\ \lambda_{E4} = (1/2)\left(3W + \delta_2\right), \\ \lambda_{E5} = (1/2)\left(3W - \delta_2\right),\ \lambda_{E6} = (1/2)\left(3W + \delta_2\right)\end{gathered} \tag{3.54}$$

Due to the tensor product of the quantum states $|j,k\rangle = |j\rangle \otimes |k\rangle$ form a four-dimensional basis in the Hilbert space $\mathrm{SU(2)} \otimes \mathrm{SU(2)}$. So in this way the basis vectors take the form, for instance:

$$\begin{gathered}|0,n\rangle = |0\rangle \otimes |n\rangle = [0,0,0,1,0,1]^T;\ |2,n-2\rangle = |2\rangle \otimes |n-2\rangle = [1,0,1,0,0,0]^T; \\ |0,n+2\rangle = |0\rangle \otimes |n+2\rangle = [0,0,0,1,1,1]^T\end{gathered}$$

Etc. And the corresponding normalized eigenvectors take the form

$$\begin{aligned}
|\lambda_1\rangle &= -\sqrt{\frac{n-1}{2n-1}}|0,n\rangle + \sqrt{\frac{n}{2n-1}}|2,n-2\rangle; \\
|\lambda_2\rangle &= -\sqrt{\frac{n+1}{2n+1}}|0,n+2\rangle + \sqrt{\frac{n+2}{2n+3}}|2,n\rangle; \\
|\lambda_{3,4}\rangle &= \sqrt{\frac{4g^2 n}{\delta_1(\delta_1 - W)}}|0,n\rangle \mp \sqrt{\frac{\delta_1 - W}{2\delta_1}}|1,n-1\rangle + \sqrt{\frac{4g^2(n-1)}{\delta_1(\delta_1 - W)}}|2,n-2\rangle; \\
|\lambda_{5,6}\rangle &= \sqrt{\frac{4g^2(n+2)}{\delta_2(\delta_2 - W)}}|0,n+2\rangle \mp \sqrt{\frac{\delta_2 - W}{2\delta_2}}|1,n+1\rangle + \sqrt{\frac{4g^2(n+1)}{\delta_2(\delta_2 - W)}}|2,n\rangle
\end{aligned} \tag{3.55}$$

Where the constants δ_1, δ_2 as defined above. Then we determine the wave function at any time with the help of the previous eigenvectors. In this way we need to consider the initial state of the system of quantum dots. A choice of suitable initial state is a state of Bell, i.e. for the sake of generality, we consider

the initial state of the QDs to be $|\psi_{qd}(0)\rangle = [a_0|0\rangle + a_2 e^{i\phi}|2\rangle]$, where a_0 and a_2 are real constants satisfying the condition $a_0^2 + a_2^2 = 1$. We will consider the initial state of the field to be coherent, or thermal. In this paper we analyze only the coherent case. The coherent states can be expressed as a superposition of number states $|\alpha\rangle = |\Psi_{Ch}(0)\rangle = \Lambda(n)|n\rangle$, with the probability distribution given as $|\Lambda(n)|^2 \equiv P(n)$, is the probability that the intra-cavity field has *n* photons and depends on the state of the intra-cavity field. Then, the initial state for the coupled QD-field system can then be written as

$$|\Psi(0)\rangle = \sum_{n=0}^{\infty} \Lambda(n)[a_0|0\rangle + a_2 e^{i\phi}|2\rangle] \otimes |n\rangle \tag{3.56}$$

We are now able to find the wave vector of the system, because the energy eigenstates form a complete set, so using the eigenvalues and eigenvectors of the equations (3.53) and (3.54), together with the initial state (3.55), we obtain the following state vector at the time *t* as

$$|\Psi(t)\rangle = \sum_{n=0}^{\infty}\sum_{k=1}^{6} \exp(-i\lambda_{Ek}t)\langle \lambda_{Ek}|\Psi(0)\rangle |\lambda_{Ek}\rangle = \sum_{n=0}^{\infty} \Lambda(n)|\varphi_n(t)\rangle \tag{3.57}$$

Where $|\varphi_n(t)\rangle$ function should be in terms of the coefficients related to the eigenvalues and eigenvectors above, so that we can express as $|\varphi_n(t)\rangle = \sum_{k=1}^{6} x_k(n,t)|jm,n\rangle$, where $|jm,n\rangle$, represents the fundamental base used in the matrix Hamiltonian (8), the coefficients and the function are explicitly expressed as

$$\begin{aligned} |\varphi_n(t)\rangle = {} & x_1(n,t)|0,n\rangle + x_2(n,t)|0,n+2\rangle + x_3(n,t)|1,n-1\rangle \\ & + x_4(n,t)|1,n+1\rangle + x_5(n,t)|2,n\rangle + x_6(n,t)|2,n-2\rangle \end{aligned} \tag{3.58}$$

due to orthonormality of the basis vectors we obtain the coefficients in the form $\langle jm,n|\varphi_n(t)\rangle$ as,

$$
\begin{aligned}
x_1(n,t) &= a_0\left[\frac{n-1}{2n-1}e^{-i\lambda_1 t}+\frac{4g^2 n}{\delta_1}\left(\frac{e^{-i\lambda_3 t}}{\delta_1-W}+\frac{e^{-i\lambda_4 t}}{\delta_1+W}\right)\right];\\
x_2(n,t) &= a_2 e^{i\phi_0}\sqrt{(n+1)(n+2)}\left[-\frac{e^{-i\lambda_2 t}}{2n+3}+\frac{4g^2 n}{\delta_1}\left(\frac{e^{-i\lambda_5 t}}{\delta_2-W}+\frac{e^{-i\lambda_6 t}}{\delta_2+W}\right)\right];\\
x_3(n,t) &= a_0\frac{g\sqrt{2n}}{\delta_1}\left(e^{-i\lambda_4 t}-e^{-i\lambda_3 t}\right);\\
x_4(n,t) &= a_2 e^{i\phi_0}\frac{g\sqrt{2(n+1)}}{\delta_2}\left(e^{-i\lambda_6 t}-e^{-i\lambda_5 t}\right);\\
x_5(n,t) &= a_2 e^{i\phi_0}\left[-\left(\frac{n+2}{2n+3}\right)e^{-i\lambda_2 t}+\frac{4g^2(n+1)}{\delta_2}\left(\frac{e^{-i\lambda_5 t}}{\delta_2-W}+\frac{e^{-i\lambda_6 t}}{\delta_2+W}\right)\right]\\
x_6(n,t) &= a_0\left[-\frac{\sqrt{n(n-1)}}{2n-1}e^{-i\lambda_1 t}+\frac{4g^2\sqrt{n(n-1)}}{\delta_1}\left(\frac{e^{-i\lambda_3 t}}{\delta_1-W}+\frac{e^{-i\lambda_4 t}}{\delta_1+W}\right)\right]
\end{aligned}
\tag{3.59}
$$

Based upon these results that were obtained, we will use later and the following sections and chapters to applications. For example, we find the density matrix, as well as reduced density matrix for the entanglement of formation in chapter 4.

3.7 Collective Atomic Systems: Dicke Model

With the JCM theoretical success, the experimental realization of their predictions were also a success, so it is much interest in finding systems of many atoms with new phenomena from precisely the interaction between atoms. These types of phenomena arising from the interaction of many particles are known as Collective Phenomena. Collective phenomena are central to the matter-radiation interaction, particularly for Cavity Quantum Electrodynamics (CQED). One such phenomenon is the Cooperative Spontaneous Emission, first discussed by Dicke [53]. As Dicke was the first consider a system of this type in 1954, the model is called commonly Dicke Model (DM), but also sometimes is used the name Tavis-Cummings Model (TCM) [59].

This model has a collection of identical atoms in a very small cavity such that the wavelength of the electric field does not very greatly with the cavity and each atom "feels" approximately same electric field. This field must be mono-

mode. Another assumption in this model is that the atoms wave-function are not overlap each other, i.e. forces are neglected dipole-dipole type between atoms. The discussion up to now has been for a single atom coupled to radiation, as the case at JCM. In later sections we will discuss lasing, involving many atoms, but where (due to decoherence) each atom can be considered independently. This brief section, in contrast, discusses coherent effects with many atoms. We consider the generalization of the Jaynes-Cummings model, to consider many atoms coupled to a single photon mode, known as the Dicke model:

$$H = \omega a^{\dagger} a + \sum_j \varepsilon_j \sigma_j^z + \sum_j g_j \left[\sigma_j^- a^{\dagger} + a \sigma_j^+ \right] \tag{3.60}$$

Here σ_j are Pauli matrices, representing the two-level systems on each site. In order to illustrate what effects coherence between two-level systems can have, it is simplest to consider the uniform case, $\varepsilon_j = \varepsilon$ and $g_j = g$. In this case, it is helpful to introduce new so called collective operators, $J = \sum_j \sigma_j$. This describes the product of *N* or *L* spin 1/2 representations being decomposed as a sum of higher-spin representations of the rotation group. Then,

$$H = \omega a^{\dagger} a + \varepsilon J_z + g \left(J_- a^{\dagger} + a J_+ \right) \tag{3.61}$$

Considering *L* two levels energy systems (in beginning distinguishable) that do not interact each other, and denoting the states of the *j-th* atom for $|j,1\rangle$ or $|j,2\rangle$, as is in the ground or excited state, and let n^+ is number of excited atoms while n^- those found in the ground state, so that $n^+ + n^- = L$. Therefore the energy system will be

$$E = \frac{\hbar \varepsilon}{2} \left(n^+ - n^- \right) \tag{3.62}$$

We will are $n^+ = k$, (remember that at general at this dissertation $\hbar = 1$, is normalized)

$$E = \hbar\varepsilon\left(k - L/2\right), \qquad k = 0,1,...,L \tag{3.63}$$

And the spectrum is equidistant and bounded. A vector that described a system with *k* excited atoms is

$$\left|1,2\right\rangle...\left|k,2\right\rangle\left|k+1,1\right\rangle...\left|L,1\right\rangle \tag{3.64}$$

With degeneration of

$$C_k^L = \frac{L!}{k!\left(L-k\right)!} \tag{3.65}$$

Because a permutation of particles remain the same energy, now assume that the degenerate states are indistinguishable, then a normalized linear combination of all these states is

$$\left|k,L\right\rangle = \sqrt{\frac{k!\left(L-k\right)!}{L!}}\sum_p \left|j_1,2\right\rangle...\left|j_k,2\right\rangle\left|j_{k+1},1\right\rangle...\left|j_L,1\right\rangle \tag{3.66}$$

Where the sum is over all possible permutations of the excited particles and no excited. The above expression is known as Dicke Atomic State.

The collective operators for a *L* atomic system, is defined by

$$J_i = \frac{1}{2}\sum_{j=1}^{L}\sigma_i^{(j)}, \qquad (i = x, y, z = 1,2,3) \tag{3.67}$$

Once again $\sigma_i^{(j)}$ are Pauli matrices and superscript (*j*) denoting the matrix of the *j-th* atom. From the definition of collective basis (3.66) we have

$$J_3\left|k,L\right\rangle = J_z\left|k,L\right\rangle = m\left|k,L\right\rangle = \left(k - L/2\right)\left|k,L\right\rangle \tag{3.68}$$

Where

$$m=\frac{2k-L}{2}=\frac{n^{+}-n^{-}}{2} \tag{3.69}$$

Inversion is defined by the system at time zero: the difference between the atoms number in excited state and no excited state. Moreover the same definition of Pauli's matrices follows that

$$J_{\pm}=\sum_{j=1}^{L}\sigma_{\pm}^{(j)}=J_{x}\pm iJ_{y} \tag{3.70}$$

That act over symmetric states $|k,L\rangle$ as follows

$$\begin{aligned} J_{-}|k,L\rangle &= \sqrt{\frac{k!(L-k)!}{L!}}(L-k+1)\sum_{p}|j_1,2\rangle...|j_{k-1},2\rangle|j_k,1\rangle...|j_L,1\rangle \\ &= \sqrt{k(L-k+1)}\,|k-1,L\rangle \end{aligned} \tag{3.71}$$

Similarly, we get the action of the other collective operators on the basis of the subspaces of symmetric states (3.66), this is given as

$$\begin{aligned} J_{+}|k,L\rangle &= \sqrt{(k+1)(L-k)}\,|k+1,L\rangle \\ J_{-}|k,L\rangle &= \sqrt{k(L-k+1)}\,|k-1,L\rangle \\ J_{-}|k,L\rangle &= \left(\frac{k-L}{2}\right)|k,L\rangle \end{aligned} \tag{3.72}$$

These collective operators satisfied the standard commutative relations of the angular momentum

$$\left[J_i, J_j\right] = J_k \varepsilon_{ijk}, \quad \left[J_z, J_\pm\right] = \pm J_\pm, \quad \left[J_+, J_-\right] = 2J_z, \tag{3.73}$$

Return to Dicke Hamiltonian (3.61), similarly to JCM we can define an Excitation Number Total operator

$$\hat{N} = \hat{n} + J_z + L/2, \qquad \left(\text{with} \quad \hat{n} = a^\dagger a\right) \tag{3.74}$$

Which obviously commute with the Hamiltonian; however unlike JCM in DM do not possible to associate a scalar C^2 to this operator. This means that if initial state belongs to a subspace defined with the given *e* excitation number, thus the system will always evolve into that subspace. So a suitable system basis atom-field is

$$\left|e,n\right\rangle = \left|L, e-n\right\rangle_a \otimes \left|n\right\rangle_f \tag{3.75}$$

To be $\left|n\right\rangle_f$ the Fock state of the electric field, $\left|L, e-n\right\rangle_a$ is the Dicke atomic state. This basis is interpreted as follows, the atomic system have a total of excitations, i.e. , photons of the field more excited atoms. If in the field there are n photons, then there can only be *e-p* excited atoms, since the excitation number is constant. To illustrate this fact, we apply number operator to this base

$$\begin{aligned}\hat{N}\left|e,n\right\rangle &= \left(\hat{n} + J_z + L/2\right)\left|e-n\right\rangle = \hat{n}\left|L, e-n\right\rangle_a \otimes \left|n\right\rangle_f + J_z\left|L, e-n\right\rangle_a \otimes \left|n\right\rangle_f \\ &\quad + \frac{L}{2}\left|L, e-n\right\rangle_a \otimes \left|n\right\rangle_f \\ &= n\left|e-n\right\rangle + \left(e-n-L/2\right)\left|e-n\right\rangle + L/2\left|e-n\right\rangle \\ &= \left(n+e-n-L/2+L/2\right)\left|e-n\right\rangle = e\left|e-n\right\rangle\end{aligned} \tag{3.76}$$

In practice as theory of angular momentum is common use a standard notation, this means one can label the atomic states by $|m, j\rangle$, with

$$J^2|m, j\rangle = j(j+1)|m, j\rangle; \qquad J_z|m, j\rangle = m|m, j\rangle$$

And using $\left[J^2, J_{x,y,z}\right] = 0$ with $|m| < j$, and *1<2j<L*. Then summarizing the standard results, $J_{\pm} = J_x \pm iJ_y$ implies

$$\begin{aligned} & J_-|m, j\rangle = \lambda|m-1, j\rangle \\ \Rightarrow \quad & |\lambda|^2 = \langle m, j|J_+J_-|m, j\rangle = \langle m, j|J^2 - J_z^2 - J_z|m, j\rangle \\ & \qquad = \left[j(j+1) - m(m-1)\right] \end{aligned} \tag{3.77}$$

From this result, we can directly calculate the rate of radiation emission from the state $|m, j, n\rangle$ (with *n* representing the number of photons) with the Hamiltonian (3.60)

$$\begin{aligned} W &= \left|\langle m-1, j, n+1|ga^{\dagger}J_-|m, j, n\rangle\right|^2 \\ &= g^2\left[j(j+1) - m(m-1)\right](n+1) \end{aligned} \tag{3.78}$$

Factorizing this expression, one has $W = g^2(j + m)(j - m + 1)(n + 1)$. Considering emission into an empty cavity, the maximum rate of radiation occurs when *2j = L* and *m =0*, then $W \simeq g^2L^2/4$. i.e., radiation intensity is proportional to the square of the number of atoms. If emission from each atom were incoherent, radiation would be proportional to the total number of excited atoms, *L/2* in this case. This enhancement of rate of radiation, due to the interatomic coherence is known as superradiance [59]. Note also that if *m = –j + 1*, so that on average only one atom is excited, one can still see superradiant effects: With *2j = L*, and

$m = -j + 1$, $W = g^2 2(j+1) \simeq g^2 L$. This state $|1-L/2, L/2\rangle$ is a superposition of excitations of each two-level system. In contrast, the emission rate for a single two-level system being excited is just g^2. Note also, that destructive interference is possible; the state $|0,0\rangle$ has a vanishing radiation rate, despite having on average half the atoms in the excited state.

3.8 Atomic Coherent States or Angular Momentum Coherent States

The atomic coherent states (ACS) or angular momentum coherent states, also known as Spin coherent states, are important in many models in quantum optics. ACS was first introduced in references [55-57]. ACS are defined as a linear combination of eigenstates of the angular momentum operator J_z. To generate through the interaction of a classical field with the dipole moment of an atom described by the angular momentum operator J_x of the atom, taking the atom in its lower level with eigenstate $|-j\rangle$ of the operator J_z. Although interest in these states is not limited to limited to rotating systems, it is simplest to define these states of the angular momentum eigenstates $|j,m\rangle$ where j takes any integer or half-integer value and $m=-j,-j+m,\ldots,j$. The actions of the angular momentum operators J_z, $\mathbf{J^2}$, J_+ and J_- on the state are given by

$$\begin{aligned} J^2|j,m\rangle &= j(j+1)|j,m\rangle \\ J_z|j,m\rangle &= m|j,m\rangle \qquad \text{with} \qquad |m| \le j \end{aligned} \tag{3.79}$$

The operations of the operators J_+, J_- and their powers on $|j,m\rangle$ are given by

$$J_{\pm}\left|j,m\right\rangle=\sqrt{(j\pm m)(j\pm m+1)}\left|j,m\pm1\right\rangle$$
$$J_{\pm}^{k}\left|j,m\right\rangle=\sqrt{\frac{(j\mp m)!(j\pm m+k)!}{(j\mp m-k)!(j\pm m)!}}\left|j,m\pm k\right\rangle;\quad m+k\le j,\quad m-k\ge -j \tag{3.80}$$
$$\exp(-\eta J_{-})\left|j,m\right\rangle=\sqrt{\frac{(j+m)!}{(j-m)!}}\sum_{k=0}^{m+j}\frac{(-\eta)^{k}}{k!}\sqrt{\frac{(j-m+k)!}{(j+m-k)!}}\left|j,m-k\right\rangle;$$

So that $J_{+}\left|j,j\right\rangle=0$ and $J_{-}\left|j,-j\right\rangle=0$. It follows from the first equation (3.80) that we can write $\left|j,m\right\rangle$ as

$$\left|j,m\right\rangle=\frac{1}{(j+m)!}\left(C_{j+m}^{2j}\right)^{-1/2}J_{+}^{j+m}\left|j,-j\right\rangle \tag{3.81}$$

Where $\left(C_{j+m}^{2j}\right)^{-1/2}$ is the binomial coefficient. The atomic coherent state $\left|\theta,\phi\right\rangle$ defined earlier [55, 56], with $\left|j,m=-j\right\rangle=\left|j,-j\right\rangle=\left|-j\right\rangle$, thus

$$\left|\theta,\phi\right\rangle=\exp\left[\frac{1}{2}\theta\left(e^{-i\phi}J_{+}-e^{+i\phi}J_{-}\right)\right]\left|-j\right\rangle=\hat{R}(\theta,\phi)\left|-j\right\rangle \tag{3.82}$$

This operator is unitary since $\hat{R}^{\dagger}(\theta,\phi)=\hat{R}(-\theta,\phi)=\hat{R}^{-1}(\theta,\phi)$ and rotates the angular momentum vector through an angle θ about the axis $\hat{i}\sin(\phi)-\hat{j}\cos(\phi)$. We can write the operator $\hat{R}(\theta,\phi)$ at (3.82) in the ordered form

$$\begin{aligned}\left|\theta,\phi\right\rangle&=\hat{R}(\theta,\phi)\left|j,-j\right\rangle=\hat{R}(\theta,\phi)\left|-j\right\rangle\\&=\left(\exp\left[\tan\frac{\theta}{2}e^{-i\phi}J_{+}\right]\right)\left(\sec^{2}\frac{\theta}{2}\right)^{J_{z}}\left(\exp\left[-\tan\frac{\theta}{2}e^{+i\phi}J_{-}\right]\right)\left|-j\right\rangle\\&=\left(\cos\frac{\theta}{2}\right)^{2j}\sum_{m=-j}^{j}\sqrt{\binom{2j}{j+m}}\left(\tan\frac{\theta}{2}e^{-i\phi}\right)^{j+m}\left|m\right\rangle\end{aligned} \tag{3.83}$$

Using the ordering theorem [57]. Then follows from (3.83), and with help of the exponential operator function and together with (3.81)

$$\left|\theta,\phi\right\rangle = \left(\cos\frac{\theta}{2}\right)^{2j} \sum_{m=-j}^{j} \left(C_{j+m}^{2j}\right)^{-1/2} \left[\tan\frac{\theta}{2} e^{-i\phi}\right]^{j+m} \left|j,m\right\rangle \tag{3.84}$$

In the case of the probability distribution *P(m)* for the operator J_z is type binomial since

$$P(m) = \left(\cos\frac{\theta}{2}\right)^{4j} C_{j+m}^{2j} \left[\tan\frac{\theta}{2}\right]^{2(j+m)} \tag{3.85}$$

These states ACSs are not mutually orthogonal, in way similar to coherent and squeezed states of the EM field; the inner product between the states $\left|\theta,\phi\right\rangle$ and $\left|\theta',\phi'\right\rangle$ being,

$$\left\langle\theta,\phi\middle|\theta',\phi'\right\rangle = \left[\cos^2(\theta/2)\cos^2(\theta'/2)\left(1+e^{i(\phi-\phi')}\right)\tan^2(\theta/2)\tan^2(\theta'/2)\right]^j \tag{3.86}$$

Hence

$$\left|\left\langle\theta,\phi\middle|\theta',\phi'\right\rangle\right|^2 = \left(\cos(\Theta/2)\right)^{4j} \tag{3.87}$$

Here Θ is defined as the angle between the directions made by (θ,ϕ) and (θ',ϕ'). Regardless of the lack of orthogonality of the ACS, they form a over-complete set in that the identity on the space with total angular momentum *j* can be resolved as

$$\frac{(2j+1)}{4\pi}\int d\Omega\left|\theta,\phi\right\rangle\left\langle\theta,\phi\right| = 1 \tag{3.88}$$

This is a spherical integral; the integration must be over the entire surface of the sphere, i.e.

$$\int d\Omega = \int_0^{2\pi} d\phi \int_0^{\pi} \sin\theta d\theta$$

To calculate we plug in the expression (3.84) on the left side of (3.88) and integrate over the angle ϕ, with the help of gamma and beta functions we obtained

$$\frac{(2j+1)}{4\pi}\int d\Omega \left|\theta,\phi\right\rangle\left\langle\theta,\phi\right| =$$

$$= (2j+1)\sum_{m=-j}^{j} C_{j+m}^{2j} \left|j,m\right\rangle\left\langle j,m\right| \int_0^{\pi} d\theta \left(\sin(\theta/2)\right)^{2(j+m)+1} \left(\cos(\theta/2)\right)^{2(j-m)+1} \quad (3.89)$$

$$\Rightarrow \frac{(2j+1)}{4\pi}\int d\Omega \left|\theta,\phi\right\rangle\left\langle\theta,\phi\right| = \sum_{m=-j}^{j} \left|j,m\right\rangle\left\langle j,m\right| = 1$$

From the above, the trace can be obtained for some operator ***A***, which can be expressed as

$$\mathrm{Tr}\left(\hat{\mathrm{A}}\right) = \frac{(2j+1)}{4\pi}\int d\Omega \left\langle\theta,\phi\right|\hat{\mathrm{A}}\left|\theta,\phi\right\rangle \quad (3.90)$$

Since the state $\left|j,m=-j\right\rangle = \left|j,-j\right\rangle = \left|-j\right\rangle$ is an eigenstate of J_z with eigenvalue $-j$ and right eigenstate of J_- with eigenvalue 0.

3.8.1 Excited Atomic Coherent States (EACs)

Now let us state the generalization of these states ACS, which are introduced by [56, 58]. The results obtained in the references cited above, plus these states will help us to get some results of our thesis. So introduce the Excited Atomic Coherent (EAC) state $\left|\theta,\phi,s\right\rangle$ by the expression

$$\left|\theta,\phi,s\right\rangle = \hat{R}(\theta,\phi)\left|s\right\rangle = \exp\left[\frac{1}{2}\theta\left(e^{-i\phi}J_+ - e^{+i\phi}J_-\right)\right]\left|s\right\rangle = \sum_{m=-j}^{j} A_m(\theta,\phi,s)\left|m\right\rangle \quad (3.91)$$

Where $|s\rangle = |j,s\rangle$ is any state of the angular momentum states. Obviously $|\theta,\phi\rangle$ is the state (3.91) when s=-j. The state (3.84) we can obtain in similar way, thus the coefficients $A_m(\theta,\phi,s)$ are given by

$$\begin{aligned} A_m(\theta,\phi,s) &= \sqrt{\frac{(j+m)!(j+s)!}{(j-m)!(j-s)!}}(-1)^s\left(\tan\frac{\theta}{2}\right)^{m+s} e^{i(s-m)\phi}\sum_{k=-j}^{\min(m,s)}\frac{(j-k)!\left(-\cos\sec^2(\theta/2)\right)^k}{(j+k)!(m-k)!(s-k)!} \\ &= \sqrt{\frac{(j+m)!(j+s)!}{(j-m)!(j-s)!}}\left(\frac{2j!}{(j+m)!(j+s)!}\right)(-1)^{s+j}\left(\sin\frac{\theta}{2}\right)^{2j}\left(\tan\frac{\theta}{2}\right)^{m+s} e^{i(s-m)\phi} \\ &\times {}_2F_1\left(-(m+j),-(s+j),2j,-\left(\cos\sec^2(\theta/2)\right)\right) \end{aligned} \quad (3.92)$$

Where the hypergeometric function is defined by

$${}_2F_1(\alpha,\beta,\gamma,z) = \sum_{l=0}\frac{(\alpha)_l(\beta)_l z^l}{(\gamma)_l l!}, \qquad \text{with } (\alpha)_l = \alpha(\alpha+1)\cdots(\alpha+l-1)$$

We can prove that the state $|\theta,\phi,s\rangle$ is an eigenfunction to the operator $\hat{R}(\theta,\phi)J_z\hat{R}^{-1}(\theta,\phi)$ with eigenvalue s. Then we will use the following formulae later,

$$\begin{aligned} \hat{R}^{-1}(\theta,\phi)J_z\hat{R}(\theta,\phi) &= J_z\cos\theta + \sin\theta\left[e^{-i\phi}J_+ + e^{+i\phi}J_-\right] \\ \hat{R}^{-1}(\theta,\phi)J_+\hat{R}(\theta,\phi) &= J_+\cos^2(\theta/2) - J_-\sin^2(\theta/2)e^{2i\phi} - J_z\sin\theta e^{i\phi} \\ \hat{R}^{-1}(\theta,\phi)J_-\hat{R}(\theta,\phi) &= J_-\cos^2(\theta/2) - J_+\sin^2(\theta/2)e^{-2i\phi} - J_z\sin\theta e^{-i\phi} \end{aligned} \quad (3.93)$$

With help of the above expressions we find the expectation values of the angular momentum components J_x, J_y, J_z, with the relation (3.91)

$$\begin{aligned} \langle\theta,\phi,s|J_z|\theta,\phi,s\rangle &= s\cos\theta \\ \langle\theta,\phi,s|J_x|\theta,\phi,s\rangle &= -s\sin\theta\cos\phi \\ \langle\theta,\phi,s|J_y|\theta,\phi,s\rangle &= -s\sin\theta\sin\phi \end{aligned} \quad (3.94)$$

In the early treatments [see references] do not is treated the excited state at general, but in transformations (3.94) just have to do *s=-j*, thus we obtain

$$\begin{aligned}\langle\theta,\phi,s|J_z|\theta,\phi,s\rangle &= -j\cos\theta \\ \langle\theta,\phi,s|J_x|\theta,\phi,s\rangle &= j\sin\theta\cos\phi \\ \langle\theta,\phi,s|J_y|\theta,\phi,s\rangle &= j\sin\theta\sin\phi\end{aligned} \tag{3.95}$$

The application of the operator $\hat{R}(\theta,\phi)$ on these states as expectation values cause a rotation of the operator $\boldsymbol{J}$ because

$$\begin{aligned}&\langle j,-j|\mathrm{J}|j,-j\rangle = (0,0,-j) \qquad \text{and} \\ &\langle\theta,\phi|\mathrm{J}|\theta,\phi\rangle = (j\sin\theta\cos\phi,\, j\sin\theta\sin\phi,\, -j\cos\theta)\end{aligned} \tag{3.96}$$

For example the ACS arisen naturally in Rabi oscillations in two level systems. Such as two-level atom (TLA) which has j=1/2, and we make the choice of the ground and excited states as $|1\rangle = |\downarrow\rangle$ and $|2\rangle = |\uparrow\rangle$ with $|1/2,-1/2\rangle$ and $|1/2,1/2\rangle$, respectively, so the ACSs for the TLA is

$$|\theta,\phi\rangle = \cos\left(\frac{\theta}{2}\right)|\downarrow\rangle + e^{-i\phi}\sin\left(\frac{\theta}{2}\right)|\uparrow\rangle \tag{3.97}$$

For now finished with the treatment of ACS, in the next chapters will deal with several results in this and early chapters to show some results of our research.

References

[1] G. Prinz, Phys. Today **45**(4), 58 (1995); G. A. Prinz, Science **282**, 1660 (1998).

[2] J.M. Kikkawa, I.P. Smorchkova, N. Samarth, and D.D. Awschalom, Science **277**, 1284 (1997); J.M. Kikkawa and D.D. Awschalom, Phys. Rev. Lett. **80**, 4313 (1998); D.D. Awschalom and J.M. Kikkawa, Phys. Today **52**(6), 33 (1999).

[3] R. Fiederling *et al.*, Nature **402**, 787 (1999).

[4] Y. Ohno *et al.*, Nature **402**, 790 (1999).

[5] F.G. Monzon and M.L. Roukes, J. Magn. Magn. Mater. **198**, 632 (1999).

[6] S. Lüscher *et al.*, cond-mat/0002226.

[7] D. Loss and D.P. DiVincenzo, Phys. Rev. A **57**, 120 (1998); cond-mat/9701055.

[8] A. Steane, Rep. Prog. Phys. **61**, 117 (1998).

[9] D.P. DiVincenzo and D. Loss, J. Magn. Magn. Mater. **200**, 202 (1999); cond-mat/9901137.

[10]C. H. Bennett and D. P. DiVincenzo, Nature **404**, 247 (2000).

[11] D.P. DiVincenzo, G. Burkard, D. Loss, and E. Sukhorukov, in *Quantum Mesoscopic Phenomena and Mesoscopic Devices in Microelectronics*, eds. I.O. Kulik and R. Ellialtoglu (NATO ASI, Turkey, June 13-25, 1999); see cond-mat/99112445.

[12]E.F. Schubert, Delta-doping of Semiconductors, Cambridge University Press, Cambridge, 1996.

[13] J.H. Blokland, M. Bozkurt, J. M. Ulloa, D. Reuter, A.D. Wieck, P.M. Koenraad, P.C.M. Christianen, and J.C. Maan, Ellipsoidal InAs quantum dots observed by cross-sectional scanning tunneling microscopy, Appl. Phys. Lett. 94 (2009), 023107:1–3.

[14] H. Haug and S.W. Koch, Quantum Theory of the Optical and Electronic Properties of Semiconductors, 3rd ed., World Scientific, Singapore, 2001, pp. 44 48.

[15] G. Bester, S. Nair, and A. Zunger, Pseudopotential calculation of the excitonic fine structure of million-atom self-assembled In17x GaxAs/GaAs quantum dots, Phys. Rev. B 67 (2003), 161306:1–4.

[16] A. Zunger, Pseudopotential theory of semiconductor quantum dots, Phys. Stat. Sol. (b) 224 (2001), pp. 727–734.

[17] M. Bayer, G. Ortner, O. Stern, A. Kuther, A.A. Gorbunov, A. Forchel, P. Hawrylak, S. Fafard, K. Hinzer, T.L. Reinecke, S.N. Walck, J.P. Reithmaier, F. Klopf, and F. Scha¨ fer, Fine structure of neutral and charged excitons in self-assembled In(Ga)As/(Al)GaAs quantum dots, Phys. Rev. B 65 (2002), 195315:1–23.

[18] R.J. Warburton, B.T. Miller, C.S. Durr, C. Bodefeld, K. Karrai, J.P. Kotthaus, G. Medeiros-Ribeiro, P.M. Petroff, and S. Huant, Coulomb interactions in small charge-tunable quantum dots: a simple model, Phys. Rev. B 58 (1998), pp. 16221–16231.

[19] E. M. Purcell, Phys. Rev. 69, 681 (1946).

[20] D. Kleppner, Phys. Rev. Lett. 47, 233 (1981).

[21] P. Goy, J. M. Raimond, M. Gross, and S. Haroche, Phys. Rev. Lett. 50, 1903 (1983).

[22] J.-M. Gérard, B. Sermage, B. Gayral, B. Legrand, E. Costard, and V. Thierry-Mieg, Phys. Rev. Lett. 81, 1110 (1998).

[23] J. J. Hopfield, Phys. Rev. 112, 1555 (1958).

[24] E. Jaynes and F. Cummings, Proc. IEEE 51, 89 (1963).

[25] A. N. Vamivakas, and M. Atatüre, *Contemporary Physics* Vol. 51, No.1. (January-February 2009), 17-36.

[26] A. Boca, R. Miller, K. M. Birnbaum, A. D. Boozer, J. McKeever, and H. J. Kimble, Phys. Rev. Lett. 93, 233603 (2004).

[27] L. Jacak, P. Hawrylak and A. Wojs, *Quantum Dots*, Springer-Verlag, Berlin, 1998.

[28] L. Bányai and S.W. Kock, *Semiconductor Quantum Dots*, World Scientific, Singapore, 1993.

[29] Y. Masumoto and T. Takagahara (Eds.), *Semiconductor Quantum Dots*, Springer, Berlin, 2002.

[30] L. Quiroga and N.F. Johnson**,** Phys. Rev. Lett. **83**, 2270 (1999).

[31] J.H. Reina, L. Quiroga and N.F. Johnson, Phys. Rev. A **62**, 012305 (2000).

[32] D. Erenso, R. Vyas and S. Singh, Phys. Rev. A (submitted).

[33] A Zunger L.W. Wang, J. Kim. Electronic structures of self-organized inas/gaas quantum dots bounded by 136 facets. Physical Review B, 61:2784, 2000.

[34] A Zunger L.W. Wang, J. Kim. Electronic structures of [110]-faceted selfassembled pyramidal inas/gaas quantum dots. Physical Review B, 59:5678, 1999.

[35] D. Bimberg O. Stier, M. Grundmann. Electronic and optical properties of strained quantum dots modeled by 8-band k · k theory. Physical Review B, 59:5688, 1999.

[36]C. Pryor. Eight-band calculations of strained inas/gaas quantum dos compared with one-,four-, and six-band approximations. Physical Review B, 57:7190, 1998.

[37] B. Krummheuer, V. M. Axt, and T. Kuhn, "Theory of pure dephasing and the resulting absorption line shape in semiconductor quantum dots," *Phys. Rev. B*, vol. 65, p. 195313, May 2002.

[38] I. D'Amico and F. Rossi, "Field-induced coulomb coupling in semiconductor macroatoms: Application to single-electron quantum devices," *Appl. Phys. Lett.*, vol. 79, pp. 1676–1678, Sept. 2001.

[39] M. Califano and P. Harrison, "Approximate methods for the solution of quantum wires and dots: Connection rules between pyramidal, cuboidal, and cubic dots," *J. Appl. Phys.*, vol. 86, pp. 5054–5059, Nov. 1999.

[40] S. Gangopadhyay and B. R. Nag, "Energy levels in three-dimensional quantum-confinement structures," *Nanotechnology*, vol. 8, pp. 14–17, Mar. 1997.

[41] M. V. R. Krishna and R. A. Friesner, "Exciton spectra of semiconductor clusters," *Phys. Rev. Lett.*, vol. 67, pp. 629–632, July 1991.

[42] L. W. Wang and A. Zunger, "Electronic-structure pseudopotential calculations of large (approximate-to-1000 atoms) Si quantum dots," *J. Phys. Chem*, vol. 98, pp. 2158–2165, Feb. 1994.

[43] E. Biolatti, I. D'Amico, P. Zanardi, and F. Rossi, "Electro-optical properties of semiconductor quantum dots: Application to quantum information processing," *Phys. Rev. B*, vol. 65, p. 075306, Feb. 2002.

[44] G. Bastard, "Super-lattice band-structure in the envelope-function approximation," *Phys. Rev. B*, vol. 24, pp. 5693–5697, 1981.

[45] P. Harrison, *Quantum Wells, Wires and Dots*. New York: Wiley, 2001.

[46] B. W. Lovett, J. H. Reina, A. Nazir, and G. A. D. Briggs. (2003) Optical schemes for quantum computation in quantum dot molecules. [Online]. Available: http://xxx.lanl.gov/abs/quant-ph/0307021

[47] A. Franceschetti, H. Fu, L. W. Wang, and A. Zunger, "Many-body pseudopotential theory of excitons in InP and CdSe quantum dots," *Phys. Rev. B*, vol. 60, pp. 1819–1829, July 1999.

[48] L. I. Schiff, *Quantum Mechanics*, 2nd ed. McGraw-Hill, 1955.

[49] T. Förster, "Transfer mechanism of electronic excitation," *Disc. Farad. Soc.*, vol. 27, pp. 7–29, 1959.

[50] D. L. Dexter, "A theory of sensitized luminescence in solids," *J. Chem. Phys.*, vol. 21, pp. 836–850, 1953.

[51] (a) J. Sanchez-Mondragon, A. Alejo-Molina, S. Sanchez-Sanchez and M. Torres-Cisneros, "Comparison of the Dicke Model and the Hamiltonianfor n Quantum Dots", *Quantum Dots, Nanoparticles, and Nanoclusters II*, edited by Diana L. Huffaker, Pallab K. Bhattacharya, *Proceedings of SPIE* Vol. 5734 (SPIE, Bellingham, WA, 2005) (b) A. Alejo-Molina, J. J. Sánchez-Mondragón, S. Sánchez-Sánchez, *DETUNING COLECTIVO DEL MODELO DE L PUNTOS CUÁNTICOS,* XLVIII CONGRESO NACIONAL SMF / XVIII REUNION ANUAL AMO GUADALAJARA JALISCO 2005. (c) **Representación de Puntos Cuánticos en la Base Atómica Coherente, S. Sánchez Sánchez,** J. J. Sánchez Mondragón, F. R. Castillo Soria,

Memorias en extenso del LII Congreso Nacional de Física (SMF)/ Reunión Anual de Óptica (AMO). Acapulco Guerrero Octubre de **2009.**

[52] S. Rudin and T. L. Reinecke, Phys. Rev. B 59, 10227 (1999).

[53] R. H. Dicke, Phys. Rev. 93, 99 (1954).

[54] M. Bienert, W. Merkel, and G. Morigi, Phys. Rev. A 69, 013405 (2004).

[55] J. M. Radcliffe, *J. Phys. A* 4 (1971) 313.

[56] (a) F. T. Arecchi, E. Courtens, R. Gilmore and H. Thomas, *Phys. Rev. A* 6 (1972) 2211. (b) A. Perelomov, *Generalized Coherent States and Their Applications* (Berlin: Springer-Verlag, 1986)

[57] S. M. Barnett and P. M. Radmore, *Methods in Theoretical Quantum Optics* (Oxford: Clarendon Press, 1997).

[58] A. S. F. Obada and G. M. Abd Al-Kader, *Journal Of Modern Optics* vol. 50, no. 14 (2003) 2163

[59] M. Tavis and F. W. Cummings, *Phys. Rev.* 170 (1968) 379

[60] Clegg, Robert. *The Vital Contributions of Perrin and Förster*. Biophotonics International, September 2004. Förster, Theodor (1946). *Naturwissenschaften*., Vol. 6, pp 166-175. Förster, Theodor (1948). *Annalen der Physik*, 2, pg. 55-75.

[61] Lackowicz, Joseph. *Principles of Fluorescence Spectroscopy*. Kluwer Academic, 2nd Edition, 1999.

[62] Förster, Theodor (1951). *Fluoreszenz Organischer Verbindungen*. Vandenhoeck & Ruprecht, Göttingen.

[63] Kawaski, A., Kuten, E., & Kaminski, J. *Fluorescence Quenching and Nonradiative Energy Transfer in Solutions*. J. Phys. B: Atom. Molec. Phys., Vol. 6, September 1973. Printed in Great Britain, 1973.

CHAPTER 4

COLLECTIVE AND COOPERATIVE EFFECTS OF QUANTUM DOTS SYSTEMS

Collective and cooperative phenomena are central to the radiation field interaction, particularly for Cavity Quantum Electrodynamics (CQED). The corresponding Dicke model has been studied extensively and is an appropriate reference for the study of the interaction of L Quantum Dots (QDs) with electromagnetic radiation interaction. The collective behavior patterns characteristic of radiation, is not the only evidence of collective response in the case of QDs. Comparison of Rabi frequencies system of the L QDs with the Dicke model frequency is distinguished in that the former has a detuning dynamic mainly due to the Coulomb interaction between QDs force (Förster). We discuss the insight of the detuning of Förster and collective conditions that optimize or minimize the effects of the decoherence thereby we obtaining a highly coherent system. With help of EACs representation we factor out the atomic operators of angular momentum that represent the QDs system. This strategy gives us a very

well alternative way to reach to insight the quantum dynamics involve in this system that in other techniques is more difficult become calculate.

4.1 QDs Hamiltonian in the Basis of Excited Atomic Coherent States (EACs)

EACs as we saw in Chapter 3 are generalized angular momentum states, which by its algebraic features are excellent tools for synthesizing collective systems that can be represented by these operators (in fact made with the same angular momentum operators alone). In the following we will use them to generalize the calculation of matrix elements and diagonalization of the Hamiltonian of QDs. In addition we will use the same basis for the excitons, which allows a broader understanding by viewing these states in the sphere of Bloch.

In this way we use the Hamiltonian for QDS equation (3.50), especially in the rotating frame with equation (3.51)

$$\begin{aligned} H &= \omega\left(a^{\dagger}a + J_z\right) + \Delta' J_z + g\left(J_+ a + a^{\dagger} J_-\right) + W J_+ J_-; \\ &\qquad \Delta' = \Delta + W = \varepsilon - \omega + W \\ H &= \omega a^{\dagger}a + \varepsilon' J_z + g\left(J_+ a + a^{\dagger} J_-\right) + W J_+ J_-; \quad \varepsilon' = \varepsilon - W \\ H_r &= \Delta' J_z + g\left(J_+ a + a^{\dagger} J_-\right) + W J_+ J_- \end{aligned} \tag{4.1}$$

Now with the basis used in the subsection (3.6.1) where the basis that we choose is the basis of eigenstates of J^2 and J_z , $|0\rangle = |j=1, s=-1\rangle$, $|1\rangle = |j=1, s=0\rangle$, $|2\rangle = |j=1, s=1\rangle$. The advantage of using this combined basis with the EACS is that the parameters allows us to use any value *s=m*, for all *m=s= -j,–j+*1*,…,j-*1*,j*. Remaining the matrix elements in terms of ACS, which is a more general solution of this system as we mentioned above. Therefore the analytic matrix elements [2] for the QDs Hamiltonian for the state

$$\begin{aligned} |\theta, \phi, s, n\rangle &= |\theta, \phi, s\rangle \otimes |n\rangle = \hat{R}(\theta, \phi)|s\rangle \otimes |n\rangle \\ &= \exp\left[\frac{1}{2}\theta\left(e^{-i\phi} J_+ - e^{+i\phi} J_-\right)\right]|s\rangle \otimes |n\rangle = \sum_{m=-j}^{j} A_m(\theta, \phi, s)|m\rangle \otimes |n\rangle \end{aligned} \tag{4.2}$$

Where θ, φ, are the spherical coordinates associate with the symmetries of the ACS [2, 7, 8], also *s* is the generalized parameter of the EACS, and *n* represent the number state of field. Thus the analytic matrix elements for the QDs Hamiltonian are

$$\begin{aligned}\left\langle H_r\right\rangle_\tau &= \left\langle \theta',\phi',s',n'\right|H_r\left|\theta,\phi,s,n\right\rangle \\ &= \left\langle \theta',\phi',s',n'\right|\Delta_F J_z + g\left(J_+ a + a^\dagger J_-\right) + WJ_+J_-\left|\theta,\phi,s,n\right\rangle \\ &= \Delta_F\left\langle \theta',\phi',s',n'\right|J_z\left|\theta,\phi,s,n\right\rangle + g\left\langle \theta',\phi',s',n'\right|\left(J_+ a + a^\dagger J_-\right)\left|\theta,\phi,s,n\right\rangle \\ &\quad + W\left\langle \theta',\phi',s',n'\right|J_+J_-\left|\theta,\phi,s,n\right\rangle \\ \left\langle H_r\right\rangle_\tau &= \Delta_F f_{zs}\delta_{n',n} + gf_{+s}\sqrt{n}\delta_{n',n-1} + gf_{-s}\sqrt{n+1}\delta_{n',n+1} + Wf_{\pm s}\delta_{n',n}\end{aligned} \tag{4.3}$$

Where the $f_{(\pm,z)s}$ are the matrix elements for each operator set of the Hamiltonian and $\tau=(\theta,\phi,s)$. Elements are explicitly (see appendix 1) calculated given by

$$\begin{aligned}f_{zs} &= \left[s\delta_{s',s}\delta_{j',j}\cos\theta + \frac{1}{2}\sqrt{(j-s)(j+s+1)}\delta_{s',s+1}\delta_{j',j}\sin\theta e^{-i\phi}\right. \\ &\quad \left. + \frac{1}{2}\sqrt{(j+s)(j-s+1)}\delta_{s',s-1}\delta_{j',j}\sin\theta e^{i\phi}\right] \\ f_{+s} &= \left[\sqrt{(j-s)(j+s+1)}\delta_{s',s+1}\delta_{j',j}\cos^2(\theta/2)\right. \\ &\quad \left. - \sqrt{(j+s)(j-s+1)}\delta_{s',s-1}\delta_{j',j}\sin^2(\theta/2)e^{i2\phi} - s\delta_{s',s}\delta_{j',j}\sin\theta e^{i\phi}\right] \\ f_{-s} &= \left[\sqrt{(j+s)(j-s+1)}\delta_{s',s-1}\delta_{j',j}\cos^2(\theta/2)\right. \\ &\quad \left. - \sqrt{(j-s)(j+s+1)}\delta_{s',s+1}\delta_{j',j}\sin^2(\theta/2)e^{-i2\phi} - s\delta_{s',s}\delta_{j',j}\sin\theta e^{-i\phi}\right]\end{aligned} \tag{4.4}$$

In For a more detailed calculation with these matrix elements, we let them in Appendix 1. After calculating all matrixes element involved in the angular momentum basis we obtain

$$
\begin{aligned}
f_{\pm s} = {} & (j+s)(j-s+1)\delta_{s',s}\cos^4(\theta/2)+(j-s)(j+s+1)\delta_{s',s}\sin^4(\theta/2) \\
& -\sqrt{(j-s)(j+s+1)}\sqrt{(j-s-1)(j+s+2)}\delta_{s',s+2}\cos^2(\theta/2)\sin^2(\theta/2)e^{-2i\phi} \\
& -\sqrt{(j+s)(j-s+1)}\sqrt{(j+s-1)(j-s+2)}\delta_{s',s-2}\cos^2(\theta/2)\sin^2(\theta/2)e^{2i\phi} \\
& +(s+1)\sqrt{(j-s)(j+s+1)}\delta_{s',s+1}\sin^2(\theta/2)\sin\theta e^{-i\phi} \\
& -s\sqrt{(j-s)(j+s+1)}\delta_{s',s+1}\cos^2(\theta/2)\sin\theta e^{-i\phi} \\
& -(s-1)\sqrt{(j+s)(j-s+1)}\delta_{s',s-1}\cos^2(\theta/2)\sin\theta e^{i\phi} \\
& +s\sqrt{(j+s)(j-s+1)}\delta_{s',s-1}\sin^2(\theta/2)\sin\theta e^{i\phi}+s^2\delta_{s',s}\sin^2\theta
\end{aligned}
\tag{4.5}
$$

With the help of Equations (4.4) and (4.5), we compute explicitly the matrix elements in the dual basis, i.e. EACs and excitonic basis in QDs, as shown in the preceding paragraphs and in chapter 3. For this system we have a combined base of six vectors, therefore span a Space Hilbert with a array matrix of 6 x 6 with 36 matrix elements, good many of them null. The matrix is given by

$$
\langle H_r \rangle_s = \begin{pmatrix}
\langle H_{rs} \rangle_{11} & \langle H_{rs} \rangle_{12} & 0 & 0 & 0 & 0 \\
\langle H_{rs} \rangle_{21} & \langle H_{rs} \rangle_{22} & \langle H_{rs} \rangle_{23} & \langle H_{rs} \rangle_{24} & 0 & 0 \\
0 & \langle H_{rs} \rangle_{23} & \langle H_{rs} \rangle_{33} & \langle H_{rs} \rangle_{34} & \langle H_{rs} \rangle_{35} & 0 \\
0 & \langle H_{rs} \rangle_{42} & \langle H_{rs} \rangle_{34} & \langle H_{rs} \rangle_{44} & \langle H_{rs} \rangle_{45} & 0 \\
0 & 0 & \langle H_{rs} \rangle_{53} & \langle H_{rs} \rangle_{45} & \langle H_{rs} \rangle_{55} & \langle H_{rs} \rangle_{56} \\
0 & 0 & 0 & 0 & \langle H_{rs} \rangle_{56} & \langle H_{rs} \rangle_{66}
\end{pmatrix}
\tag{4.6}
$$

Where the no null elements area given by

$$
\begin{aligned}
\langle H_{rs}\rangle_{11} &= -\Delta_F \cos\theta + W\left[2\sin^4(\theta/2)+\sin^2\theta\right],\\
\langle H_{rs}\rangle_{22} &= \frac{\sqrt{2}}{2}\Delta_F \sin\theta e^{i\phi} + 2W\left[\cos^4(\theta/2)+\sin^2\theta\right],\\
\langle H_{rs}\rangle_{33} &= \Delta_F \cos\theta + W\left[2\cos^4(\theta/2)+\sin^2\theta\right]\\
\langle H_{rs}\rangle_{44} &= -\Delta_F \cos\theta + W\left[2\sin^4(\theta/2)+\sin^2\theta\right],\\
\langle H_{rs}\rangle_{55} &= 2W\left[\cos^4(\theta/2)+\sin^4(\theta/2)\right],\\
\langle H_{rs}\rangle_{66} &= \Delta_F \cos\theta + W\left[2\cos^4(\theta/2)+\sin^2\theta\right]
\end{aligned}
\tag{4.7}
$$

The off diagonal symmetric terms and nor symmetric are given by:

$$
\begin{aligned}
\langle H_{rs}\rangle_{23} &= \langle H_{rs}\rangle_{32} = \sqrt{2(n+1)}g\cos^2(\theta/2),\\
\langle H_{rs}\rangle_{34} &= \langle H_{rs}\rangle_{43} = -2W\cos^2(\theta/2)\sin^2(\theta/2)e^{-i2\phi},\\
\langle H_{rs}\rangle_{45} &= \langle H_{rs}\rangle_{54} = \sqrt{2n}g\cos^2(\theta/2)\\
\langle H_{rs}\rangle_{56} &= \langle H_{rs}\rangle_{65} = \sqrt{2(n-1)}g\cos^2(\theta/2)\\
\langle H_{rs}\rangle_{12} &= \frac{\sqrt{2}}{2}\Delta_F \sin\theta e^{i\phi} + \sqrt{2(n+2)}g\cos^2(\theta/2) + \sqrt{2}W\cos^2(\theta/2)\sin^2\theta e^{i\phi},\\
\langle H_{rs}\rangle_{21} &= \sqrt{2(n+2)}g\cos^2(\theta/2),\\
\langle H_{rs}\rangle_{24} &= -\sqrt{2(n+1)}g\sin^2\theta e^{-2i\phi} + \sqrt{2}W\cos^2(\theta/2)\sin\theta e^{-i\phi}\\
\langle H_{rs}\rangle_{42} &= -\sqrt{2(n+1)}g\sin^2(\theta/2)e^{i2\phi}\\
\langle H_{rs}\rangle_{35} &= \sqrt{2n}g\sin^2(\theta/2)e^{-i2\phi}\\
\langle H_{rs}\rangle_{53} &= -\sqrt{2n}g\sin^2(\theta/2)e^{2i\phi},
\end{aligned}
\tag{4.8}
$$

In this matrix, it elements are characterized by trigonometric functions that describe the respective EACs, and they allow for a broader perspective of the behavior of states in the Bloch sphere. It should also be noticed that by making $\theta = 0$, it is obtained the matrix (3.53) computed in chapter 3 as a particular case.

The diagonalization of this matrix is not easy in general form, due to the Hilbert dimensionality span for the vector basis, which is of 6 X 6. The simplest case is when $\theta = 0$, that already was studied in chapter 3. However, in this case, this correspond to a more general type of matrices with elements as function of the EACs which provided more system information through of diagonalization and Bloch's states sphere.

4.2 Förster Collective Dynamic Detuning in the Basis of EACs

In this section we analyze the collective dynamic detuning of Förster on the ESCs basis. This analysis has already demonstrated in references [1, 2, 3, 4] in the case of SU(2) algebra of collective angular momentum operators. In equation (4.3) we have the matrix elements for QDs Hamiltonian

$$\left\langle H_r \right\rangle_\tau = \Delta_F f_{zs}\delta_{n',n} + gf_{+s}\sqrt{n}\delta_{n',n-1} + gf_{-s}\sqrt{n+1}\delta_{n',n+1} + Wf_{\pm s}\delta_{n',n} \tag{4.9}$$

Where $f_{\pm,z,s}$ are the matrix elements given by the expressions (4.4) and (4.5) in general analytic form.

Let us briefly discuss the collective role of this dipole term. According to the JCM and Collective Dicke model, we can rewrite the Hamiltonian for L QDs as

$$H = \omega\hat{N} + \hat{Q}_L - \frac{\omega L}{2} \tag{4.10}$$

Note that the Hamiltonian is in terms of two constants of motion, namely, $[H,N]=[H,Q_L]=0$, such that $[N,Q_L]=0$. The number Operator N, the number of photons and excited atoms that characterize the states in this manifold, is given by

$$\hat{N} = a^\dagger a + J_z + \frac{L}{2} \tag{4.11}$$

The excitation operator off diagonal is

$$\hat{Q}_L = H_{Dk} + H_F \tag{4.12}$$

It is expected that the concept of collectivity that gives rise to the cooperative superradiance in the QDs system, as in the Dicke model, shows in this system. This is confirmed by noticinng that H, $\hat{N}$, and $\hat{Q}_L$ in addition to $\boldsymbol{J^2}$ is also a constant of motion, which commutes with all the others constants of motion.

$$\left[J^2, H\right] = \left[J^2, \hat{N}\right] = \left[J^2, \hat{Q}_L\right] = 0 \tag{4.13}$$

But in particular $J^2, \hat{N}$ commute with H_{Dk}, and H_F respectively, although the latter two do not commute with each other

$$\left[\hat{N}, H_F\right] = \left[\hat{N}, H_{Dk}\right] = 0, \text{ and } \left[J^2, H_F\right] = \left[J^2, H_{Dk}\right] = 0 \tag{4.14}$$

The Förster's term, in the Hamiltonian of the QDs, introduces considerable dynamic implications in their eigenfunctions [3, 4], even at the lower order terms. This section shows that the Förster detuning has an atomic dependence and therefore a collective variation. For convenience, we will work on resonance $(\Delta = 0)$. The terms H_F and H_{Dk} are not diagonal in an atomic Dicke states representation, and with help of the EACS have they will have the following matrix elements:

$$\begin{aligned}
f_s &= \langle L, \theta', \phi', s', n' | H_F | L, \theta, \phi, s, n \rangle = \langle L, s' | H_F | L, s \rangle = \langle L, s' | J_+ J_- - J_z | L, s \rangle \\
h_{+,s} &= \langle L, \theta', \phi', s', n' | H_{Dk} | L, \theta, \phi, s-1, n \rangle = \langle L, s' | H_{Dk} | L, s-1 \rangle = \langle L, s' | J_+ a | L, s-1 \rangle \\
h_{-,s} &= \langle L, \theta', \phi', s'-1, n' | H_{Dk} | L, \theta, \phi, s, n \rangle = \langle L, s'-1 | H_{Dk} | L, s \rangle = \langle L, s'-1 | J_- a^\dagger | L, s \rangle
\end{aligned} \tag{4.15}$$

Whose explicit expressions are given with the help of Equations (4.4) and (4.5), where

$$\begin{aligned}
f_s &= \left(f_{\pm s} - f_{zs}\right)\delta_{n',n} \\
h_{+,s} &= f_{+,s-1}\sqrt{n}\,\delta_{n',n-1} \\
h_{-,s} &= f_{-,s'-1}\sqrt{n+1}\,\delta_{n',n+1}
\end{aligned} \tag{4.16}$$

As demonstrated above N is a constant of motion, and in that manifold the states that are directly coupled by the interaction can be diagonalized in Dicke states representation. An interesting and solvable case is given when we chose $\theta = 0$ in the EACs. Those elements are reduced to a simpler form at function of normal matrix elements of quantum angular momentum.

Let us assume that we could diagonalize that Hamiltonian, in that case the respective eigenvalues could take the form $\lambda_{\pm} = \gamma_0 \pm \gamma$ and they should share some general properties:

$$\gamma_0 = \frac{1}{2}\mathrm{Trace}\langle H_F \rangle = \frac{1}{2}(\lambda_+ + \lambda_-) = \frac{1}{2}(f_s + f_{s-1}) \tag{4.17}$$

And

$$\lambda_+\lambda_- = \mathrm{Det}\langle Q_L \rangle = \gamma_0^2 + \gamma^2 = f_s f_{s-1} - h_{\pm,s}h_{\pm s}^* \tag{4.18}$$

Where, from equations (4.16) we have $h_{\pm,s}$ which meaning that $h_{+,s} = h_{-,s}$, it is because as already we discuss more above, these elements are draw with the first term, therefore

$$\gamma^2 = \left|h_{\pm,s}\right|^2 + \frac{1}{4}\mathrm{W}^2\langle L,s'|J_+J_-|L,s\rangle \frac{\left[\langle L,s'|J_+J_- - J_z|L,s\rangle - \langle L,s'-1|J_+J_- - J_z|L,s-1\rangle\right]^2}{\langle L,s'|J_+J_-|L,s\rangle} \tag{4.19}$$

Or in more compact form

$$\gamma^2 = \left|h_{\pm,s}\right|^2 + \frac{\mathrm{W}^2}{4}\frac{L+1-s}{s}\left(1 - \frac{s}{L+1-s}\right)^2 \tag{4.20}$$

$\left|h_{\pm,s}\right|^2$ is identified as the diagonalization of the Dicke Hamiltonian, and therefore as the Rabi's frequency Ω_{QD}. Therefore, this term is given as a correction to the Dicke's frequency Ω_{Dk}, previously determined in references [1], as

$$\Omega_{QD}^2 = \Omega_{Dk}^2 + \Delta_F^2 \tag{4.21}$$

Where the Förster's dynamic detuning is given by

$$\Delta_F^2 = \frac{\mathrm{W}^2}{4}\frac{L+1-s}{s}\left(1-\frac{s}{L+1-s}\right)^2$$

$$\Delta_F = \sqrt{\frac{\mathrm{W}^2}{4}\frac{L+1-s}{s}\left(1-\frac{s}{L+1-s}\right)^2} \tag{4.22}$$

$$\Delta_F = \frac{\mathrm{W}}{2}\sqrt{\frac{L-s+1}{s}}\left(1-\frac{s}{L-s+1}\right)$$

The plot of equations (4.18) is show at figures 4.1 and 4.2 in order to values of *L* and *s*:

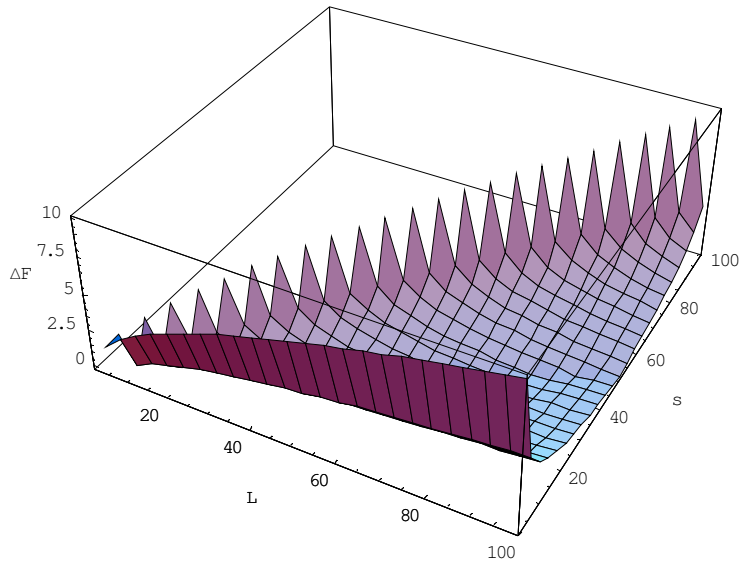

Figure 4.1 Förster Dynamic Collective Detuning: The plot shows Δ_F as a function of *L* and *s*. Note that detuning becomes meaningful only if *s*=1 or *s=L.*

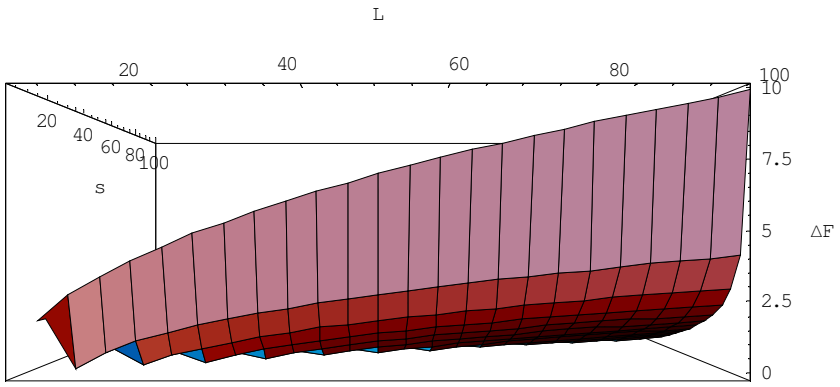

Figure 4.2 another perspective of the Förster Dynamic Collective Detuning: The plot shows Δ_F as a function of *L* and *s*. Note that detuning becomes meaningful only if *s*=1 or *s=L.*

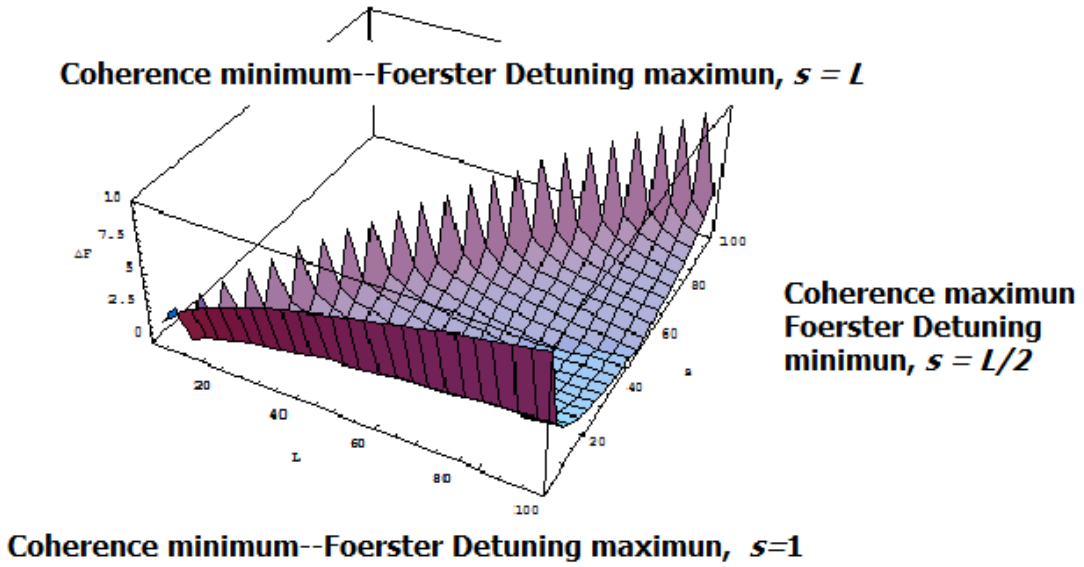

Figure 4.3 In this picture we show more specifically the Förster Dynamic Collective Detuning with maximum and minimum coherence: The plot shows Δ_F as a function of L and s. Note that detuning becomes meaningful only if s=1 or s=L.

We should note that it is very interesting to atomic dependence shown in figure 4.1 and 4.2, but in particular the values that are relevant to occurrence of a collective behavior $s=L/2$; with equations (4.21) and (4.22), we get

$$\Omega_{QD}^2 = \Omega_{Dk}^2 + \frac{\mathrm{W}^2(L-1)}{4L} \qquad s=1 \quad \text{and} \quad s=L$$

$$\Omega_{QD}^2 = \Omega_{Dk}^2 + \frac{\mathrm{W}^2}{L(L+2)} \qquad s=L/2 \tag{4.23}$$

These expressions show that the Förster frequency dynamics for L large become negligible when collective behavior is dominant. The contribution of Förster term the QDs Hamiltonian produces a dynamic detuning, which is not noticeable in the case of a QD and in collective behavior. Therefore, there is no difference significant to the JCM, although with increasing the number of QDs becomes substantial differences with Dicke model, but is evident that they must appear for

a large group of QDs. It shows further that the in Förster dynamics detuning, there are two phases: one of them is a constant detuning and other one is proportional to the atomic state- These features point out the difference between the semiclassical model descriptions, and Quantum Electrodynamics model.

4.3 Representation of Quantum Dots in the Basis of ACs

In this section once again we used the ACS [5-7] to find a system of coupled differential equations in the Heisenberg picture and the full QDs Hamiltonian in turn reduces the equations to find a semiclassical collective dynamics of the system.

QED interaction between EM fields and atomic systems has been crucial for understand the radiative properties, its complexity has made it known accurately and completely to a single atom, first described by a classical EN field (semiclassical model) and then fully QED, which correspond to the Tavis-Cummings model [9] or JCM. These multi-atomics systems have been derived and the Dicke model [10] which has been studied in an approximate collective effects [1, 2, 11, 12].

As we talked earlier in previous sections and chapter 3, more realistic systems require consideration of other interactions, such as Förster interaction in semiconductor QDs, which is an interaction between QDs, but not through electromagnetic field. This is the difference introduced by Quiroga in collective Hamiltonian [4] as a system of Cavity Quantum Electrodynamics (CQED) for the QDs and Dicke system. These systems are of great interest because it has been show experimentally the entanglement or quantum entanglement [5], "antibunching" and Rabi oscillations [6], but has not explored the interaction between non-radiative QDs corresponding to non-linear Förster term in the Hamiltonian [7], (see expressions (3.47) and (3.49)).

Atomic Coherent States (ACS) have been used only in a context purely atomic, i.e. systems a few atoms to many two level atoms [8]. In this work we give them a wider use, when applied to groups of L QDs systems in order to factoring the expectation value of the nonlinear Förster term in the Hamiltonian.

The description of the ACS was carried out in chapter 3, and previous sections as particular case of the EACS. In this section we calculate the evolution equations for operators [2, 11] in the Heisenberg picture. These equations are calculated using the Heisenberg equation brackets, giving a differential system with the Hamiltonian operators, i.e. with the Hamiltonian (3.49) or equation (4.1) in this chapter, here we have the Förster term as a non-linearity. Starting from this Hamiltonian we find their commutator and switches with each operator involved to find the respective equations, this are

$$\frac{dJ_+}{dt} = i\left[H, J_+\right] + \frac{\partial J_+}{\partial t} = i\left(\varepsilon' J_+ - 2ga^\dagger J_z - 2WJ_+ J_z\right),$$

$$\frac{dJ_-}{dt} = i\left[H, J_-\right] + \frac{\partial J_-}{\partial t} = -i\left(\varepsilon' J_- + 2ga^\dagger J_z + 2WJ_z J_-\right), \tag{4.24}$$

$$\frac{dJ_z}{dt} = i\left[H, J_z\right] + \frac{\partial J_z}{\partial t} = -ig\left(J_+ a - a^\dagger J_-\right);$$

$$\frac{da^\dagger}{dt} = i\left[H, a^\dagger\right] + \frac{\partial a^\dagger}{\partial t} = i\left(\omega a^\dagger + gJ_+\right); \qquad \frac{da}{dt} = i\left[H, a\right] + \frac{\partial a}{\partial t} = -i\left(\omega a + gJ_-\right)$$

In this system we have that only three equations are independent because only we need a conjugate operator or well only a conjugate into the operators of angular momentum and the quantized EM field.

4.3.1 Semiclassical Model and numerical solutions

The semiclassical picture that arises from the EM coherent states is one of the most interesting and useful for practical purposes. Therefore, it is a convenient question to consider if we could carry on a similar analysis in the collective atomic case. In this subsection we discuss a simpler model of the system Eq. (4.24). Let us assume that initial atomic state correspond to the ACS, therefore the collective

atomic operator could be changed by its corresponding amplitudes in the angular momentum operators (with SU(2) algebra). This is derived simply by calculating the expectation values with the ACS basis, making the equations in scalar form, where the products of the expectation value operators are factorized. However the Förster term becomes nonlinear and our possibility is to numerically solve it. We have conveniently denoted by [2]:

$$\langle\theta,\phi|J_+|\theta,\phi\rangle = f_+; \quad \langle\theta,\phi|J_-|\theta,\phi\rangle = f_-; \quad \langle\theta,\phi|J_z|\theta,\phi\rangle = f_z \tag{4.25}$$

And analogously for the operators $J_x,\ J_y$ by

$$\langle\theta,\phi|J_x|\theta,\phi\rangle = f_x; \quad \langle\theta,\phi|J_y|\theta,\phi\rangle = f_y; \quad \langle\theta,\phi|J_z|\theta,\phi\rangle = f_z \tag{4.26}$$

Therefore to obtain the actual semiclassical system, we have to consider that the interaction electromagnetic field is time independent, defined as real amplitude, i.e. $a \Rightarrow \alpha$, we get a coupled differential equations system nonlinear scalar, which can be solved numerically, so

$$\begin{aligned} f_x' &= \frac{df_x}{dt} = (-\varepsilon')f_y + 2Wf_yf_z \\ f_y' &= \frac{df_x}{dt} = (\varepsilon')f_x - 2g\alpha f_z - 2Wf_xf_z \\ f_z' &= \frac{df_x}{dt} = 2g\alpha f_y. \end{aligned} \tag{4.27}$$

Where $\varepsilon'=\varepsilon - W$ is the Förster detuning defined at equation (4.1) and chapter 3, W is interaction Förster constant. The constant α is amplitude of classical field and g is interaction constant coupling between field and dots.

This coupled differential system can be solved by numerical techniques. But we have careful to observe that the variables are not only coupled by the field but also by the nonlinearity in the terms J_zJ_y and J_zJ_x for (4.27) in the Real part. It is easy to realize that in spite of this nonlinearity, these equations preserve the

Norm, and that in the absence of field this term corresponds to a detuning correction in terms of the expectation value of the atomic inversion constant. If we choose α as a parameter very small, we can see clearly the impact of Förster constant *W*. This should lead us to sinusoidal oscillations to the QDs operators, as we display below where we are going to keep constant the EM field α and the dipole coupling g, but vary the collective ε detuning and the dipole-dipole coupling W, as the competing variables. Before we show the analytic limit cases for de system (4.27), and we perform the solutions in this limit, i.e. if we have that the Förster constant is W =0, then

$$\begin{aligned} f_x' &= \frac{df_x}{dt} = -\varepsilon' f_y \\ f_y' &= \frac{df_x}{dt} = \varepsilon' f_x - 2g\alpha f_z \\ f_z' &= \frac{df_x}{dt} = 2g\alpha f_y \end{aligned} \tag{4.28}$$

In this case we have harmonic solutions with frequency $\Omega = \sqrt{4g^2\alpha^2 + \varepsilon'^2}$

Another case is when $\Omega = \varepsilon' = \alpha = 0$, so we have,

$$\begin{aligned} f_z' &= 0 \Rightarrow f_z = f_0 \ \text{ Constant} \\ f_x' &= \frac{df_x}{dt} = 2Wf_0 f_y \\ f_y' &= \frac{df_x}{dt} = -2Wf_0 f_x \end{aligned} \tag{4.29}$$

Too harmonic solutions with frequency $\Omega_W = 2Wf_0$.

We can concluded that

$$\begin{aligned} & f_x f_x' + f_z f_z' + f_y f_y' = 0 \\ & \Rightarrow \text{ Constant Norm} \end{aligned} \tag{4.30}$$

Now we give the numerical results of the system (4.27), with parameters:

$$W = 0.0,\ \ \varepsilon = 1.8,\ \ g = 3.0,\ \ \alpha = 1/25.$$
$$W = 0.5,\ \ \varepsilon = 1.8,\ \ g = 3.0,\ \ \alpha = 1/25.$$
$$W = 0.3,\ \ \varepsilon = 2.0,\ \ g = 3.0,\ \ \alpha = 1/25.$$
$$W = 0.3,\ \ \varepsilon = 2.0,\ \ g = 3.0,\ \ \alpha = 1/25.$$

So with these parameters the plots are

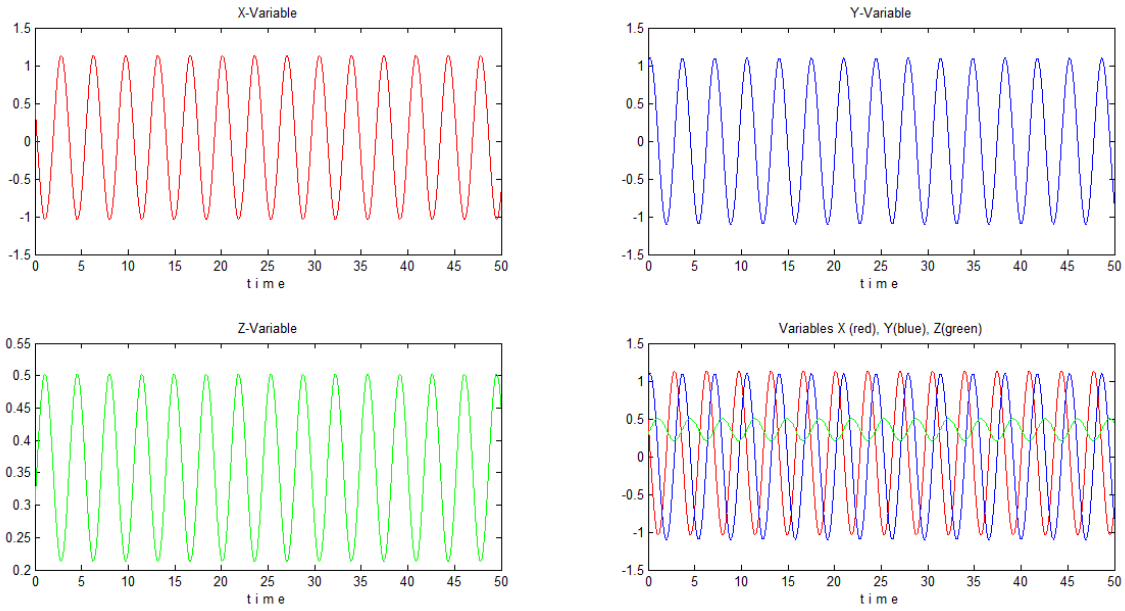

Figure 4.4 Semiclassical behaviors by the system of QDs with parameters: $W = 0.0,\ \ \varepsilon = 1.8,\ \ g = 3.0,\ \ \alpha = 1/25.$ We can observe that oscillations correspond to a case when there are not Förster Interaction, but there are collective radiation (classical)-matter interaction, type Dicke with Rabi oscillations, this indicate that behavior is correct with respect to the Dicke Hamiltonian.

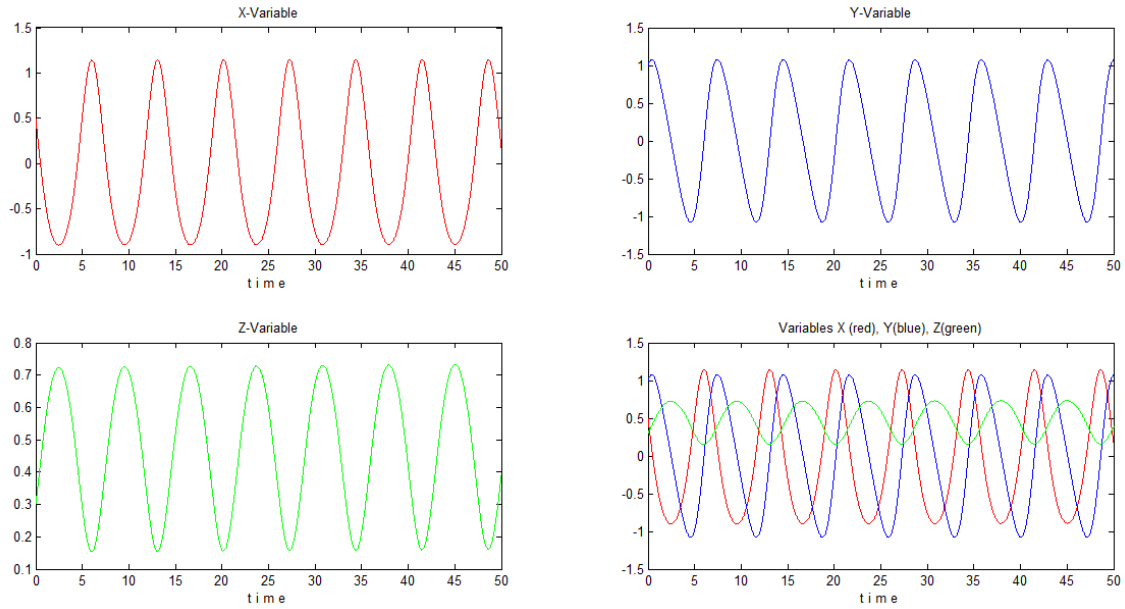

Figure 4.5 Semiclassical behaviors of a QDs system with parameters: $W = 0.5,\ \varepsilon = 1.8,\ g = 3.0,\ \alpha = 1/25.$ In this case we can observe that there is Förster Interaction, with oscillations type Rabi too. This collective radiation (classical)-matter interaction type show Rabi oscillations, however notice the role of the dipole-dipole.

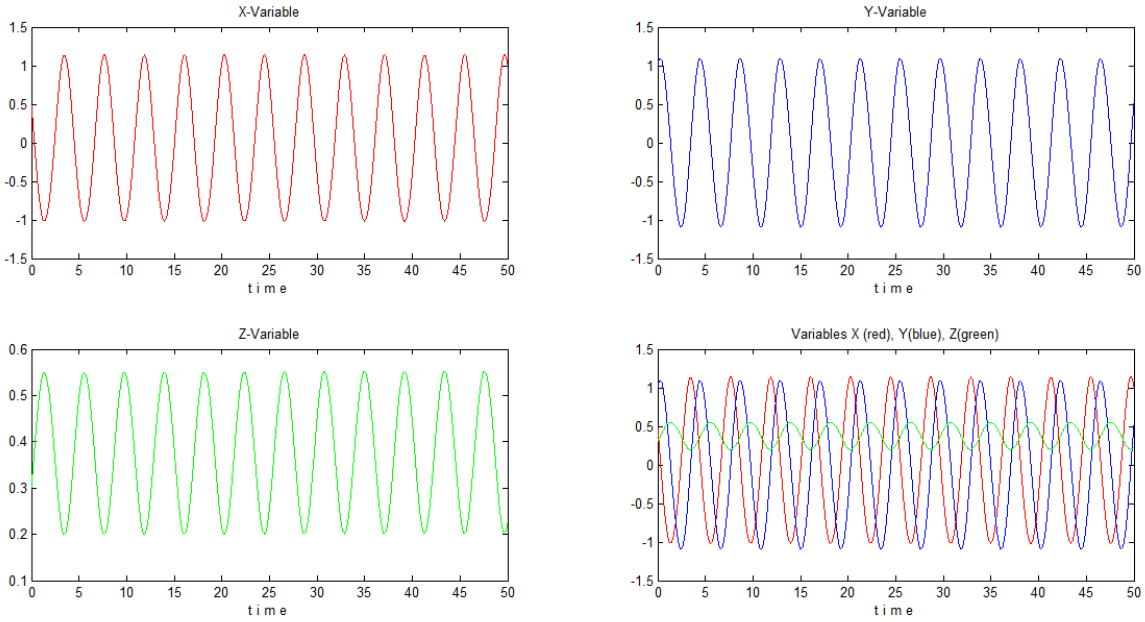

Figure 4.6 Semiclassical behavior of a QDs system with parameters: $W = 0.3,\ \varepsilon = 2.0,\ g = 3.0,\ \alpha = 1/25.$ In this case we can observe that there is Förster Interaction, with oscillations type Rabi too, and dipole-dipole coupling.

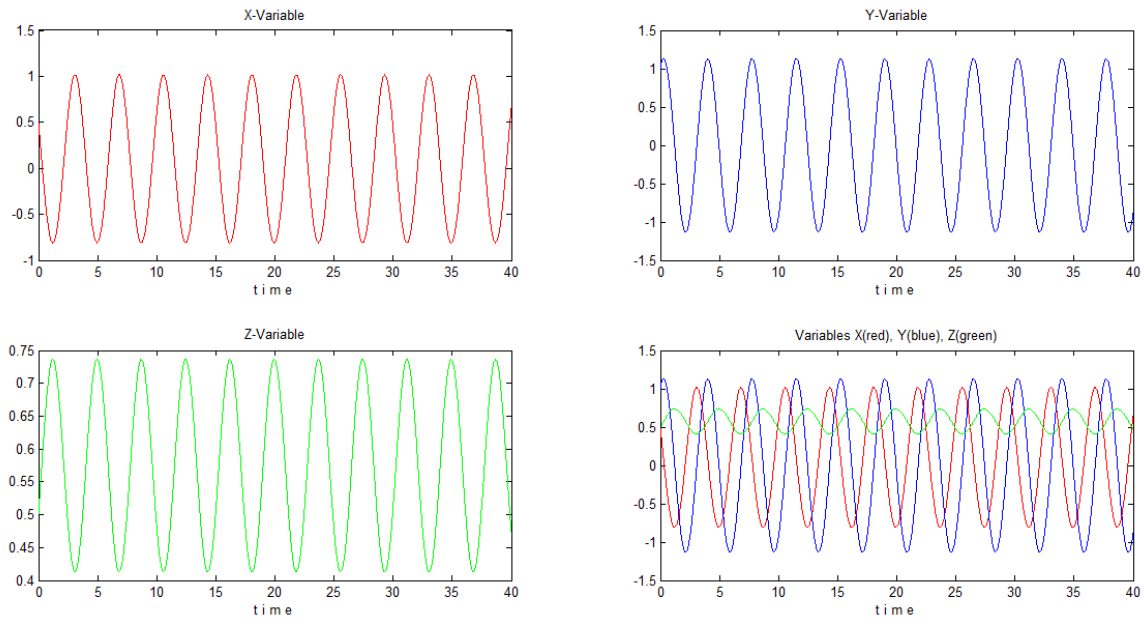

Figure 4.7 Semiclassical behaviors by the system of QDs with parameters: $W = 0.3,\ \varepsilon = 2.0,\ g = 3.0,\ \alpha = 1/25.$ In this case we can observe that there is Förster Interaction, with oscillations type Rabi too. This collective radiation (classical)-matter interaction type show Rabi oscillations. With Runge-Kutta numerical method

CONCLUSIONS OF CHAPTER 4

In this chapter we research the collective dynamics of QDs systems at different stages. On the hand we compare the QDs Hamiltonian which includes the Förster term, with that Dicke model. We were able to calculate and plotting display different behaviors as limiting cases, noting that for a QD the difference with atomic model for a single atom, better known as JCM there is no big difference. For collective case of the Dicke model versus nonlinear QDs Hamiltonian becomes substantial because to the interaction of Förster (FRET). On the other hand we study the implementation of EACS in order to factor out as a resource for the atomic operators, and so we able to work in the Heisenberg picture with a Differential Equation Coupled System.

Besides EACS serving to factor out the atomic operators representing the nonlinearity in the QDs Hamiltonian, the use of coherent atomic states allows us to easily recognize the modulation produced by the interaction of Förster. We show that the oscillations are similar to the collective dynamics of quantum dots due to the Förster interaction term with those of the Dicke model dynamics, which is

collective but with linear characteristics. This opens a wide panorama of exploration than usual with help of these atomic states.

REFERENCES

[1] (a) J. Sanchez-Mondragon, A. Alejo-Molina, S. Sanchez-Sanchez and M. Torres-Cisneros, "Comparison of the Dicke Model and the Hamiltonianfor *L* Quantum Dots", *Quantum Dots, Nanoparticles, and Nanoclusters II*, edited by Diana L. Huffaker, Pallab K. Bhattacharya, *Proceedings of SPIE* Vol. 5734 (SPIE, Bellingham, WA, 2005) (b) A. Alejo-Molina, J. J. Sánchez-Mondragón, S. Sánchez-Sánchez, *DETUNING COLECTIVO DEL MODELO DE L PUNTOS CUÁNTICOS,* XLVIII CONGRESO NACIONAL SMF / XVIII REUNION ANUAL AMO GUADALAJARA JALISCO 2005.

[2] S. Sánchez Sánchez, J. J. Sánchez Mondragón, F. R. Castillo Soria, *Representación de Puntos Cuánticos en la Base Atómica Coherente*; Memorias en extenso del LII Congreso Nacional de Física (SMF)/ Reunión Anual de Óptica (AMO). Acapulco Guerrero Octubre de 2009.

[3] L. Quiroga and N. F. Johnson, Phys. Rev. Lett. 83, 2270 (1999).

[4] J. H. Reina, L. Quiroga, and N. F. Johnson, Phys. Rev. A. 62, 012305 (2000).

[5] J. M. Radcliffe, *J. Phys. A* 4 (1971) 313.

[6] (a) F. T. Arecchi, E. Courtens, R. Gilmore and H. Thomas, *Phys. Rev. A* 6 (1972) 2211. (b) A. Perelomov, *Generalized Coherent States and Their Applications* (Berlin: Springer-Verlag, 1986)

[7] S. M. Barnett and P. M. Radmore, *Methods in Theoretical Quantum Optics* (Oxford: Clarendon Press, 1997).

[8] A. S. F. Obada and G. M. Abd Al-Kader, *Journal Of Modern Optics* vol. 50, no. 14 (2003) 2163

[9] M. Tavis and F. W. Cummings, *Phys. Rev.* 170 (1968) 379

[10] R. H. Dicke, *Phys. Rev.* 93 (1954) 99.

[11] Edited by L. Mandel and E. Wolf, *Coherence and Quantum Optics.*, vol. 5**,** (New York, Plenum).

[12] S. M. Chumakov, A. B. Klimov and J. J. Sanchez-Mondragon, "Collective atomic dynamics in a strong quantum field".

CHAPTER 5

Q-BIT ENTANGLEMENT MESURMENT FOR A REDUCED QDs SYSTEM

The greatest challenge of quantum computing and quantum information is the physical realization and implementation of a real quantum computer. The first problem which is designing a physical system that allows us to build and control the so call Quantum bit (qubit). The qubit is the fundamental unit of quantum processing, so unlike his classic bit counterpart, the latter has been implemented satisfactorily, but the implementation of qubit is more problematic because it is a mathematical entity type yet. Wherefore become to a physical reality is no easy task for two reasons: first because it is not to keep a quantum system with feature that the superposition without being destroyed by the environment, the other one is perhaps the most complex to perform, is due to Quantum Entanglement of qubits to be kept in order to transferring and processing information, which is also dissipated and destroyed by the classical physical environment that they are surrounded. Because these qubits suffer a loss of coherence (Decoherence), which is indispensable in quantum system if want to keep all the quantum properties of superposition and entanglement. Already Di Vincenzo [42-44] gave the main criteria (*Di Vincenzo Criteria*) in order to the physical implementation and performs

of quantum processor (For more complete study sees Appendix 2 and references [1, 42-44]). The Entanglement of quantum systems is a key aspect in order to understand the dynamics and behavior of mixed systems (density matrix) as bipartite systems of quantum bits (q-bits). A quantifiable measure widely used is the *Entanglement of Formation* [12, 13] of a mixed state, defined as the minimum number of singlets needed to create an ensemble of pure states that represents the density matrix of the system. In this chapter considering a double quantum dot system coupled cavity type Jaynes-Cummings investigate the entanglement between two quantum dots, immersed each in its own cavity, showing analytically that entanglement has a very interesting effects such as temporal evolution including the so-called sudden death effect.

In this chapter we research a system compose for two QDs embedded in own cavity, where this pair is previously entangled before that these QDs are introduced into cavity. We will study in Cavity-Quantum Electrodynamics (CQED) context. We will give an introduction to the concepts and subjects we needed for insights the study of our system, into sections 5.1, 5.2 and 5.3. For more complete reviews of these affairs about quantum computing and quantum information you refer to Appendix 2 and the references cited here and there in. We want to clarify that this is neither a chapter nor thesis on the implementation of physical systems (QDs) for quantum computing. It is just a proposal on CQED context where we develop the main calculations, supported also by Entanglement of Formation theory [12, 13] (see section 5.3) as a quantitative measure for the entanglement between our qubits: i.e. our two QDs more cavities system.

5.1 Introduction

For several years, many authors have studied entanglement because its enormous importance at its fundamental level and because its applications to quantum information and quantum computing [1]. Entanglement has marked a new way to reinterpret the quantum nature of computer technology due to the incorporation of quantum processing units with so-called quantum bits (q-bits), represented as dual units that open up infinite possibilities of parallel processing, at least theoretically, much faster than any classical computational process. However this has been the case at the theoretical level, therefore it is essential to implement physical models that allow the incorporation of this development into feasible systems or where the technological inertia may lead to, and one of the most visible are Quantum Dots. In spite that we usually refer to Quantum Dots as Atom like structures, there are substantial differences such as the exchange

interaction (Forster interaction) [20] which has been used as the basis for proposals of quantum computation, and therefore deserve a careful analysis.

Quantum entanglement has played very important roles in quantum information processing such as quantum teleportation, [1, 2] quantum cryptographic, [3] quantum dense coding,[4] and parallel computing [5]. Therefore a precise measurement is needed to quantify the degree of entanglement for those q-bits system in collaboration or competition with such exchange interaction. This is more interesting because the physical character and mathematical structure of entangled states have not been well understood and the Forster interaction tuning opens new possibilities to deal with its fundamental questions. There are two important problems for entanglement. One is to find a method to determine whether a given state is separable (or not entangled), and the other one, it is to define the best measurement quantifying an amount of entanglement of a given state. In order to solve the first problem, much effort has been made. [6-8]. The quest for proper measurement of entanglement has received also a great deal of attention. The entanglement of formation, distillation, and relative entropy, [9-11] negativity, [12] concurrence, [12, 13] concurrence related measures, or positive operator are used to investigate entanglement. Although the entanglement of formation is defined for arbitrary-dimensional bipartite systems, so far no explicit analytic formulates for entanglement of formation have been found for systems larger than a pair of qubits, except for some special symmetric states. [14].

Another serious problem that must be considered in entanglement, as mentioned earlier, in a quantum system is it may deteriorate due to interaction with background noise or with other systems usually called environments. Interest was originally concerned with the consequences for quantum measurement and the quantum-classical transition [15–17]. More recently, entanglement decoherence has been studied in connection with obstacles to realize various quantum information processing schemes. T. Yu and Eberly have shown that entanglement can decay to zero abruptly, in a finite time, a phenomenon termed entanglement sudden death [18, 19].

Such quantum correlations are responsible for much of the challenge in understanding interacting many-body quantum systems, and it is therefore of fundamental importance to have quantitative knowledge of these correlations. Progress in quantum information theory has led to the development of new measures of the inseparability of a quantum state, and in the last few years these measures have been used to assess the quantum correlations in diverse physical systems. Concurrence [12, 13] is an especially useful metric for such studies because it can be applied to mixed as well as pure states. It therefore can be used to quantify the thermal entanglement in a system at nonzero temperature. It can also be applied to evaluate the inseparablilty of an equal incoherent mixture of degenerate energy eigenstates. However as we mentioned above, concurrence is defined only for a pair of qubits. Since a qubit is formally equivalent to a spin-1⁄2

particle when only the spin degree of freedom of the latter is considered, this has led to several analyses of the thermal entanglement between a pair of interacting spin-1/2 particles.

The entanglement of formation, another important entanglement measure, can be calculated directly from the concurrence and is monotonically related to it. The method of calculating the concurrence for more general density matrices can be found in Wootters [13].

The importance of this issue is to find necessary and sufficient conditions for the development of quantum computer systems in their physical implementation (hardware) and the new rules of quantum processing (software). In our case we focus on studying the physical implementation on a fundamental level [20], seeking the most appropriate quantum physical system of many systems studied in quantum physics for many decades to more sophisticated atomic systems with cooperative and collective effects. Up until now, such quantum-mechanical computers have been proposed in terms of trapped ions and atoms [21], cavity quantum electrodynamics (QED) [22], nuclear magnetic resonance [23], Josephson junctions [24], and semiconductor nanostructures [25] schemes. All of the above proposals have decoherence and operational errors as the main obstacles for their experimental realization, which pose much stronger problems here than in classical computers. There is much current excitement about the possibility of using solid-state-based devices for the achievement of quantum computation tasks. In particular, semiconductor nanostructure fabrication technology is well developed and hence offers us a wide and promising arena for the challenging project of building quantum information processors. Because of their quantum-mechanical nature and their potential scalability properties, semiconductor quantum dots (QDs) are very promising candidates for the implementation of quantum computing processes. Several solid-state design schemes for quantum computation have been proposed to date: Kane [25] has proposed a scheme that encodes information onto the nuclear spins of donor atoms in doped silicon electronic devices where externally applied electric fields are used to perform logical operations on individual spins. Loss and Di-Vincenzo[25] have presented a scheme based on electron spin effects, in which coupled quantum dots are used as a quantum gate. This scheme is based on the fact that the electron spins on the dots have an exchange interaction (Forster interaction) [20] which changes sign with increasing external magnetic field.

5.2 Quantum Computing and Quantum Information Theory

Strictly spoken, the mathematical formulation of quantum mechanics, which was shortly introduced in chapter 2, is not a physical theory in its own right, but rather provides a framework to formulate physical theories within. Depending on how exactly the Hilbert spaces and Hamiltonians are constructed, different theories to arise, from non-relativistic quantum electrodynamics, which still maintains many formal analogies to classical physics, to quantum chromo-dynamics which introduces entities like quarks and gluons which are completely meaningless outside the scope of quantum mechanics. Quantum computing is yet another theory on top of the abstract quantum mechanical formalism. It is, however, not a physical theory in the sense that it tries to accurately describe natural processes, but is built on abstract concepts like quantum-bits (qbits) and quantum gates, without regard to the underlying physical quantum-dynamical model.

The basic idea of modern computing science is the view of computation as a mechanical, rather than a purely mental process. In 1936, Alan Turing formalized this concept by constructing an abstract device, now called *Turing-Machine*, which he proved to be capable of performing any effective (i.e. mechanical, algorithmic) computation. At about the same time, Alonzo Church showed that any function of positive integers is effectively calculable only if recursive. Both findings are, in fact, equivalent and are commonly referred to as the *Church-Turing Thesis*. In its strong form, it can be summarized as: *Any algorithmic process can be simulated efficiently using a Turing machine.*

This means that, no matter what type of machine is actually used for a certain computation, an equivalent Turing Machine can be found which solves the same problem with only polynomial overhead. The strong Church-Turing Thesis came under attack when in 1977 Robert Solovay and Volker Strassen published a fast Monte-Carlo test for primality [1, 31], a problem for which no efficient deterministic algorithm was known at that time [In 2002, Manindra Agrawal, Neeraj Kayal and Nitin Saxena eventually found a deterministic primality test [32] with a worst case time complexity of $O(n12)$.]

While this challenge could easily be resolved by using a probabilistic Turing Machine, it raises the question whether even more powerful models of computation exists. In 1985, David Deutsch adopted a more general approach and tried to develop an abstract machine, the Universal Quantum Computer, which is not targeted at some formal notion of computability, but should be capable of effectively simulating an arbitrary *physical system* and consequently any realizable computational device [33, 36].

Deutsch also described a simple quantum algorithm which would be capable of determining in a single step whether a given one-bit oracle function $f:\mathrm{B}\to\mathrm{B}$ *f*is either constant or balanced. The algorithm was later generalized for *n*-bit functions $f:\mathrm{B}^n\to\mathrm{B}$ (Deutsch-Jozsa problem [35]) and demonstrates that a quantum computer is indeed more powerful than a probabilistic Turing machine.

At the same time, Richard Feynman showed how local Hamiltonians can be constructed to perform arbitrary classical computations [38]. In 1994, Peter Shor demonstrated how prime factorization and the calculation of the discrete logarithm could be efficiently performed on a quantum computer [40]. The immense practical importance of these problems for cryptography made Shor's algorithm the *killer-application* of quantum computing. One year later, Lov Grover designed a quantum algorithm for finding a unique solution to *Q(x)* = 1 in an unstructured search space of size *n*, requiring only *O*(*p n*) evaluations of the black-box oracle function *Q* [39]. At this time, Peter Zoller and Ignacio Cirac demonstrated how a linear ion trap can be used to store qubits and perform quantum computations [41]. In 2001, a team at IBM succeeded to implement Shor's algorithm on an NMR based 7-qubit quantum computer to factorize the number 15, [37].

5.3 Concurrence and Entanglement of Formation

Entanglement is a quality of quantum mechanics, which corresponds to the presence of nonlocal correlations between different parts of a system that cannot be explained classically. A pure state of a pair of quantum systems (bipartite) is called entangled if it is not factorizable (i.e., if the state total cannot be written as a product of states of the particle) and a mixed state is entangled if it can be represented as the mixed state pure factorizable [12]. One can define the concept of entanglement for mixed quantum states, as mixed state is entangled if it cannot be represented as a mixture of unentangled pure states. For both pure and mixed quantum states, there are good measures of the degree of entanglement. In the case of pure states of a bipartite system there is a single widely accepted measure of entanglement, whereas for mixed states of such systems there are three measures [9, 11, 26] that have been extensively studied. One of these, entanglement of formation, is a subject of this paper. We will use Wootters' concurrence [12, 13] as our measure in this discussion, mainly for its relevance for mixed states and the convenience of its definition and normalization.

A pure $|m\rangle\otimes|n\rangle$, ($m\le n$) quantum state $|\psi\rangle$ is a normalized vector in the tensor product $H_A\otimes H_B$ of two Hilbert spaces H_A and H_B for systems *A* and *B*. The entanglement of formation is defined to be $E(|\psi\rangle)=S(\rho_A)$ where $\rho_A\equiv Tr_B(|\psi\rangle\langle\psi|)$ is the reduced density matrix. Here $S(\rho_A)$ is the entropy.

$$S(\rho_A) \equiv -\sum_{i=1}^{m} \mu_i \log_2(\mu_i) = H(\vec{\mu}) \tag{5.1}$$

Where μ_i are the eigenvalues of ρ_A and $\vec{\mu}$ is the Schmidt vector $(\mu_1, \mu_2, ..., \mu_m)$. It is evident that $E(|\psi\rangle)$ vanishes only for product states. This definition can be extended to mixed states ρ by the convex roof,

$$E(\rho) \equiv \min_{\{p_i, |\psi_i\rangle\}} \sum_i p_i E(|\psi_i\rangle) \tag{5.2}$$

for all possible ensemble realizations $\rho = \sum_i p_i |\psi_i\rangle\langle\psi_i|$, where $p_i \geq 0$ and $\sum_i p_i = 1$ Consequently, a state ρ is *separable* if and only if $E(\rho) = 0$ and hence can be represented as a convex combination of product states as $\rho = \sum_i p_i \rho_i^A \otimes \rho_i^B$ where ρ_i^A and ρ_i^B, are pure state density matrices associated to the subsystems *A* and *B*, respectively [29]. The measure Eq. (5.2) satisfies all the essential requirements of a good entanglement measure: convexity, no increase under local quantum operations and classical communications on average, no increase under local measurements, asymptotic continuity, and other properties [9, 30].

5.3.1 for a pair of quantum bits (q-bits)

For a pair of qubits, there exists a general formula for E_f , proved first for special cases [9, 12] and later for all states. The formula is based on the quantity called concurrence, which at this point has a standard definition only for a pair of qubits [3, 12]. Let us first consider a pure state $|\psi\rangle$ of a pair of qubits. The concurrence $C(|\psi\rangle)$ of this state is defined to be $C(|\psi\rangle) = |\langle\psi|\tilde{\psi}\rangle|$ where the tilde represents the ***spin-flip*** operation, $|\tilde{\psi}\rangle = (\sigma_y \otimes \sigma_y)|\psi^*\rangle$. Here $|\psi^*\rangle$ is the complex conjugate of $|\psi\rangle$ in the standard basis $\{|00\rangle, |01\rangle, |10\rangle, |11\rangle\}$, and σ_y is the Pauli operator $\sigma_y = \begin{pmatrix} 0 & -i \\ i & 0 \end{pmatrix}$. The spin-flip operation, when applied to a pure product state, takes the state of each qubit to the orthogonal state, that is, the state diametrically opposite on the Bloch sphere. The concurrence of a pure product state is therefore zero. On the other hand, a completely entangled state such as the singlet state is left invariant by the spin flip (except possibly for a phase

factor), so that for such states C takes the value one, which is its maximum possible value. It is not hard to obtain the following relation between concurrence and entanglement of a pure state.

$$E\left(|\psi\rangle\right) = \mathrm{E}\left(C\left(|\psi\rangle\right)\right) \tag{5.3}$$

Where the function $\mathrm{E} = E_f(C)$ is defined by

$$\mathrm{E} = E_f(C) = h\left(\frac{1+\sqrt{1-C^2}}{2}\right) \tag{5.4}$$

And

$$h(x) = -x\log_2(x) - (1-x)\log_2(1-x) \tag{5.5}$$

The function $E_f(C)$ is monotonically increasing for $0 \le C \le 1$; so the concurrence can be regarded as a measure of entanglement in its own right, though unlike entanglement of formation, it is not a resource-based or information theoretic measure. The connection between concurrence and entanglement is particularly clear if we express the state in the standard basis: $|\psi\rangle = a|00\rangle + b|01\rangle + c|10\rangle + d|11\rangle$. One can show that $|\psi\rangle$ is factorizable if and only if $ad = bc$, so that one might take the difference between ad and bc as a measure of entanglement. Indeed, this is what concurrence does: $C\left(|\psi\rangle\right) = 2|ad - bc|$. We can define the concurrence of a *mixed state* ρ of two qubits to be the average concurrence of an ensemble of pure states representing ρ, minimized over all decompositions of ρ. That is, according to equation (5.2),

$$C(\rho) = \inf \sum_i p_i C\left(|\psi_i\rangle\right) \tag{5.6}$$

Where once again $\rho = \sum_i p_i |\psi_i\rangle\langle\psi_i|$. Now it happens that the function $E_f(C)$ defined by Eq. (5.4), in addition to being monotonically increasing, is also convex. It follows that

$$\mathrm{E}(C(\rho)) = \inf \mathrm{E}\left(\sum_i p_i C\left(|\psi_i\rangle\right) \right) \leq \sum_i p_i \mathrm{E}\left(|\psi_i\rangle\right) = E_f(\rho) \tag{5.7}$$

That is, $\mathrm{E}(C(\rho))$ is a lower bound on $E_f(\rho)$. At this point we invoke, but do not prove, two remarkable facts about concurrence. First, there always exists a decomposition of ρ that achieves the minimum in Eq. (5.6) with a set of pure states having the same concurrence. This fact makes the inequality in Eq. (5.7) and equality, so that $\mathrm{E}(C(\rho))$ actually gives us the entanglement of formation. Second, one can find an explicit formula for $C(\rho)$ [13]. It is

$$C(\rho) = \max\{0, \lambda_1 - \lambda_2 - \lambda_3 - \lambda_4\} \tag{5.8}$$

Where the λ_i are the square roots of the eigenvalues of $\rho\tilde{\rho}$ in descending order. Here $\tilde{\rho}$ is the result of applying the spin-up operation to ρ:

$$\tilde{\rho} = (\sigma_y \otimes \sigma_y)\rho^*(\sigma_y \otimes \sigma_y) \tag{5.9}$$

And the complex conjugation is again taken in the standard basis (Even though $\rho\tilde{\rho}$ is not necessarily a Hermitian matrix, its eigenvalues are all real and non-negative because it is the product of two non-negative definite matrices.). Alternatively, we can say that the λ_i are the singular values (in descending order) of the symmetric matrix

$$\mathrm{A}_{ij} = \sqrt{r_i r_j}\left\langle \Psi_i \middle| \tilde{\Psi}_j \right\rangle \tag{5.10}$$

Where the $|\Psi_i\rangle$'s are the eigenvectors of ρ and the r_i's are the corresponding eigenvalues. One can see that Eq. (21) reduces to the pure state formula

$C(|\psi\rangle) = |\langle\psi|\tilde{\psi}\rangle|$ when ρ is the pure state $\rho = |\psi\rangle\langle\psi|$. We now have our formula for the entanglement of a pair of qubits in any mixed state ρ

$$E_f(\rho) = \mathrm{E}\big(C(\rho)\big) \tag{5.11}$$

With *C* given by Eq. (5.8) and the function E given by Eq. (5.4).

5.4. Entanglement of Formation for a System of two QDs

The key element in the quantum information processing is the so-called quantum bit. For this reason, understanding their behavior in quantum computing environments is essential to carry out external operations that perform specific calculations in locations on qubits by logic operations with new algorithms adapted to these qubits. So we should form networks of qubits at different intervals making full operations. In our case we have a small network of two QDs at the nodes of network under this study we will provide the means to insight the transfer at a distance of entanglement in the lattice network.

Our qubits are a system of two quantum dots which are located in their respective single-mode ($a,\ a^{\dagger}$ and $b,\ b^{\dagger}$), lossless cavities so that a cavity includes only one such dots. Thus, each node of our network consists of a cavity in which there is a QD. We will restrict our attention to the dynamics of entanglement between two such nodes. We will denote the dot at the first node by *A*, cavity at the first node by *a*, dot at the second node by *B* and cavity at the second node by *b*, as sketched in Fig. 5.1. We are going to be using the QDs Hamiltonian model [20, 27, 28] to specify the interactions in our system, this include the Förster interaction. The QDs Hamiltonians (remember that $\hbar = 1$) is the same we seed in chapter 3 and 4, i.e. equations (3.45), (3.46) and (3.47). We consider *L* identical semiconductor quantum dots that are equally coupled to each other via coulombic interaction. The QDs interact with a quantized field (dipole interaction) in a high-Q cavity. Then the coupled QD-field system is described by the Hamiltonian [20, 27],

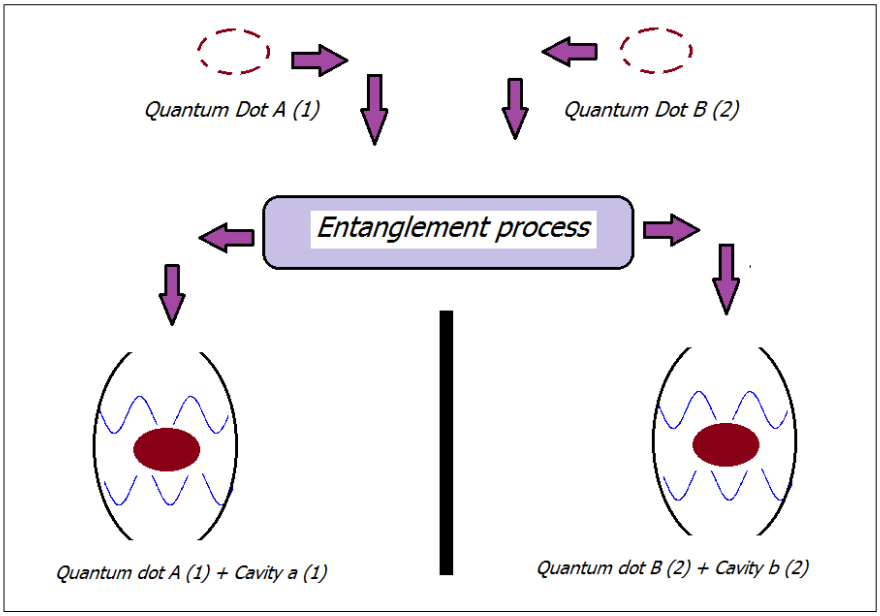

FIGURE 5.1 This diagram show our system of two QDs previously entangled. The QDs are placed in their respective cavity, which there are not interaction between them.

in order to two subsystems A and B

$$H^{(A)} = \omega a^{\dagger} a + \varepsilon J_z + g\left(J_+ a + a^{\dagger} J_-\right) + W\left(J^2 - J_z^2\right)$$

$$H^{(B)} = \omega b^{\dagger} b + \varepsilon J_z + g\left(J_+ b + b^{\dagger} J_-\right) + W\left(J^2 - J_z^2\right) \tag{5.12}$$

Where ε is the QD band gap, g is the coupling strength between the field and the QDs, ω is the field frequency, and W represents the interdot coulomb interaction. The coulomb interaction process known as Forster process exchanges energy, but does not require the physical transfer of the electrons and holes. For equal coupling these QDs are equidistant from each other so that the dots lie on a line for L = 2, at the vertices of an equilateral triangle for L = 3, and at the vertices of a regular pyramid for L = 4. The Hamiltonian (5.12) can be rewritten in a much more suitable in the representation of angular momentum, with the changes point out into references: [20, 27] and chapter 2. In reference [20] we obtained that may consist of two parts, one with the Dicke H_{Dk} Hamiltonian itself and the other is the interaction Hamiltonian Förster H_F, defined as

$$
\begin{aligned}
H_{Dk_A} &= \Delta J_z + g\left(J_+ a + a^\dagger J_-\right), \qquad \Delta = \varepsilon - \omega; \\
H_{Dk_B} &= \Delta J_z + g\left(J_+ b + b^\dagger J_-\right), \\
H_F &= W\left(J^2 - J_z^2\right) \quad \text{or} \quad H_F = W J_+ J_-
\end{aligned}
\tag{5.13}
$$

Where Δ is the detuning between the electromagnetic field and the band gap. The Hamiltonian of L QDs can be rewritten in the form: $H = \omega N + Q_L$, with $N = a^\dagger a + J_z + L/2$ is the number of atoms and photons and $Q_L = H_{Dk} + H_F$ are constants of motion. However there is another way to rewrite the Hamiltonian (5.12), using the relations of the algebra of angular momentum given as follows

$$
\begin{aligned}
H^{(A)} &= \omega a^\dagger a + \varepsilon' J_z + g\left(J_+ a + a^\dagger J_-\right) + W J_+ J_-; \\
\varepsilon' &= \varepsilon - W \\
H^{(B)} &= \omega b^\dagger b + \varepsilon' J_z + g\left(J_+ b + b^\dagger J_-\right) + W J_+ J_-
\end{aligned}
\tag{5.14}
$$

Here we see the term of Förster WJ_+J_- as a non-linearity and we has introduced a new constant ε', as defined above. Again we rewrite the Hamiltonian to include explicitly the detuning (Δ) which now call *Förster Detuning* (Δ'), so we get

$$
\begin{aligned}
H^{(A)} &= \omega\left(a^\dagger a + J_z\right) + g\left(J_+ a + a^\dagger J_-\right) - \Delta' J_z + W J_+ J_-; \\
H^{(B)} &= \omega\left(b^\dagger b + J_z\right) + g\left(J_+ b + b^\dagger J_-\right) - \Delta' J_z + W J_+ J_-
\end{aligned}
\tag{5.15}
$$

$$
\Delta' = \Delta + W = \omega - \varepsilon + W = \omega - \varepsilon'
$$

In a frame rotating with the field frequency ω, Eq. (5.15) takes the form

$$H_F^{(A)} = \Delta' J_z + g\left(J_+ a + a^\dagger J_-\right) + W J_+ J_-$$
$$H_F^{(B)} = \Delta' J_z + g\left(J_+ b + b^\dagger J_-\right) + W J_+ J_- \tag{5.16}$$

5.4.1 Two QDs interacting with their own quantized cavity field: Hamiltonian Diagonalization.

In this section we use the Hamiltonian (5.14), for each of the systems and we diagonalization in similarly way to section 3.6 into chapter 3, i.e. splits into two subsystems which are represented as $H_T = H^{(A)} + H^{(B)} = H^{(1)} + H^{(2)}$. This will simplify the task of studying the time evolution of the QD-field system. Starting with the initial condition representing the vacuum of excitons [see for example: 20, 27, 28 and 50], $|j = 1/2, m = -1/2\rangle = |\downarrow\rangle$, only the $j = 1/2$ subspace is optically active while the $j = 0$ subspace remains dark. We choose the basis of eigenstates of J^2 and J_z, $|\downarrow\rangle = |j = 1/2, m = -1/2\rangle$, $|\uparrow\rangle = |j = 1/2, m = 1/2\rangle$, as an appropriate representation for this problem $|\downarrow\rangle$ represents the vacuum for excitons, $|\uparrow\rangle$ denotes a symmetric delocalized single-exciton state. If we represent the field state intro each cavity by the Fock state $|n_a, n_b\rangle$ and consider the QDs in the entangled state involving the vacuum and exciton states $\left[|\uparrow\downarrow\rangle \pm |\downarrow\uparrow\rangle\right]$, then we will have an invariant subspace spanned by $\left\{|\uparrow\downarrow\rangle \otimes |00\rangle; |\downarrow\uparrow\rangle \otimes |00\rangle; |\downarrow\downarrow\rangle \otimes |10\rangle; |\downarrow\downarrow\rangle \otimes |01\rangle\right\}$ With these basis vectors we determine the matrix elements of the Hamiltonian in Eq. (5.14) and obtain the eigenvalues, and the eigenvectors by mean of diagonalization. Thus the explicit matrix is,

$$H_T = H^{(A)} + H^{(B)} = \begin{pmatrix} W & 0 & g & 0 \\ 0 & W & 0 & g \\ g & 0 & \omega - \varepsilon' & 0 \\ 0 & g & 0 & \omega - \varepsilon' \end{pmatrix}$$

$$H_T = H^{(A)} + H^{(B)} = \begin{pmatrix} W & 0 & g & 0 \\ 0 & W & 0 & g \\ g & 0 & \Delta' & 0 \\ 0 & g & 0 & \Delta' \end{pmatrix} \tag{5.17}$$

where $\Delta' = \omega - \varepsilon' = \Delta + W$

A interesting case is when $\Delta' = \omega - \varepsilon' = \Delta + W = 0 + W = W$, when we have resonance. In next subsection we will use this case in order to calculate the Concurrence function and thus the Entanglement of Formation, for now we calculate the general case for the Hamiltonian diagonalization. The characteristic polynomial is for matrix (5.17) is

$$P(\lambda) = \left[g^2 + (W - \lambda)\lambda - (W - \lambda)\Delta' \right]^2$$

At both cavities with the same field frequency ω, and we define the constants for simplicity as $\delta = \left[4g^2 + W^2 - 2W\Delta' + (\Delta')^2 \right]^{1/2} = \left[W(W - 2\Delta') + (4g^2 + (\Delta')^2) \right]^{1/2}$, the eigenvalues, take the form,

$$\lambda_{E1} = (1/2)\left(W + \Delta' - \delta\right), \quad \lambda_{E2} = (1/2)\left(W + \Delta' - \delta\right)$$

$$\lambda_{E3} = (1/2)\left(W + \Delta' + \delta\right), \quad \lambda_{E4} = (1/2)\left(W + \Delta' + \delta\right) \tag{5.18}$$

Due to the tensor product of the quantum states $|j,k\rangle = |j\rangle \otimes |k\rangle$ form a four-dimensional basis in the Hilbert space $\mathrm{SU(2)} \otimes \mathrm{SU(2)}$. And the corresponding normalized eigenvectors take the form,

$$|\lambda_1\rangle = \sqrt{\frac{1}{4g^2 + \Omega_1{}^2}}\left[(\Omega_1 |\uparrow\downarrow, 00\rangle + 2g |\downarrow\downarrow, 10\rangle\right]$$

$$|\lambda_2\rangle = \sqrt{\frac{1}{4g^2 + \Omega_1{}^2}}\left[(\Omega_1 |\uparrow\uparrow, 00\rangle + 2g |\downarrow\uparrow, 01\rangle\right] \qquad (5.19)$$

$$|\lambda_3\rangle = \sqrt{\frac{1}{4g^2 + \Omega_2{}^2}}\left[\Omega_2 |\uparrow\downarrow, 00\rangle + 2g |\downarrow\downarrow, 00\rangle\right]$$

$$|\lambda_4\rangle = \sqrt{\frac{1}{4g^2 + \Omega_2{}^2}}\left[\Omega_2 |\uparrow\uparrow, 00\rangle + 2g |\downarrow\uparrow, 00\rangle\right]$$

The constant δ as defined above. Also we define $\Omega_1 = W - \delta - \Delta'$, $\Omega_2 = W + \delta - \Delta'$. Then we determine the wave function at any time with the help of the previous eigenvectors. In this way we need to consider the initial state of the quantum dots system. A choice of suitable initial state is a state of Bell, i.e. for the sake of generality, we consider the initial state of the QDs to be $|\psi_{qd}(0)\rangle = \left[c_1 |\uparrow\downarrow\rangle + c_2 e^{i\phi} |\downarrow\uparrow\rangle\right]$, where a_1 and a_2 are real constants satisfying the condition $c_1^2 + c_2^2 = 1$. We will consider the initial state of the field to be coherent, or thermal. Then, the initial state for the coupled QD-field system can then be written as

$$|\Psi(0)\rangle = |\psi_{qd}(0)\rangle \otimes |00\rangle = \left[c_1 |\uparrow\downarrow\rangle + c_2 e^{i\phi} |\downarrow\uparrow\rangle\right] \otimes |00\rangle \qquad (5.20)$$

We are now able to find the wave vector of the system, because the energy eigenstates form a complete set, so using the eigenvalues and eigenvectors of the equations (5.18) and (5.19), together with the initial state (5.20), [50] we obtain the following state vector at the time *t* as

$$\left|\Psi(t)\right\rangle = \sum_{k=1}^{N=4} \exp(-i\lambda_{Ek}t)\left\langle \lambda_{Ek}\left|\Psi(0)\right\rangle\right|\lambda_{Ek}\rangle \tag{5.21}$$

This expression is written explicitly as

$$\begin{aligned}\left|\Psi(t)\right\rangle = {} & e^{-i\lambda_1 t}\left\langle \lambda_1\left|\Psi(0)\right\rangle\right|\lambda_1\rangle + e^{-i\lambda_2 t}\left\langle \lambda_2\left|\Psi(0)\right\rangle\right|\lambda_2\rangle \\ & + e^{-i\lambda_3 t}\left\langle \lambda_3\left|\Psi(0)\right\rangle\right|\lambda_3\rangle + e^{-i\lambda_4 t}\left\langle \lambda_4\left|\Psi(0)\right\rangle\right|\lambda_4\rangle\end{aligned} \tag{5.22}$$

Because to orthonormality of the basis vectors we obtain the coefficients in the form $\left\langle jm,n\left|\Psi(t)\right\rangle\right.$ as

$$\begin{aligned} x_1(\Omega,t) &= c_1 \frac{(\Omega_1^2+\Omega_2^2)}{\left[(4g^2+{\Omega_1}^2)(4g^2+{\Omega_2}^2)\right]} e^{-i(\lambda_1+\lambda_3)t} \\ x_2(\Omega,t) &= e^{i\phi_0}\left[c_1 \frac{4g^2}{(4g^2+{\Omega_1}^2)} e^{-i\lambda_2 t} + c_2 \frac{4g^2}{(4g^2+{\Omega_2}^2)} e^{-i\lambda_4 t}\right] \\ x_3(\Omega,t) &= c_1 \frac{2g\Omega_1}{(4g^2+{\Omega_1}^2)} e^{-i\lambda_1 t} \\ x_4(\Omega,t) &= c_1 \frac{2g\Omega_2}{(4g^2+{\Omega_2}^2)} e^{-i\lambda_3 t} \end{aligned} \tag{5.23}$$

Then the solution of the system in terms of the standard basis can be written as a simple linear combination, i.e.

$$\left|\Psi(t)\right\rangle = x_1(t)\left|\uparrow\downarrow\right\rangle + x_2(t)\left|\downarrow\uparrow\right\rangle + x_3(t)\left|\downarrow\downarrow\right\rangle + x_4(t)\left|\downarrow\downarrow\right\rangle \tag{5.24}$$

Where the coefficients $x_i(t)$ are given by expressions (5.23). Based on these results that were obtained, in the following section we find the density matrix, as well as reduced density matrix in order to calculate the concurrence and entanglement of formation.

5.4.2 Entanglement of Formation for two QDs as qubits implementation

For sake of simplicity, let us assume that both cavities are prepared initially in the vacuum state $|0_a\rangle \otimes |0_b\rangle$ and the two QDs are in a pure entangled state specified below as a Bell state. Under these assumptions, there is never more than one photon in each cavity, so the cavity mode is essentially equivalent to a two-level system. This allows a uniform measure of quantum entanglement together to concurrence, for both dots and the cavity modes.

According to the above we must note that there are, in principle, six different concurrences that provide information about the overall entanglements that may arise. We can denote for sake of simplicity as follows: [48, 49] C^{AB}, C^{Ab}, C^{Aa}, C^{Bb}, C^{Ab}, C^{Ba}. Symmetry considerations can provide natural relations among these, which we can see into references [46]. Here we confine our attention to C^{AB}. So, it should note that we in reality have six *individual* systems and four qubits: i.e. the two QDs (*A* and *B*, see figure 5.1) represent two qubits and two cavities (*a* and *b*) represent other two qubits itself, plus the combinations in interaction between these system as we showed in concurrences. However, we focus only in the *AB* combination in order to measure the entanglement.

For calculate the Entanglement of formation we need find the density matrix in general terms of the coefficients $x_i(t)$, [see for example: 18, 19 and 45 to 48] I.E. we must to compute the matrix elements, for density reduced matrix, which serving us in order to find out *Spin-flipped matrix* which is an ingredient essential in *Concurrence function* for entanglement of formation. The explicit calculate is showed in Appendix 3. Here we show the resulting matrix. This matrix is

$$\hat{\rho} = |\Psi\rangle\langle\Psi| = \begin{pmatrix} 0 \\ x_1 \\ x_2 \\ x_3 + x_4 \end{pmatrix} \begin{pmatrix} 0 & x_1^* & x_2^* & x_3^* + x_4^* \end{pmatrix}$$

$$\hat{\rho} = \begin{pmatrix} 0 & 0 & 0 & 0 \\ 0 & |x_1|^2 & x_1 x_2^* & x_1\left(x_3^* + x_4^*\right) \\ 0 & x_1^* x_2 & |x_2|^2 & x_2\left(x_3^* + x_4^*\right) \\ 0 & x_1^*\left(x_3 + x_4\right) & x_2^*\left(x_3 + x_4\right) & |x_3|^2 + |x_4|^2 \end{pmatrix} \tag{5.25}$$

In the combination of the four qubits that we use as system, appear most characteristics of character universal. But the simplest is first, all reduction to a two-qubit form, obtained by tracing over the two qubits, will yield a two-qubit mixed state always having the *X-form* [47, 49]. The form standard is as

$$\hat{\rho} = \begin{pmatrix} a & 0 & 0 & w \\ 0 & b & z & 0 \\ 0 & z^* & c & 0 \\ w^* & 0 & 0 & d \end{pmatrix} \tag{5.26}$$

Where $a + b + c + d = 1$. Second, since the concurrence of this mixed state is easily found to be

$$C = 2\max\left\{0, |z| - \sqrt{ad}, |w| - \sqrt{bc}\right\} \equiv 2\max\left\{0, Q\right\} \tag{5.27}$$

For the cases we will encounter $w = 0$, and this equation turns into

$$C = 2\max\left\{0, |z| - \sqrt{ad}\right\} \equiv 2\max\{0, Q\} \tag{5.28}$$

So it is clear that *Q*, defined as

$$Q = |z| - \sqrt{ad} \tag{5.29}$$

This will be an important quantity. We will mention at the end certain *conservation* properties that derive from *Q* in some cases because it can be negative, whereas *C* cannot.

The information about the entanglement of two QDs is contained in the reduced density matrix ρ^{AB} for the two dots which can be obtained from expressions (5.24) and (5.25) by tracing out the photonic parts of the total pure state. The explicit 4 × 4 matrix written in the basis $\{|\uparrow\uparrow\rangle;|\uparrow\downarrow\rangle;|\downarrow\uparrow\rangle;|\downarrow\downarrow\rangle\}$ [47, 49] is given by

$$\hat{\rho}^{AB} = \begin{pmatrix} 0 & 0 & 0 & 0 \\ 0 & |x_1|^2 & x_1 x_2^* & 0 \\ 0 & x_1^* x_2 & |x_2|^2 & 0 \\ 0 & 0 & 0 & |x_3|^2 + |x_4|^2 \end{pmatrix} \tag{5.30}$$

This is in the standard form of the two-qubit (quantum dots) mixed state, which was noted previously by [47] in order to two level atoms case. Once again the time-dependent matrix elements are given by (5.23), which we analyzing the case when the detuning is zero, i.e. $\Delta' = \omega - \varepsilon' = \Delta + W = 0 + W = W$, this is in resonance. It must be note that only to keep the Förster interaction constant. So the total of constants defined into equations in order to coefficients in eq. (5.23) and eigenvectors (5.19) are: $\Omega_1 = W - \delta - \Delta' = -2g$, $\Omega_2 = W + \delta - \Delta' = 2g$ and $\delta = \left[W(W - 2\Delta') + (4g^2 + (\Delta')^2)\right]^{1/2} = 2g$, thus the equations (5.19) and (5.23) now given by

$$|\lambda_1\rangle = \frac{1}{\sqrt{2}}\left[|\downarrow\downarrow,10\rangle - |\uparrow\downarrow,00\rangle\right]$$

$$|\lambda_2\rangle = \frac{1}{\sqrt{2}}\left[|\downarrow\uparrow,01\rangle - |\uparrow\uparrow,00\rangle\right]$$

$$|\lambda_3\rangle = \frac{1}{\sqrt{2}}\left[|\uparrow\downarrow,00\rangle + |\downarrow\downarrow,00\rangle\right] \tag{5.31}$$

$$|\lambda_4\rangle = \frac{1}{\sqrt{2}}\left[|\uparrow\uparrow,00\rangle + |\downarrow\uparrow,00\rangle\right]$$

And for the coefficients:

$$x_1(t) = x_1(t;W,g) = c_1 \frac{e^{-i2Wt}}{8g^2}$$

$$x_2(t) = x_2(t;W,g) = e^{i\phi_0}\left[c_1 \frac{1}{2} e^{-i(W-g)t} + c_2 \frac{1}{2} e^{-i(W+g)t}\right] \tag{5.32}$$

$$x_3(t) = x_3(t;W,g) = -c_1 \frac{1}{2} e^{-i(W-g)t}$$

$$x_4(t) = x_4(t;W,g) = c_2 \frac{1}{2} e^{-i(W+g)t}$$

It should be note that the constants c_1 and c_2 into equations (5.32) must to obey the normalization condition, also if compared to the eigenvectors obtained in eqs. (5.31), the latter are entangled states of Bell (resonant case) where the constants

are actually of $1/\sqrt{2}$, except for the sign. Thus the equations for the coefficients are:

$$x_1(t) = \frac{e^{-i2Wt}}{8\sqrt{2}g^2}$$

$$x_2(t) = e^{i\phi_0}\frac{1}{\sqrt{2}}\frac{1}{2}\left[e^{-i(W-g)t} + e^{-i(W+g)t}\right] = \frac{1}{\sqrt{2}}\cos(gt)e^{-iWt}e^{i\phi_0} \tag{5.33}$$

$$x_3(t) = -\frac{1}{2\sqrt{2}}e^{-i(W-g)t}$$

$$x_4(t) = \frac{1}{2\sqrt{2}}e^{-i(W+g)t}$$

Now we show that the concurrence of the density matrix (5.30), with references to eqs. (5.27) to (5.29), also section 5.3, this is given first by function $Q_{AB}(t)$ as

$$\begin{aligned} Q_{AB}(t) &= |z| - \sqrt{ad} = \left|x_1^* x_2 + x_1 x_2^*\right| - \sqrt{0} \\ &= \frac{1}{16g^2}\left|\cos(gt)\left(e^{-iWt}e^{-i\phi_0} + e^{iWt}e^{i\phi_0}\right)\right| \end{aligned} \tag{5.34}$$

$$Q_{AB}(t) = \frac{1}{8g^2}\begin{cases} \left|\cos(\phi_0)\cos(gt)\cos(Wt)\right| & \text{Real Part} \\ \left|\sin(\phi_0)\cos(gt)\sin(Wt)\right| & \text{Imaginary Part} \end{cases}$$

So that the Concurrence function can be think in dual way, the first one as a function just of time and the phase term is keeping constant, and the another one as a function of two variables, i.e. as function of the time and phase parameter. For sake of simplicity we use only the real part in terms of the cosines functions. The imaginary part has a similar behavior. In the figures below we showed several cases for both functions with different values of parameters *W* and *g*. It must be

noted that the plots have a behavior of cosine oscillations type, but self-modulate with a function of the same nature, i.e. cosine-cosine, and the amplitude not exceeding the one, as it should be for *Entanglement of Formation*. The graphics results are showed in next figures; and the functions for Concurrences are

$$C_{AB}(t) = \frac{1}{8g^2}\left|\cos(\phi_0)\cos(gt)\cos(Wt)\right| \quad \text{with} \quad \phi_0 = \text{constant}$$

$$C_{AB}(t,\phi_0) = \frac{1}{8g^2}\left|\cos(\phi_0)\cos(gt)\cos(Wt)\right| \quad \text{with} \quad \phi_0 = \text{independent variable} \tag{5.35}$$

Before us presenting of plots, we show the analytical results without approach with the limit cases on the physical parameters

$$\begin{aligned} Q_{AB}(t) &= \frac{1}{16g^2}\left|\begin{matrix}\cos(\phi_0)\left(\cos(g+W)t+\cos((g-W)t)\right)\\ +i\sin(\phi_0)\left(\sin(g+W)t-\sin((g-W)t)\right)\end{matrix}\right| \\ Q_{AB}(t) &= \frac{1}{8g^2}\cos(\phi_0)\cos(g)t \qquad W=0 \end{aligned} \tag{5.36}$$

Now, when $g \gg W$, in this case, is the dominant parameter, i.e. the coupling constant between the radiation field and the QDs,

$$\begin{aligned} Q_{AB}(t) &= \frac{1}{8g^2}\left|\cos(\phi_0)\cos Wt\cos gt + i\sin(\phi_0)\cos gt\sin Wt\right| \\ Q^2_{AB}(t) &= \left(\frac{1}{8g^2}\right)^2\left(\cos^2(\phi_0)\cos^2 Wt\cos^2 gt+\sin^2(\phi_0)\cos^2 gt\sin^2 Wt\right) \\ Q^2_{AB}(t) &= \left(\frac{1}{8g^2}\right)^2\cos^2 gt\left(\cos^2(\phi_0)\cos^2 Wt+\sin^2(\phi_0)\sin^2 Wt\right) \\ Q_{AB}(t) &= \frac{1}{16g^2}\left|\begin{matrix}\cos(\phi_0)\left(\cos(g+W)t+\cos((g-W)t)\right)\\ +i\sin(\phi_0)\left(\sin(g+W)t-\sin((g-W)t)\right)\end{matrix}\right| \end{aligned} \tag{5.37}$$

Another interesting case is when we add a parameter δ to the others parameters, which enables us to get analytical expressions more general, besides being able to manipulate this parameter numerically and perturbative way.

$$W = g + \delta; \qquad W \succ \delta,\ g \succ \delta$$

$$\begin{aligned} Q_{AB}(t) &= \frac{1}{16g^2}\left|\begin{array}{l}\cos(\phi_0)\left(\cos(2g+\delta)t + \cos(\delta t)\right) \\ +i\sin(\phi_0)\left(\sin(2g+\delta)t + \sin\delta t\right)\end{array}\right| \\ &= \frac{1}{16g^2}\left|\begin{array}{l}\cos(\phi_0)\left(\cos\delta t\left(1+\cos 2gt\right) - \sin 2gt\sin\delta t\right) \\ +i\sin(\phi_0)\left(\sin 2gt\cos\delta t + \left(1+\cos 2gt\right)\sin\delta t\right)\end{array}\right| \end{aligned} \tag{5.38}$$

$$\begin{aligned} Q_{AB}^2(t) &= \left(\frac{1}{16g^2}\right)^2\left(\begin{array}{l}\left(1+\cos 2gt\right)^2\left(\cos^2\delta t\cos^2(\phi_0) + \sin^2\delta t\sin^2(\phi_0)\right) \\ +\sin^2 2gt\left(\sin^2\delta t\cos^2(\phi_0) + \cos^2\delta t\sin^2(\phi_0)\right)\end{array}\right) \\ &\quad -2\left(\frac{1}{16g^2}\right)^2\left(1+\cos 2gt\right)\cos(2\phi_0)\sin 2gt\cos\delta t\sin\delta t \end{aligned}$$

Now we show the Concurrence plots in order to different parameters values, also in two, and three-dimensionally. The case 3D we consider the ϕ_0 as variable, which enables us visualize the contour zones of Sudden Death of concurrence.

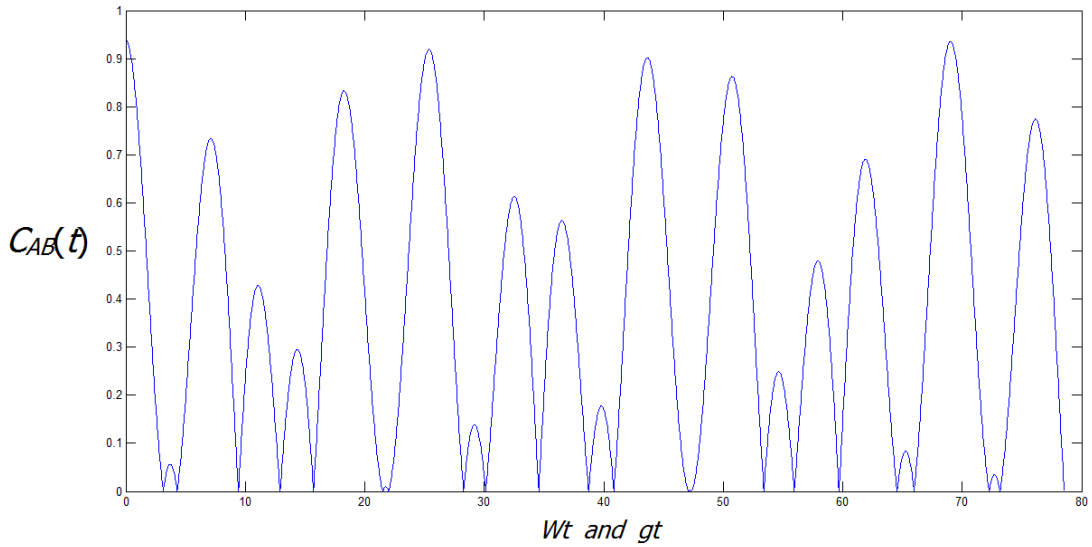

Figure5.2. Plot of the Concurrence for parameters: W=0.5; g=0.365; $\phi_0 = 0$. In this plot the oscillations fluctuate into of the time interval, almost become of top for entanglement of formation of one.

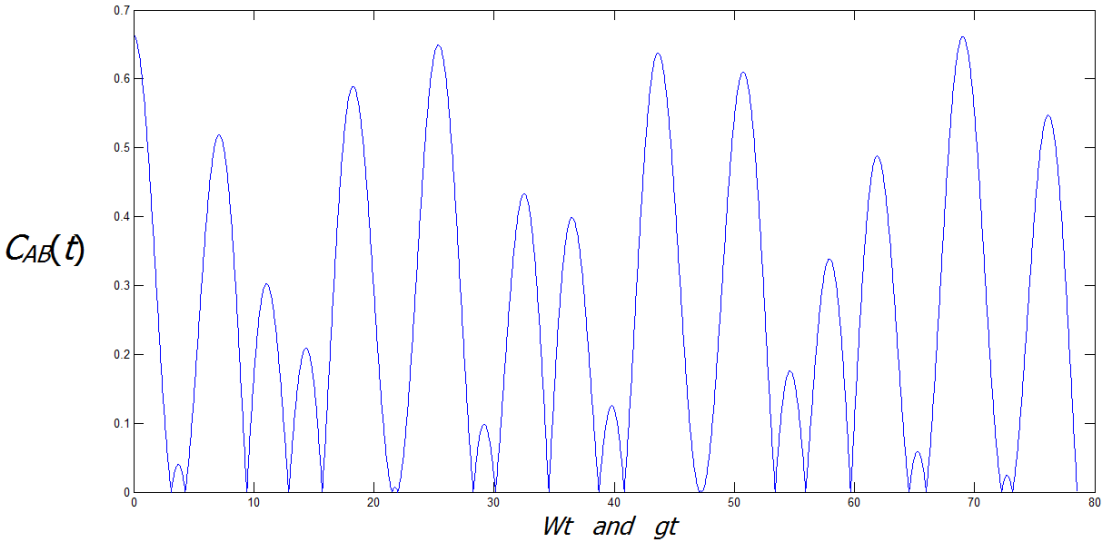

Figure5.3. Plot of the Concurrence for parameters: W=0.5; g=0.365; $\phi_0 = \pi/4$. In this case the plot decreases the amplitudes of the oscillations, because we do a change of $\pi/4$ to the phase.

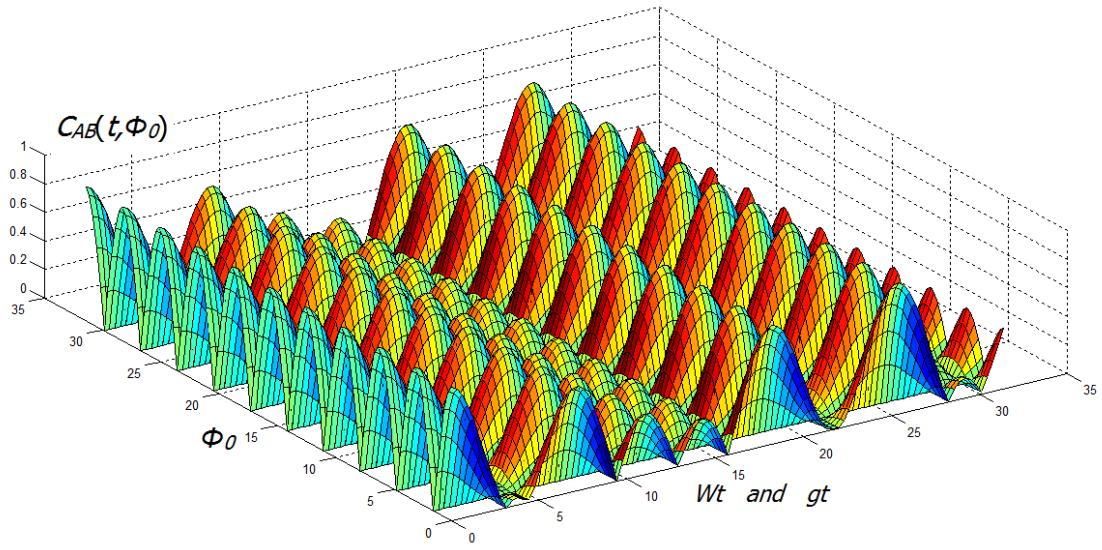

Figure5.4. Plot 3D for the Concurrence $C_{AB}(t,\Phi_0)$; for parameters: W=0.5; g=0.365

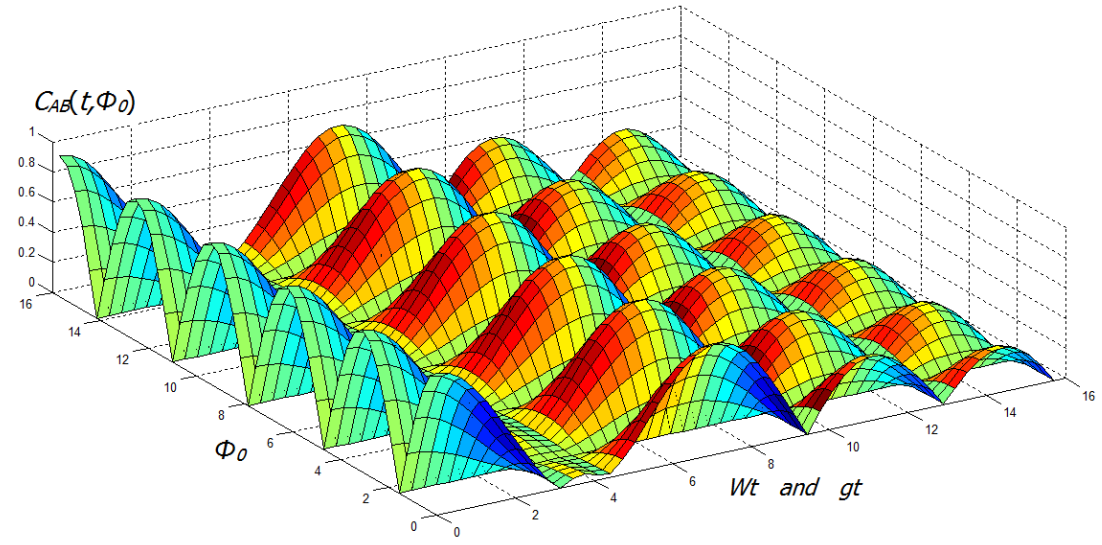

Figure5.5. Plot 3D for the Concurrence $C_{AB}(t,\Phi_0)$, is same plot that fig. 5.4, but on reduce scale; for parameters: W=0.5; g=0.365

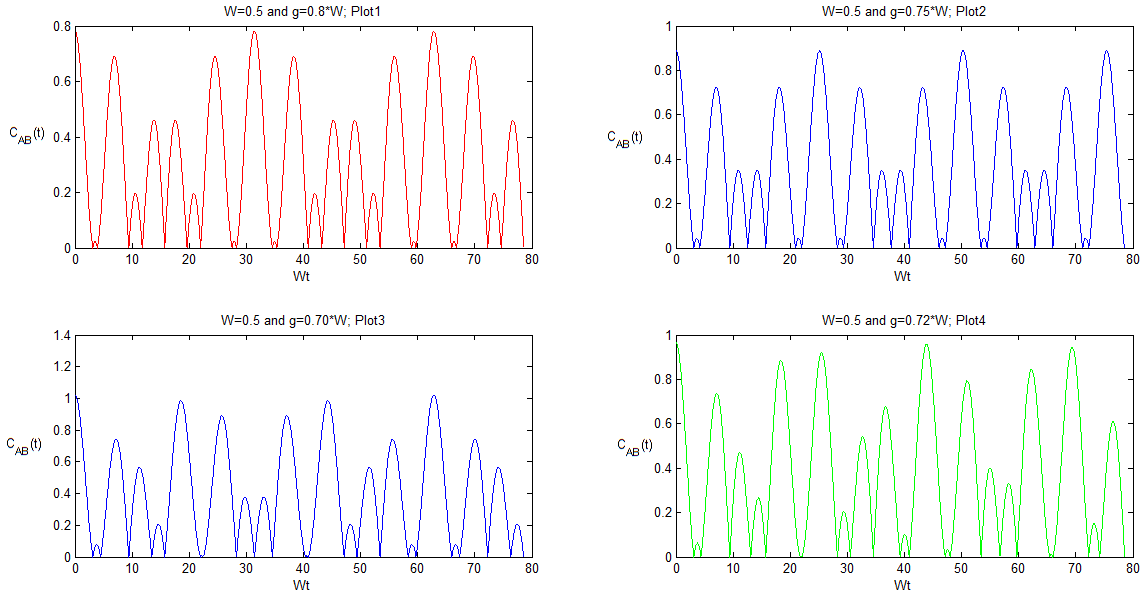

Figure5.6. Plots for the Concurrence $C_{AB}(t)$; for parameters: W=0.5 and plot1 g=0.8W, plot2 g=0.75W, Plot3 g=0.70W, plot4 g=0.72W. We can see that four combinations for constant g proportional to W. The more optimums combination is in order to plot2 in blue, and plot4 in green. Plot3 in blue slightly exceeds the allowable bound for Entanglement of formation and Concurrence of one. This is because the interaction constants differ by a percentage equal (or greater) to 30%, as is clearly noted in the data above.

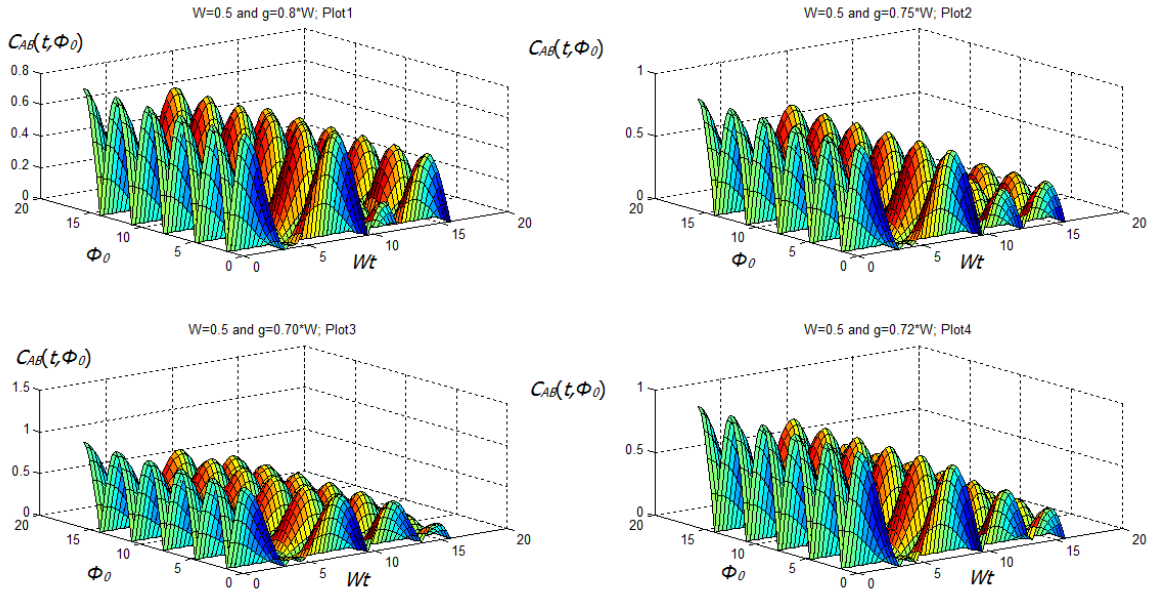

Figure5.7. Plots in 3D for the Concurrence $C_{AB}(t,\Phi_0)$; for parameters: W=0.5 and plot1 g=0.8W, plot2 g=0.75W, Plot3 g=0.70W, plot4 g=0.72W. We can see those four combinations in 3D for constant g proportional to W and the parameter of phase Φ_0.

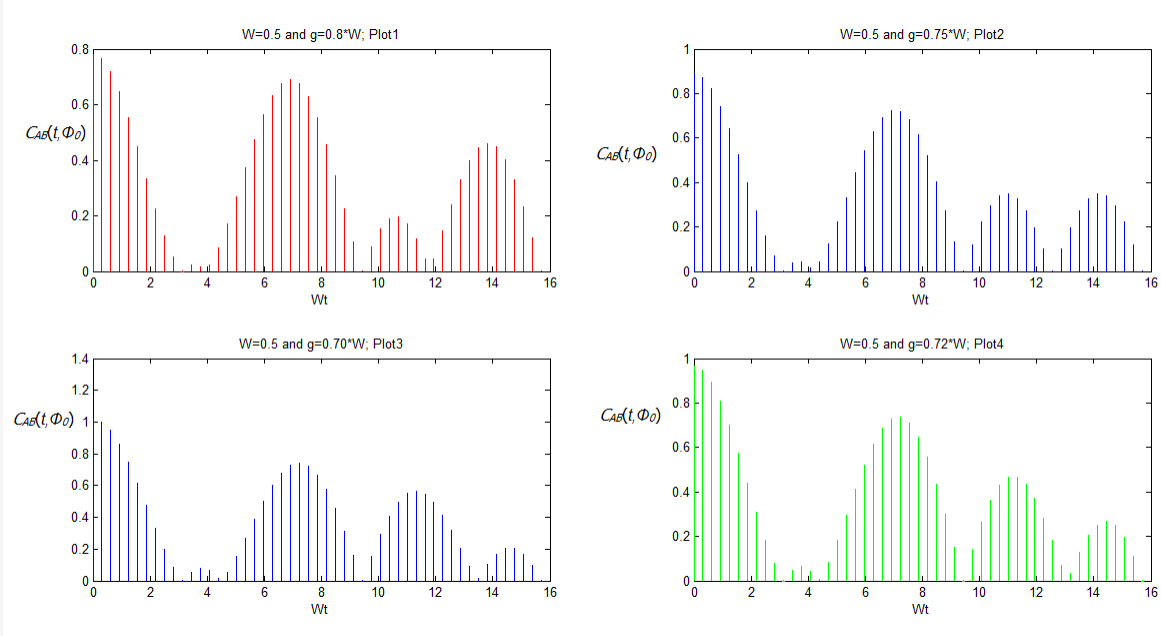

Figure5.8. Plots in 2D for the Concurrence $C_{AB}(t,\Phi_0)$; for same parameters: W=0.5 and plot1 g=0.8W, plot2 g=0.75W, Plot3 g=0.70W, plot4 g=0.72W. We can see the height as a profile without plotting the parameter phase Φ_0. This allows us to visualize how the concurrence behaves in their maxim bound.

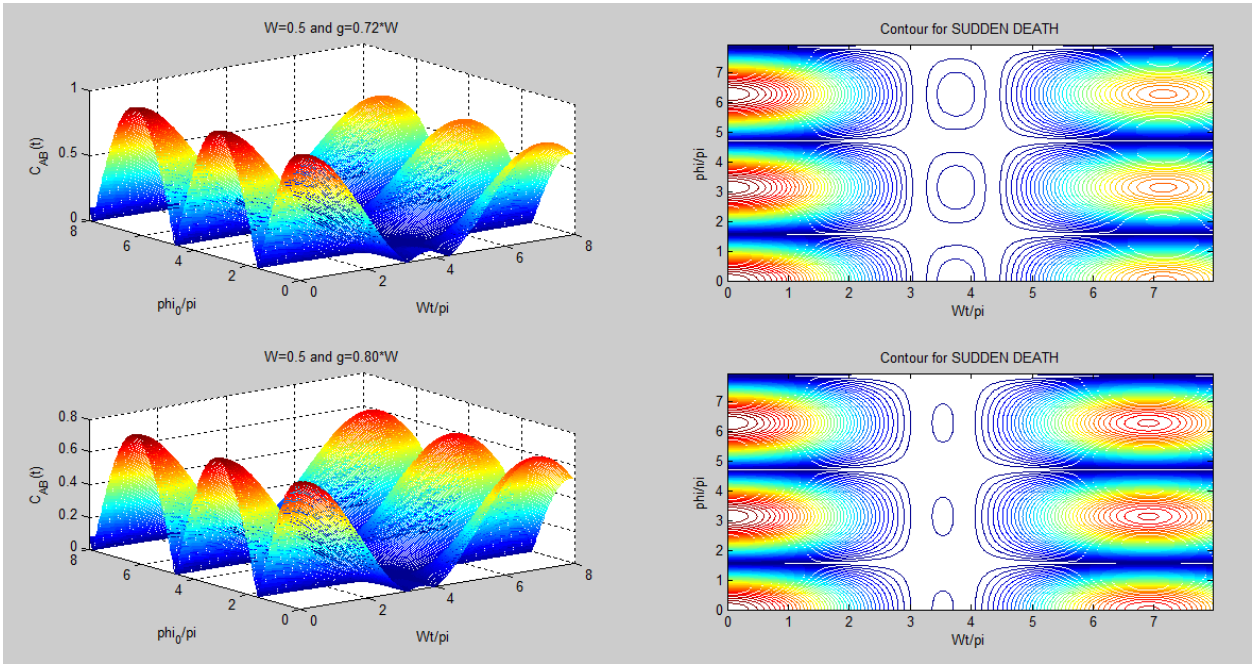

Figure5.9. Plots in 3D and Contours for so-called SUDDEN DEATH ZONES by $C_{AB}(t,\Phi_0)$; with two cases: W=0.5 and g=0.72W, g=0.80W and the parameter Φ_0 is variable, this is consequence of the initial state of Bell. We can see that contour zones of sudden death are minimums of the plots on the right. The interesting is to note that in this small zone rescaled for sake of simplicity that there is not a total sudden death as in the atomic case of the other authors [45-50]. What is also seen in previous plots from figures 5.2 to 5.8 into their minimum points.

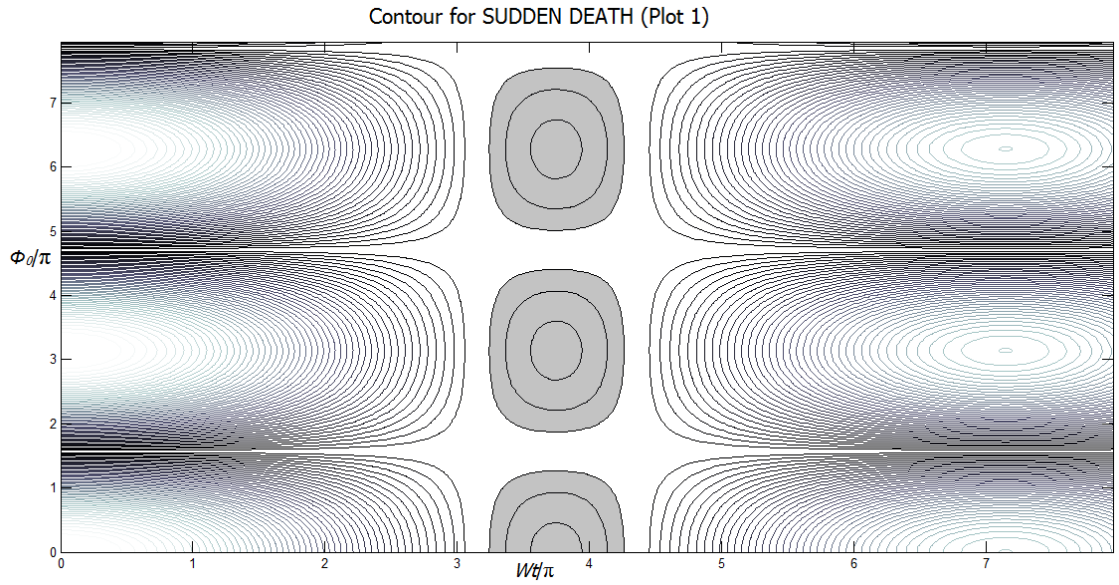

Figure5.10. Plots of Contours for so-called SUDDEN DEATH ZONES by $C_{AB}(t,\Phi_0)$; for the case: W=0.5 and g=0.72W, and the parameter Φ_0 is variable, this is consequence of the initial state of Bell. We can see the contour zones for sudden death that are minimums on the plots in gray color, but without become null totally.

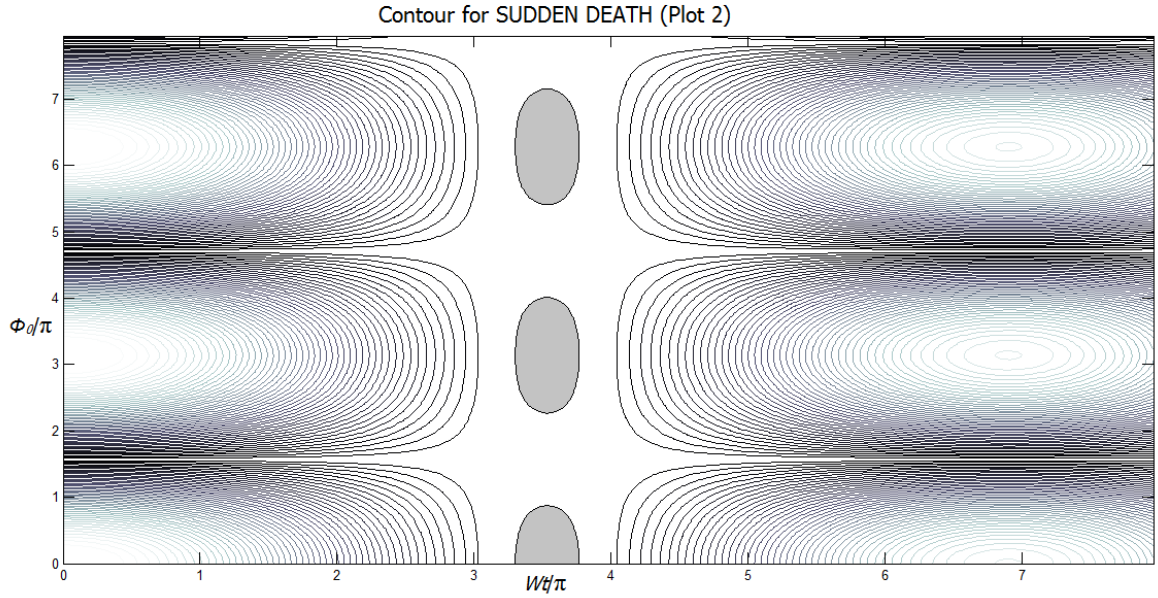

Figure5.11. Plots of Contours for so-called SUDDEN DEATH ZONES by $C_{AB}(t,\Phi_0)$; for the case: W=0.5 and g=0.80W, and the parameter Φ_0 is variable, this is consequence of the initial state of Bell. We can see only a contour zone for sudden death that is a minimum on the plot in gray color, but similarly the previous without become null totally.

CONCLUTIONS of CHAPTER 5

In this chapter we study the dynamics behavior of a system of two QDs embedded into own cavity, previously entangled, with initial state type Bell into of the context CQED and Förster interaction included into QDs Hamiltonian. This behavior let us insight the particular dynamics of transference and quantum communication correlations between two qubits, in this case represent for our two QDs, i.e. how is the entanglement process after that qubits are entangled and input into cavity in this situation of communication to distance without interaction, i.e. how evolve this entanglement with the time and consider the initial state of type Bell, which include the Φ_0 parameter. The way in order to understand and quantify this process without ambiguity is obtain a secure measure of the entanglement. This measure is the *Concurrence and Entanglement of Formation* for two qubits (Wotters, et. al, see [12, 13]) only. The measure is defined only for two qubits as entities of two states, because there is not an extension of this method to more qubits that to allow calculate with precision their entanglement. Our results between the two cavity-QD, let us see that the entanglement depend of both parameters of interaction, i.e. the interaction field-QDs (g) and the Förster interaction (W). Both interactions must be of the same order, because if either of the two differs significantly from another the result found is that oscillations slightly exceed the bound of the one for entanglement of formation. In this way we find that the interaction parameters must be very well controlled and should not be very different in order of magnitude. Also the best way to control them is by making one of the two is in terms of another one by a minimum percentage, as we can see in figures 5.6 and 5.7. Another one very important is the so-called Sudden Death feature where we analyzed in multiples plots in figures 5.9 to but with greater accurately in contour plots 5.8 to 5.11 how the characteristics zones are *minimums*, however there is not totally sudden death of entanglement as happen in the cases study for systems of atoms for other authors [45-49] or the case for QDs studied in references: [5, 27, 28, 50], in these papers the authors do not even mentioned the case of Sudden Death as in atomic situation. We can say that for these QDs system almost there is not sudden death because minimum zones are very sharp, i.e. they are smooth curves cosine in which do not we get semi-flat zones, that in atomic case is where entanglement sudden death occurs. This allows us conclude that our QDs system featuring to two qubits is more efficient for propagation of entanglement without loss of quantum correlation.

REFERENCES

[1] M. A. Nielsen and I. L. Chuang, ***Quantum Computation and Quantum Information*** (CambridgeUniversity Press, Cambridge, England, 2000).

[2] C.H. Bennett, G. Brassard, C. Crepeau, R. Jozsa, A. Peres, and W.K. Wootters, Phys. Rev. Lett. **70** (1993) 1895.

[3] C.A. Fuchs, N. Gisin, R.B. Griffiths, C-S. Niu, and A.Peres, Phys. Rev. A **56** (1997) 1163.

[4] C.H. Bennett and S.J. Wiesner, Phys. Rev. Lett. **69** (1992) 2881.

[5] D.P. DiVincenzo, Science 270 (1995) 255.

[6] R.F. Werner, Phys. Rev. A **40** (1989) 4277; A. Peres, Phys. Rev. Lett. **77** (1996) 1413.

[7] M. Horodecki, P. Horodecki, and R. Horodecki, Phys. Lett. A 223 (1996); M. Horodecki and P. Horodecki, Phys. Rev. A **59** (1999) 4206.N.J. Cerf, C. Adami, and R.M. Gingrich, Phys. Rev. A 60 (1999) 898. M.A. Nielsen and J. Kempe, Phys. Rev. Lett. 86 (2001) 5184.

[8] W. Dur and J.I. Cirac, Phys. Rev. A 61 (2000) 042314. ;W. D¨ur, J.I. Cirac, and R. Tarrach, Phys. Rev. Lett. 83 (1999) 3562. M. Lewenstein and A. Sanpera, Phys. Rev. Lett. 80 (1998) 2261. B.M. Terhal and P. Horodecki, Phys. Rev. A 61 (2000) 040301. M.A. Nielsen, J. Phys. A: Mathematical and General 34 (2001) 6987. A. Wong and N. Christensen, Phys. Rev. A 63 (2001) 044301.

[9] C.H. Bennett, D.P. DiVincenzo, J.A. Smolin, and W.K. Wootters, Phys. Rev. A **54** (1996) 3824.

[10] C.H. Bennett, H.J. Bernstein, S. Popescu, and B. Schumacher, Phys. Rev. A 53 (1996) 2046.

[11] V. Vedral, M.B. Plenio, M.A. Rippin, and P.L. Knight, Phys. Rev. Lett. 78 (1997) 2275; V. Vedral, M.B. Plenio, K. Jacobs, and P.L. Knight, Phys. Rev. A 56 (1997) 4452; V. Vedral and M.B. Plenio, Phys. Rev. A **57** (1998) 1619.

[12] S. Hill and W. K. Wootters, Phys. Rev. Lett. **78**, 5022 (1997).

[13] W. K. Wootters, Phys. Rev. Lett. **80**, 2245 (1998). Quantum Inf. Comput. **1**, 27 (2001).

[14] B.M. Terhal, K. Gerd, and K.G.H. Vollbrecht, Phys. Rev. Lett. **85** (2000) 2625.

[15] Zurek W H 1981 *Phys. Rev.* D **24** 1516 Zurek W H 1991 *Phys. Today* **44** 36
[16] Joos E, Zeh H D, Kiefer C, Giulini D, Kupsch K and Stamatescu I-O 2003 *Decoherence and the Appearance of a Classical World in Quantum Theory* (Germany: Springer)

[17] Caldeira A and Leggett A 1985 *Phys. Rev.* A **31** 1059

[18] Yu T and Eberly J H 2004 *Phys. Rev. Lett.* **93** 140404

[19] Yu T and Eberly J H 2006 *Opt. Commum.* at press *Preprint* quant-ph/0602196

[20] (a) J. Sanchez-Mondragon, A. Alejo-Molina, S. Sanchez-Sanchez and M. Torres-Cisneros, "Comparison of the Dicke Model and the Hamiltonianfor n Quantum Dots", *Quantum Dots, Nanoparticles, and Nanoclusters II*, edited by Diana L. Huffaker, Pallab K. Bhattacharya, *Proceedings of SPIE* Vol. 5734 (SPIE, Bellingham, WA, 2005) (b) A. Alejo-Molina, J. J. Sánchez-Mondragón, S. Sánchez-Sánchez, *DETUNING COLECTIVO DEL MODELO DE L PUNTOS CUÁNTICOS,* XLVIII CONGRESO NACIONAL SMF / XVIII REUNION ANUAL AMO GUADALAJARA JALISCO 2005. (c) **Representación de Puntos Cuánticos en la Base Atómica Coherente, S. Sánchez Sánchez,** J. J. Sánchez Mondragón, F. R. Castillo Soria, Memorias en extenso del LII Congreso Nacional de Física (SMF)/ Reunión Anual de Óptica (AMO). Acapulco Guerrero Octubre de **2009.**

[21] J.I. Cirac and P. Zoller, Phys. Rev. Lett. **74**, 4091 (1995); C. Monroe, D.M. Meekhof, B.E. King, W.M. Itano, and D.J. Wineland, *ibid.* **75**, 4714 (1995).

[22] Q.A. Turchete, C.J. Hood, W. Lange, H. Mabuchi, and H.J. Kimble, Phys. Rev. Lett. **75**, 4710 (1995).

[23] N.A. Gershenfeld and I.L. Chuang, Science **275**, 350 (1997); D.G. Cory, A.F. Fahmy, and T.F. Havel, Proc. Natl. Acad. Sci. USA, **94**, 1634 (1997); E. Knill, I.L. Chuang, and R. Laflamme, Phys. Rev. A **57**, 3348 (1998); J.A. Jones, M. Mosca, and R.H. Hansen, Nature (London) **393**, 344 (1998).

[24] A. Shnirman, G. Schön, and Z. Hermon, Phys. Rev. Lett. **79**, 2371 (1997); D.V. Averin, Solid State Commun. **105**, 659 (1998); Y. Makhlin, G. Schon, and A. Shnirman, Nature (London) **398**, 305 (1999).

[25] B.E. Kane, Nature (London) **393**, 133 (1998); D. Loss and D.P. DiVincenzo, Phys. Rev. A **57**, 120 (1998); G. Burkard, D. Loss, and D.P. DiVincenzo, Phys. Rev. B **59**, 2070 (1999); A. Barenco, D. Deutsch, A. Ekert, and R. Jozsa, Phys. Rev. Lett. **74**, 4083 (1995); A. Imamoglu, D.D. Awschalom, G. Burkard, D.P. DiVincenzo, D. Loss, M. Sherwin, and A. Small, *ibid.* **83**,

[26] C. H. Bennett, G. Brassard, S. Popescu, B. Schumacher, J. Smolin, and W. K. Wootters, Phys.Rev. Lett. **76** (1996) 722.

[27] L. Quiroga and N. F. Johnson, Phys. Rev. Lett. 83, 2270 (1999).

[28] J. H. Reina, L. Quiroga, and N. F. Johnson, Phys. Rev. A. 62, 012305 (2000).

[29] R. F. Werner, Phys. Rev. A **40**, 4277 (1989).

[30] M. Horodecki, Quantum Inf. Comput. **1**, 3 (2001); D. Bruß, J. Math. Phys. (N.Y.) **43**, 4237 (2002); M. B. Plenio and S. Virmani, quant-ph/0504163.

[31] R. Solovay and V. Strassen: A Fast Monte-Carlo Test for Primality (1977). *SIAM Journal on Computing, 1977, pp. 84-85*

[32] M. Agrawal, N. Kayal, N. Saxena: PRIMES is in P (2002). *preprint,* http://www.cse.iitk.ac.in/users/manindra/primality.ps

[33] D. Deutsch: Quantum theory, the Church-Turing principle and the universal quantum computer (1985). *Proc. R. Soc., London, A 400, pp. 97-117*

[34] D. Deutsch: Quantum computational networks (1989). *Proc. R. Soc., London, A 439, pp. 553-558*

[35] D. Deutsch and R. Jozsa: Rapid solution of problems by quantum computer (1992). *Proc. Roy. Soc. London, Ser. A, vol. 439, pp. 553-558*

[36] K. Svozil: Quantum algorithmic information theory (1996). *Journal of Universal Computer Science 2, pp. 311-346*

[37] I.L. Chuang et al.: NMR quantum computing: Realizing Shor's algorithm (2001). *Nature 414, pp. 883-887*

[38] R.P. Feynman: Quantum mechanical computers (1985). *Optics News 11, pp 11-20*

[39] Lov K. Grover: A fast quantum mechanical algorithm for database search (1996). *Proceeding of the 28th Annual ACM Symposium on Theory of Computing*

[40] P.W. Shor.: Algorithms for quantum computation: Discrete logarithms and factoring (1994). *Proc. 35th Annual Symposium on Foundations of Computer Science, IEEE Press, Los Alamitos, CA*

[41] J.I. Cirac, P. Zoller: Quantum Computations with Cold trapped Ions (1995). *Phys. Rev. Lett. 74, p. 4091*

[42] D. P. DiVincenzo, Fortschr. Phys. **48**, 771 (2000).

[43] M. Nakahara, S. Kanemitsu, M. M. Salomaa and S. Takagi (eds.), *Physical Realization of Quantum Computing: Are the DiVincenzo Criteria Fulfilled in 2004?* World Scientific, Singapore (2006).

[44] M. Nakahara, T. Ohmi, *Quantum Computing: From Linear Algebra to Physical Realizations*, CRC Press Taylor and Francis Group (2008)

[45] Yu T. and Eberly J H 2002 *Phys. Rev.* B **66** 193306; Yu T. and Eberly J H 2003 *Phys. Rev.* B **68** 165322

[46] Yönac M, Yu T and Eberly J H 2006 in preparation

[47] Yu T and Eberly J H 2007 *Quantum Inf. Comp.* **7** in press (*Preprint* quant-ph/0503089)

[48] Yönac M, Yu T and Eberly J H, J. Phys. B: At. Mol. Opt. Phys. **39** (2006) S621–S625

[49] Yönac M, Yu T and Eberly J H, J. Phys. B: At. Mol. Opt. Phys. **40** (2007) S45–S59

[50] A. Mitra, R. Vyas, and D. Erenso, Phys. Rev. A **76** 052317 (2007).

CHAPTER 6

GENERAL CONCLUTIONS

The research that we did throughout this thesis was realized in two stage of study of quantum systems, especially the quantum structures so-called Quantum Dots or Artificial Atoms (chapter 3), which are able to keep the carrier charge excitons (electron-hole) into a state of almost totally confined. These features allow us to analyze their properties and potential in order to perform manipulation and control of the carriers into QDs, as well as its use completely for experimental and technological applications. The stages were studied as a Collective Phenomena in chapters 2, 3 and 4. And as systems reduced to just two components of QDs in chapter 5 that serve as qubits for quantum computation and quantum information processing. The principal objective in first instance is understand the collective behavior into the context of the CQED and Dicke model, but with difference that our system are quantum structures (QDs) most complex since the charge carriers into them have a behavior similar to natural atoms (confinement and quantized levels) but with additional features which have nonlinearities that is included in QD Hamiltonian (angular momentum representation) between other things that span the applications of these structures. The analysis done with this QDs Hamiltonian was a carried out with different techniques and approaches used in quantum theory calculations. The mathematical tools and concepts were built up based on

the theories of quantum optics (QOp), especially Cavity Quantum Electrodynamics (CQED).

In chapter 2 was a review of quantum mechanics topics most relevant and necessary in order to our later work in this dissertation, especially regarding the Jaynes-Cummings model (JCM), quantum entanglement and principles of quantum computation and information. For the chapter 3 reviewed the state of art of quantum dots and introduce the important models in QOp and CQED such as JCM and Dicke collective model. Also we diagonalized the Hamiltonian at the basis of QDs, getting the eigenenergys and eigenfunctions. We introduced the so-called Atomic Coherent States (ACS) and Excited Atomic Coherent States (EACs) equation (4.2), which was used in chapter 3 and 4. These states allowed us to factorize the nonlinear operators of QDs Hamiltonian. The principal results were obtained in chapters 4 and 5. In first one we explored the phenomenon of collectivity in quantum system conformed of L QDs, in this case we demonstrated that the collective states type Dicke are not sufficient for analyzed the collective problem of QDs, because this issue have a deeper meaning about carriers charge into the QDs, which are behave as excitons in solid state structures, however with energy level quantized and confined in 3D, as discussed in chapter 3. We apply the technique of the ACS and EACs as natural states for the QDs Hamiltonian. We showed that can be obtained more general expressions for the matrix elements, and we may treat the atomic problem, as a special case of these states because the general expressions (4.3) to (4.5) involving the states of angular momentum operators used in chapter 3 in order to diagonalized the Hamiltonian; likewise these operators contain the Spin operators (matrices) of Pauli that representing the known atoms (states) of two levels used in the JCM and Dicke model as particular case. Another grant advantage of the EACS is that it allows factorized the expressions with the angular momentum operators in equation (4.24). We can express the expectation values in the form of scalar functions. We can calculated the collective dynamics of the QDs among themselves and explore the limits cases with the physical parameters involved.

In the chapter 5, we analyzed the behavior of the reduced system of two QDs, without interaction among themselves; only we assume that they are entangled previously. The system consist of a pair the cavities that contain each a quantum dot, we calculated and showed that Concurrence function has a oscillatory behavior as well as showed so called Sudden Death Zones. These zones were first proposed by Eberly et. al. in the context of Cavities QED with two level

atoms. Our proposal in this dissertation was as we mentioned two QDs, which are technologically most feasible features in design and implementation due to that present these quantum structures are very studied experimentally and theoretically into the different technological applications. Of course there have been great theoretical and experimentally efforts for technological implementation of similar systems with other quantum objects such as aforementioned TLA of Eberly, ions, quantum wells, so on. But, these efforts appear to have met with little success. Thus our contribution in this thesis is the theoretical study of the QDs from two points of the view, first one collective and the other one reduced only to just two QDs for implementation in quantum computing systems, specially the study of the quantum entanglement between the two QDs, because is the vital importance in transfer of quantum information with high degree of coherence and no has loss of information. In following we summarized the main features of our conclusions from study of QDs systems from the point of the view of quantum optics and Cavity-QED, as has been talked since the beginning of this dissertation.

- Quantum Dot systems have been show to possess characteristics of type atomic, theoretical properties but more complex due to the Forster interaction which is non linear. It behavior is similar but not equal.
- In the theoretical study using analytically handling of the algebra SU(2) the angular momentum proved to be of enormous help, especially with the Atomic Coherent States (ACS) and EACS, which served to factor non-linear operators and we obtained a system of coupled differential equations scalar, relatively most easy in order to solve numerically.
- We show that the collective quantum dot detuning, similar to Dicke detuning, is a correction to include the Forster interaction.
- The nonlinear differential equations coupled system type Bloch we found with Heisenberg picture provides an overview to explore the limits on the QDs system dynamics.
- The Norm allows us to observe that these solutions remain in a constant oscillatory state.
- The QDs reduced system in order to implement a bipartite qubits system have showed lower zones of Sudden Death, which means that the dots kept for as long as the property of quantum entanglement, which is the great relevance for quantum information processing theory and their physical implementation.

- The QDs have the many potential technological applications and already are used in multiple systems.
- The quantum computer is still waiting to be reality; however the QDs are strong candidates in order to their implementation.
- There are still many theoretical and experimental study perspectives to be done in these structures. In our case we can still explore and research with our theoretical study schemes most scope these quantum systems.

Future perspective of research and remarks

Our research was mainly focused on the study of quantum dots systems from a few no more a half dozen until our reduced system of only two dots with own cavity. Although the Hamiltonian is essentially built to N identical semiconductor quantum dots, which must be equally coupled to each other by means of Coulomb interaction (known as the Förster process) and equidistant. This configuration is not always easy to get too large N, due to technical implementations in labs and industrial design and too theoretically. However there is still a very broad scope of theoretical and experimental studies with a lot of the applications. In the way of CQED are still many open questions related to the implementation of systems for quantum computing as we proposed in this dissertation. For example if we can increase the number of quantum dots into the each cavity, or if is possible manage nor only bipartite systems, but with greater number of members of cavity-QD, or make more complex networks such as quantum dots in cellular automata QCA.

In a purely quantum context, i.e. when we completely quantized matter-field, in this case QDs and electromagnetic field, leads us to formulate highly coherent system for efficient performance in quantum computing and information theory that allows us build entangled states with QDs systems, because these are the proposed to be the physical basis to generate the theoretical quantum bits or qubits. The physical implementation of a computer to perform quantum logic operations requires a minimum of two qubits, but would not perform more very simple tasks. Therefore we need to explore theoretical formulations that extend current capabilities to generate large amounts of physical systems (QDs) entangled that do not lose their coherence and also perform the tasks of actually computer

as a technology that greatly improves on existing classical computers with logical bits zero and one. So much work still to do in these lines of computing and quantum information.

Particularly we are interesting in the physical aspect of the theory involved in QDs in the address of optoelectronics, photonic and other applications, such as solar cells most efficient and most robust QDs systems considering approaches semiclassical (semi-quantum) where only is quantized the matter (QDs) without quantized the radiation fields due to macroscopic nature of system which only need take account the quantum insight of the matter in interaction with driven classical fields. Quantum dots as already explained in more detail in previous chapters are very interesting objects with capabilities, which can be exploited in many novel physical senses for technological applications. Depending on the type of scale and the number of dots as well as the separation between they, different effects are considered to move the charge carriers (excitons) within of dots which can be harnessed to generate different electrical responses and radiation emitted when stimulated with techniques of tunneling and transport, also transfer of energy with or without excitons, so on. In our case consider mainly studied situations where the Förster energy transfer allows do transferring without charge carriers. In the research of Solar Cells, being robust systems with a large number of quantum dots and due the solar radiation nature must be consider the inverse Auger Effect (generation of photocurrents from stimulation of the spectral solar radiation) for better performance of these devices. These studies have shown that efficiency of solar cells built (theoretically and experimentally) with QDs improving the efficiency in order to generating photocurrents of a 33% with conventional cells up to 50, 60 and almost 70% of efficiency with QDs. Are still in theoretical and experimental developing these technologies but they are in the right direction. There are also applications in biology and medicine where the QDs are being used as molecular beacons of multiplexing with different varieties of imaging modalities including highly correlated microscopy within the organic cells and tissues, to function as broad spectrum fluorescent objects. These are just some of the research paths to explore the techniques used in this thesis and expand to other methods and applications that generate novel technology and fundamental physics.

A. Explicit Calculations for Matrix Elements in EACS and the Concurrence QDs System

A.1 Matrix elements of exacted atomic coherent states (EACS)

We are going to justify the results presented in Chapter 4. Namely, we will derive analytical results for the matrix elements in the Excited Atomic Coherent States (EACS) basis. In which we explained that it is more general basis than the known Atomic coherent states (ACS). We will be making a series of calculations based principally in the momentum angular algebra together to EACs basis. All computations are analytics and accurate without approximations, although can be used to make approximated calculations in problems that involving perturbation theory.

We use the Hamiltonians (4.1), but in rotating frame, i.e.

$$
\begin{aligned}
H &= \omega\left(a^{\dagger}a + J_z\right) + \Delta' J_z + g\left(J_+ a + a^{\dagger} J_-\right) + W J_+ J_-; \\
&\qquad \Delta' = \Delta + W = \varepsilon - \omega + W \\
H &= \omega a^{\dagger} a + \varepsilon' J_z + g\left(J_+ a + a^{\dagger} J_-\right) + W J_+ J_-; \quad \varepsilon' = \varepsilon - W \\
H_r &= \Delta' J_z + g\left(J_+ a + a^{\dagger} J_-\right) + W J_+ J_-
\end{aligned}
\tag{A.1}
$$

The ACS are defined by equations (3.82) and (3.83) as

$$
\left|\theta,\phi\right\rangle = \exp\left[\frac{1}{2}\theta\left(e^{-i\phi}J_+ - e^{+i\phi}J_-\right)\right]\left|-j\right\rangle = \hat{R}(\theta,\phi)\left|-j\right\rangle
$$

$$
\begin{aligned}
\left|\theta,\phi\right\rangle &= \hat{R}(\theta,\phi)\left|j,-j\right\rangle = \hat{R}(\theta,\phi)\left|-j\right\rangle \\
&= \left(\exp\left[\tan\frac{\theta}{2}e^{-i\phi}J_+\right]\right)\left(\sec^2\frac{\theta}{2}\right)^{J_z}\left(\exp\left[-\tan\frac{\theta}{2}e^{+i\phi}J_-\right]\right)\left|-j\right\rangle \\
&= \left(\cos\frac{\theta}{2}\right)^{2j}\sum_{m=-j}^{j}\sqrt{\binom{2j}{j+m}}\left(\tan\frac{\theta}{2}e^{-i\phi}\right)^{j+m}\left|m\right\rangle
\end{aligned}
\tag{A.2}
$$

The generalized ACS are defined in equation (3.91) as

$$
\left|\theta,\phi,s,n\right\rangle = \hat{R}(\theta,\phi)\left|s,n\right\rangle = \exp\left[\frac{1}{2}\theta\left(e^{-i\phi}J_+ - e^{+i\phi}J_-\right)\right]\left|s,n\right\rangle = \sum_{m=-j}^{j} A_m(\theta,\phi,s)\left|m,n\right\rangle \tag{A.3}
$$

Where θ, φ, are the spherical coordinates associate with the symmetries of the ACS [2, 7, 8 into references chapter 4], also *s* is the generalized parameter of the EACS, and *n* represent the number state of field. In the chapter 4 we present the matrix elements in this basis, but we not showed the explicit calculations, because now we show as this are computed more explicitly. Thus the analytic matrix elements for the QDs Hamiltonian are

$$
\begin{aligned}
\left\langle H_r \right\rangle_\tau &= \left\langle \theta', \phi', s', n' \right| H_r \left| \theta, \phi, s, n \right\rangle \\
&= \left\langle \theta', \phi', s', n' \right| \Delta_F J_z + g\left(J_+ a + a^\dagger J_- \right) + W J_+ J_- \left| \theta, \phi, s, n \right\rangle \\
&= \Delta_F \left\langle \theta', \phi', s', n' \right| J_z \left| \theta, \phi, s, n \right\rangle + g \left\langle \theta', \phi', s', n' \right| \left(J_+ a + a^\dagger J_- \right) \left| \theta, \phi, s, n \right\rangle \\
&\quad + W \left\langle \theta', \phi', s', n' \right| J_+ J_- \left| \theta, \phi, s, n \right\rangle \\
\left\langle H_r \right\rangle_\tau &= \Delta_F f_{zs} \delta_{n',n} + g f_{+s} \sqrt{n} \delta_{n',n-1} + g f_{-s} \sqrt{n+1} \delta_{n',n+1} + W f_{\pm s} \delta_{n',n}
\end{aligned}
\tag{A.4}
$$

In order to computed these matrix elements plugging in the expression equation (A.3) for each operator of the Hamiltonian, i.e. element to element we obtain

$$
\begin{aligned}
\Delta_F f_{zs,n} &= \Delta_F f_{zs} \left\langle n' \middle| n \right\rangle = \Delta_F \left\langle \theta', \phi', s', n' \right| J_z \left| \theta, \phi, s, n \right\rangle \\
g f_{+s,n} &= g f_{+s} \left\langle n' \middle| a \middle| n \right\rangle = g \left\langle \theta', \phi', s', n' \right| \left(J_+ a \right) \left| \theta, \phi, s, n \right\rangle \\
g f_{-s,n} &= g f_{-s} \left\langle n' \middle| a^\dagger \middle| n \right\rangle = g \left\langle \theta', \phi', s', n' \right| \left(a^\dagger J_- \right) \left| \theta, \phi, s, n \right\rangle \\
W f_{\pm s,n} &= W f_{\pm s} \left\langle n' \middle| n \right\rangle = W \left\langle \theta', \phi', s', n' \right| J_+ J_- \left| \theta, \phi, s, n \right\rangle
\end{aligned}
\tag{A.5}
$$

So, one to one are calculate with help of the EACS and the momentum angular algebra SU(2), i.e.

$$
\begin{aligned}
J_+ \left| j, m \right\rangle &= \sqrt{(j-m)\left(j+m-1\right)} \left| j, m+1 \right\rangle \\
J_- \left| j, m \right\rangle &= \sqrt{\left(j+m\right)\left(j-m+1\right)} \left| j, m-1 \right\rangle \\
J_z \left| j, m \right\rangle &= m \left| j, m \right\rangle
\end{aligned}
\tag{A.6}
$$

$$
\left[J_i, J_j \right] = J_k \varepsilon_{ijk}, \quad \left[J_z, J_\pm \right] = \pm J_\pm, \quad \left[J_+, J_- \right] = 2 J_z,
$$

Thus using the EACs more the expressions of the angular momentum algebra (A.6), we obtain for each matrix element explicitly

$$
\begin{aligned}
f_{zs,n} = f_{zs}\delta_{n',n} &= \langle \theta',\phi',s',n' | J_z | \theta,\phi,s,n \rangle \\
&= \langle j',s',n' | \hat{R}^{\dagger}(\theta,\phi) J_z \hat{R}(\theta,\phi) | j,s,n \rangle \\
&= \langle j',s' | \left[J_z \cos\theta + 1/2 \left(e^{-i\phi} J_+ + e^{i\phi} J_- \right) \sin\theta \right] | j,s \rangle, \quad \text{where } \delta_{n',n} = \langle n' | n \rangle \\
&= \langle j',s' | J_z | j,s \rangle \cos\theta + \frac{1}{2}\Delta_F \langle j',s' | J_+ | j,s \rangle \sin\theta e^{-i\phi} + \frac{1}{2}\Delta_F \langle j',s' | J_- | j,s \rangle \sin\theta e^{i\phi} \\
&= \begin{bmatrix} s\delta_{s',s}\delta_{j',j}\cos\theta + 1/2\sqrt{(j-s)(j+s+1)}\,\delta_{j',j}\delta_{s',s+1}\sin\theta e^{-i\phi} \\ +1/2\sqrt{(j+s)(j-s+1)}\,\delta_{j',j}\delta_{s',s-1}\sin\theta e^{i\phi} \end{bmatrix} \delta_{n',n}
\end{aligned}
\tag{A.7}
$$

The next matrix element is

$$
\begin{aligned}
f_{+s,n} &= \langle \theta',\phi',s' | J_+ | \theta,\phi,s \rangle \langle n' | a | n \rangle \\
&= \langle j',s',n' | \hat{R}^{\dagger}(\theta,\phi) J_+ \hat{R}(\theta,\phi) | j,s,n \rangle \sqrt{n}\,\delta_{n',n-1} \\
&= \langle j',s' | \left[J_+ \cos^2(\theta/2) - J_- \sin^2(\theta/2) e^{i2\phi} - J_z \sin\theta e^{i\phi} \right] | j,s \rangle \sqrt{n}\,\delta_{n',n-1} \\
&= \left[\langle j',s' | J_+ | j,s \rangle \cos^2(\theta/2) - \langle j',s' | J_- | j,s \rangle \sin^2(\theta/2) e^{i2\phi} - \langle j',s' | J_z | j,s \rangle \sin\theta e^{i\phi} \right] \sqrt{n}\,\delta_{n',n-1} \\
&= \begin{bmatrix} \sqrt{(j-s)(j+s+1)}\,\delta_{j',j}\delta_{s',s+1}\cos^2(\theta/2) \\ -\sqrt{(j+s)(j-s+1)}\,\delta_{j',j}\delta_{s',s-1}\sin^2(\theta/2)e^{i2\phi} - s\delta_{s',s}\delta_{j',j}\sin\theta e^{i\phi} \end{bmatrix} \sqrt{n}\,\delta_{n',n-1}
\end{aligned}
\tag{A.8}
$$

Now we have the matrix element $f_{-s,n}$, we should clarify that we are including in these elements the part for the EM field, i.e.

$$
\begin{aligned}
f_{-s,n} = f_{-s}\langle n' | a^{\dagger} | n \rangle &= \langle \theta',\phi',s' | J_- | \theta,\phi,s \rangle \langle n' | a^{\dagger} | n \rangle \\
&= \langle j',s',n' | \hat{R}^{\dagger}(\theta,\phi) J_- \hat{R}(\theta,\phi) | j,s,n \rangle \sqrt{n+1}\,\delta_{n',n+1} \\
&= \langle j',s' | \left[J_- \cos^2(\theta/2) - J_+ \sin^2(\theta/2) e^{-i2\phi} - J_z \sin\theta e^{-i\phi} \right] | j,s \rangle \sqrt{n+1}\,\delta_{n',n+1} \\
&= \left[\langle j',s' | J_- | j,s \rangle \cos^2(\theta/2) - \langle j',s' | J_+ | j,s \rangle \sin^2(\theta/2) e^{-i2\phi} - \langle j',s' | J_z | j,s \rangle \sin\theta e^{-i\phi} \right] \sqrt{n+1}\,\delta_{n',n+1} \\
&= \begin{bmatrix} \sqrt{(j+s)(j-s+1)}\,\delta_{j',j}\delta_{s',s-1}\cos^2(\theta/2) \\ -\sqrt{(j-s)(j+s+1)}\,\delta_{j',j}\delta_{s',s+1}\sin^2(\theta/2)e^{-i2\phi} - s\delta_{s',s}\delta_{j',j}\sin\theta e^{-i\phi} \end{bmatrix} \sqrt{n+1}\,\delta_{n',n+1}
\end{aligned}
\tag{A.9}
$$

The last matrix element is much more complicated because of the appearance of the operator product is nor linear. So we must calculate more elements

$$
\begin{aligned}
f_{\pm s,n} &= f_{-s}\langle n'|n\rangle = \langle \theta',\phi',s'|J_-|\theta,\phi,s\rangle \delta_{n',n} \\
&= \langle j',s',n'|\hat{R}^{\dagger}(\theta,\phi)J_+J_-\hat{R}(\theta,\phi)|j,s,n\rangle \delta_{n',n} \\
&= \langle j',s'| \begin{bmatrix}
J_+J_-\cos^4(\theta/2)+J_-J_+\sin^4(\theta/2)-\left(J_+^2e^{-i2\phi}+J_-^2e^{i2\phi}\right)\cos^2(\theta/2)\sin^2(\theta/2) \\
+\left(J_zJ_+\sin^2(\theta/2)-J_+J_z\cos^2(\theta/2)\right)\sin\theta e^{-i\phi} \\
-\left(J_zJ_-\cos^2(\theta/2)-J_-J_z\sin^2(\theta/2)\right)\sin\theta e^{i\phi} \\
+J_z^2\sin^2\theta
\end{bmatrix} |j,s\rangle \delta_{n',n} \\
&= \begin{bmatrix}
\langle j',s'|J_+J_-|j,s\rangle\cos^4(\theta/2)+\langle j',s'|J_-J_+|j,s\rangle\sin^4(\theta/2) \\
-\langle j',s'|J_+^2|j,s\rangle\cos^2(\theta/2)\sin^2(\theta/2)e^{-2i\phi} \\
-\langle j',s'|J_-^2|j,s\rangle\cos^2(\theta/2)\sin^2(\theta/2)e^{2i\phi} \\
+\langle j',s'|J_zJ_+|j,s\rangle\sin^2(\theta/2)\sin\theta e^{-i\phi} \\
-\langle j',s'|J_+J_z|j,s\rangle\cos^2(\theta/2)\sin\theta e^{-i\phi} \\
-\langle j',s'|J_zJ_-|j,s\rangle\cos^2(\theta/2)\sin\theta e^{i\phi} \\
+\langle j',s'|J_-J_z|j,s\rangle\sin^2(\theta/2)\sin\theta e^{i\phi} \\
+\langle j',s'|J_z^2|j,s\rangle\sin^2\theta
\end{bmatrix} \delta_{n',n}
\end{aligned}
$$

(A.10)

Now we get each one of the above matrix elements independently with the help of angular momentum algebra, i.e.

$$
\begin{aligned}
\langle j',s'|J_+J_-|j,s\rangle &= (j+s)(j-s+1)\delta_{s',s}\\
\langle j',s'|J_-J_+|j,s\rangle &= (j-s)(j+s+1)\delta_{s',s}\\
\langle j',s'|J_+J_+|j,s\rangle &= \sqrt{(j-s)(j+s+1)}\sqrt{(j-s-1)(j+s+2)}\delta_{j',j}\delta_{s',s+2}\\
\langle j',s'|J_-J_-|j,s\rangle &= \sqrt{(j+s)(j-s+1)}\sqrt{(j+s-1)(j-s+2)}\delta_{j',j}\delta_{s',s-2}\\
\langle j',s'|J_zJ_+|j,s\rangle &= (s+1)\sqrt{(j-s)(j+s+1)}\delta_{j',j}\delta_{s',s+1}\\
\langle j',s'|J_+J_z|j,s\rangle &= s\sqrt{(j-s)(j+s+1)}\delta_{j',j}\delta_{s',s+1}\\
\langle j',s'|J_zJ_-|j,s\rangle &= (s-1)\sqrt{(j+s)(j-s+1)}\delta_{j',j}\delta_{s',s-1}\\
\langle j',s'|J_-J_z|j,s\rangle &= s\sqrt{(j+s)(j-s+1)}\delta_{j',j}\delta_{s',s-1}\\
\langle j',s'|J_zJ_z|j,s\rangle &= s^2\delta_{j',j}\delta_{s',s}
\end{aligned}
\tag{A.11}
$$

Therefore to putting together all the above elements is obtained

$$
f_{\pm s,n} = f_{\pm s}\delta_{n',n} = \left[\begin{array}{l}
(j+s)(j-s+1)\delta_{s',s}\cos^4(\theta/2)+(j-s)(j+s+1)\delta_{s',s}\sin^4(\theta/2)\\
\quad -\sqrt{(j-s)(j+s+1)}\sqrt{(j-s-1)(j+s+2)}\delta_{s',s+2}\cos^2(\theta/2)\sin^2(\theta/2)e^{-2i\phi}\\
\quad -\sqrt{(j+s)(j-s+1)}\sqrt{(j+s-1)(j-s+2)}\delta_{s',s-2}\cos^2(\theta/2)\sin^2(\theta/2)e^{2i\phi}\\
\quad +(s+1)\sqrt{(j-s)(j+s+1)}\delta_{s',s+1}\sin^2(\theta/2)\sin\theta e^{-i\phi}\\
\quad -s\sqrt{(j-s)(j+s+1)}\delta_{s',s+1}\cos^2(\theta/2)\sin\theta e^{-i\phi}\\
\quad -(s-1)\sqrt{(j+s)(j-s+1)}\delta_{s',s-1}\cos^2(\theta/2)\sin\theta e^{i\phi}\\
\quad +s\sqrt{(j+s)(j-s+1)}\delta_{s',s-1}\sin^2(\theta/2)\sin\theta e^{i\phi}+s^2\delta_{s',s}\sin^2\theta
\end{array}\right]\delta_{n',n}
\tag{A.12}
$$

All matrix elements obtained above are quite general, of course this can be used with any basis that involving the angular momentum states such as that obtained in chapter 4 with the matrix (4.6), and other applications that involving angular momentum and perturbation theory in any physics theory.

A.2 Matrix elements of two QDs system Hamiltonian

We must remember that our system consists of a QDs pair without mutual interaction, this is resuming into the picture (figure 5.1)

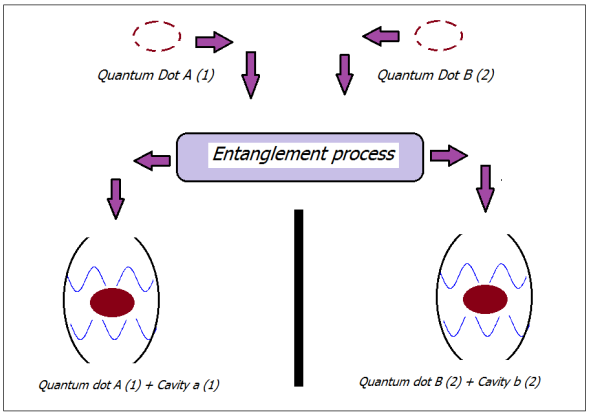

This system has the total Hamiltonian given for Hamiltonians (5.14)

$$\begin{aligned} H^{(A)} &= \omega a^{\dagger}a + \varepsilon' J_z + g\left(J_+ a + a^{\dagger} J_-\right) + W J_+ J_-; \\ \varepsilon' &= \varepsilon - W \\ H^{(B)} &= \omega b^{\dagger} b + \varepsilon' J_z + g\left(J_+ b + b^{\dagger} J_-\right) + W J_+ J_- \end{aligned} \tag{A.13}$$

These we can rewrite as

$$H^{(A)} = \omega\left(a^{\dagger}a + J_z\right) + g\left(J_+ a + a^{\dagger} J_-\right) - \Delta' J_z + W J_+ J_-;$$

$$H^{(B)} = \omega\left(b^{\dagger}b + J_z\right) + g\left(J_+ b + b^{\dagger} J_-\right) - \Delta' J_z + W J_+ J_- \tag{A.14}$$

$$\Delta' = \Delta + W = \omega - \varepsilon + W = \omega - \varepsilon'$$

The first ingredients we need in order to calculate the matrix elements are a general wavefunction that contains a combination of states of the fields $a, a^{\dagger}$ and $b, b^{\dagger}$ i.e. as equation (5.24). Also we need the spin states of the QDs, which are

explained into the chapters 4 and 5, and general terms in chapter 3. Thus we have the wavefunction

$$\left|\Psi(t)\right\rangle = x_1(t)\left|\uparrow\downarrow\right\rangle\otimes\left|0_a,0_b\right\rangle + x_2(t)\left|\downarrow\uparrow\right\rangle\otimes\left|0_a,0_b\right\rangle + x_3(t)\left|\downarrow\downarrow\right\rangle\otimes\left|1_a,0_b\right\rangle + x_4(t)\left|\downarrow\downarrow\right\rangle\otimes\left|0_a,1_b\right\rangle \quad \text{(A.15)}$$

We must note that, $\left|\uparrow\downarrow\right\rangle = \left|\uparrow\right\rangle\otimes\left|\downarrow\right\rangle$ are the spin angular momentum states, also the field states are en general $\left|0_a,0_b\right\rangle = \left|0_a\right\rangle\otimes\left|0_b\right\rangle \rightarrow \left|n_a,n_b\right\rangle = \left|n_a\right\rangle\otimes\left|n_b\right\rangle$, the number states of field. Both states (field and QDs) are in tensor product.

Or simply we can rewrite as

$$\left|\Psi(t)\right\rangle = x_1(t)\left|\uparrow\downarrow,00\right\rangle + x_2(t)\left|\downarrow\uparrow,00\right\rangle + x_3(t)\left|\downarrow\downarrow,10\right\rangle + x_4(t)\left|\downarrow\downarrow,01\right\rangle \quad \text{(A.16)}$$

In the basis $\left\{\left|\uparrow\downarrow\right\rangle\otimes\left|00\right\rangle;\left|\downarrow\uparrow\right\rangle\otimes\left|00\right\rangle;\left|\downarrow\downarrow\right\rangle\otimes\left|10\right\rangle;\left|\downarrow\downarrow\right\rangle\otimes\left|01\right\rangle\right\}$.

With this in mind, we can proceed to calculate the matrix elements with the Hamiltonian (A13), where the Hamiltonian total is $H_{Total} = H_T = H^{(A)} + H^{(B)}$, so

$$\left\langle H_T\right\rangle_\Psi = \left\langle\Psi(t)\right|H_T\left|\Psi(t)\right\rangle = \left\langle\Psi(t)\right|H^{(A)}\left|\Psi(t)\right\rangle + \left\langle\Psi(t)\right|H^{(B)}\left|\Psi(t)\right\rangle \quad \text{(A.17)}$$

Plugging the Hamiltonian explicitly we have

$$\begin{aligned}\left\langle H_T\right\rangle_\Psi = {} & \left\langle\Psi(t)\right|\omega a^\dagger a + \varepsilon' J_z + g\left(J_+ a + a^\dagger J_-\right) + WJ_+J_-\left|\Psi(t)\right\rangle \\ & + \left\langle\Psi(t)\right|\omega b^\dagger b + \varepsilon' J_z + g\left(J_+ b + b^\dagger J_-\right) + WJ_+J_-\left|\Psi(t)\right\rangle\end{aligned} \quad \text{(A.18)}$$

The matrix elements we should calculates are explicitly the following

$$\langle H_T\rangle_{11}=\langle 00\uparrow\downarrow|H_T|\uparrow\downarrow 00\rangle,\quad \langle H_T\rangle_{12}=\langle 00\uparrow\downarrow|H_T|\downarrow\uparrow 00\rangle,$$
$$\langle H_T\rangle_{13}=\langle 00\uparrow\downarrow|H_T|\downarrow\downarrow 10\rangle,\quad \langle H_T\rangle_{14}=\langle 00\uparrow\downarrow|H_T|\downarrow\downarrow 01\rangle.$$

$$\langle H_T\rangle_{21}=\langle 00\downarrow\uparrow|H_T|\uparrow\downarrow 00\rangle,\quad \langle H_T\rangle_{22}=\langle 00\downarrow\uparrow|H_T|\downarrow\uparrow 00\rangle,$$
$$\langle H_T\rangle_{23}=\langle 00\downarrow\uparrow|H_T|\downarrow\downarrow 10\rangle,\quad \langle H_T\rangle_{24}=\langle 00\downarrow\uparrow|H_T|\downarrow\downarrow 01\rangle.$$

$$\langle H_T\rangle_{31}=\langle 10\downarrow\downarrow|H_T|\uparrow\downarrow 00\rangle,\quad \langle H_T\rangle_{32}=\langle 10\downarrow\downarrow|H_T|\downarrow\uparrow 00\rangle,$$
$$\langle H_T\rangle_{33}=\langle 10\downarrow\downarrow|H_T|\downarrow\downarrow 10\rangle,\quad \langle H_T\rangle_{34}=\langle 10\downarrow\downarrow|H_T|\downarrow\downarrow 01\rangle.$$

$$\langle H_T\rangle_{41}=\langle 01\downarrow\downarrow|H_T|\uparrow\downarrow 00\rangle,\quad \langle H_T\rangle_{42}=\langle 01\downarrow\downarrow|H_T|\downarrow\uparrow 00\rangle,$$
$$\langle H_T\rangle_{43}=\langle 01\downarrow\downarrow|H_T|\downarrow\downarrow 10\rangle,\quad \langle H_T\rangle_{44}=\langle 01\downarrow\downarrow|H_T|\downarrow\downarrow 01\rangle. \qquad \text{(A.19)}$$

The application of the Hamiltonian operators on the states must act on the tensor product of the angular momentum states and the field independently, i.e. the spin-vectors and field states are

$$|\uparrow\rangle\otimes|\uparrow\rangle=[1,0,0,0]^T,\quad |\uparrow\rangle\otimes|\downarrow\rangle=[0,1,0,0]^T,\ \text{so on}$$

$$|n_a\rangle=\sqrt{n_a}\,\delta_{n'_a,n_a-1},\quad |n_a\rangle=\sqrt{n_a+1}\,\delta_{n'_a,n_a+1} \qquad \text{(A.20)}$$

$$|n_b\rangle=\sqrt{n_b}\,\delta_{n'_b,n_b-1},\quad |n_b\rangle=\sqrt{n_b+1}\,\delta_{n'_b,n_b+1}$$

These states must have their corresponding dual vectors $|\uparrow\rangle\otimes|\downarrow\rangle\rightarrow\langle\uparrow|\otimes\langle\downarrow|$ so on. Thus the calculate each matrix element, we obtain

$$H_{11}^{(A)} = \left\langle 0_a 0_b, \uparrow\downarrow \middle| H^{(A)} \middle| \uparrow\downarrow, 0_a 0_b \right\rangle = \left\langle n'_a n'_b, \uparrow\downarrow \middle| H^{(A)} \middle| \uparrow\downarrow, n_a n_b \right\rangle$$
$$= n_a \omega + \frac{\varepsilon'}{2} + W = W + \frac{\varepsilon'}{2}, \qquad n_a = 0. \qquad \left\langle n'_b \middle| n_b \right\rangle = 1.$$

$$H_{13}^{(A)} = \left\langle 0_a 0_b, \uparrow\downarrow \middle| H^{(A)} \middle| \downarrow\downarrow, 1_a 0_b \right\rangle = \left\langle n'_a n'_b, \uparrow\downarrow \middle| H^{(A)} \middle| \downarrow\downarrow, n_a n_b \right\rangle$$
$$= -\frac{\varepsilon'}{2}\delta_{n'_a, n_a} + g\sqrt{n_a}\,\delta_{n'_a, n_a - 1} = 0 + g = g, \qquad n'_a = 0, n_a = 1.$$
$$H_{22}^{(A)} = \left\langle 0_a 0_b, \downarrow\uparrow \middle| H^{(A)} \middle| \downarrow\uparrow, 1_a 0_b \right\rangle = \left\langle n'_a n'_b, \downarrow\uparrow \middle| H^{(A)} \middle| \downarrow\uparrow, n_a n_b \right\rangle$$
$$= n_a \omega - \frac{\varepsilon'}{2} = 0 - \frac{\varepsilon'}{2}, \qquad n_a = 0.$$
$$H_{31}^{(A)} = \left\langle 1_a 0_b, \downarrow\downarrow \middle| H^{(A)} \middle| \uparrow\downarrow, 0_a 0_b \right\rangle = \left\langle n'_a n'_b, \downarrow\downarrow \middle| H^{(A)} \middle| \uparrow\downarrow, n_a n_b \right\rangle$$
$$= g$$
$$H_{33}^{(A)} = \left\langle 1_a 0_b, \downarrow\downarrow \middle| H^{(A)} \middle| \downarrow\downarrow, 1_a 0_b \right\rangle = \left\langle n'_a n'_b, \downarrow\downarrow \middle| H^{(A)} \middle| \downarrow\downarrow, n_a n_b \right\rangle$$
$$= n_a \omega - \frac{\varepsilon'}{2} = \omega - \frac{\varepsilon'}{2}, \qquad n_a = 1.$$
$$H_{44}^{(A)} = \left\langle 0_a 1_b, \downarrow\downarrow \middle| H^{(A)} \middle| \downarrow\downarrow, 0_a 1_b \right\rangle = \left\langle n'_a n'_b, \downarrow\downarrow \middle| H^{(A)} \middle| \downarrow\downarrow, n_a n_b \right\rangle \qquad \text{(A.21)}$$
$$= n_a \omega \delta_{n'_a, n_a} - \frac{\varepsilon'}{2}\delta_{n'_a, n_a} = -\frac{\varepsilon'}{2}, \qquad n'_a = n_a = 0.$$

$$H_{12}^{(A)} = H_{14}^{(A)} = H_{21}^{(A)} = H_{23}^{(A)} = H_{24}^{(A)} = H_{32}^{(A)} = H_{34}^{(A)} = H_{41}^{(A)} = H_{42}^{(A)} = H_{43}^{(A)} = 0.$$

The matrix we get is,

$$H^{(A)} = \begin{pmatrix} W + \frac{\varepsilon'}{2} & 0 & g & 0 \\ 0 & -\frac{\varepsilon'}{2} & 0 & 0 \\ g & 0 & \omega - \frac{\varepsilon'}{2} & 0 \\ 0 & 0 & 0 & -\frac{\varepsilon'}{2} \end{pmatrix} \tag{A.22}$$

Similarly the matrix elements for $H^{(B)}$,

$$
\begin{aligned}
H_{11}^{(B)} &= \left\langle 0_a 0_b, \uparrow\downarrow \middle| H^{(B)} \middle| \uparrow\downarrow, 0_a 0_b \right\rangle = \left\langle n'_b, \uparrow\downarrow \middle| H^{(B)} \middle| \uparrow\downarrow, n_b \right\rangle \\
&= -\frac{\varepsilon'}{2}, \qquad n_b = 0. \qquad \left\langle n'_a \middle| n_a \right\rangle = 1. \\
H_{22}^{(B)} &= \left\langle 0_a 0_b, \downarrow\uparrow \middle| H^{(B)} \middle| \downarrow\uparrow, 1_a 0_b \right\rangle = \left\langle n'_b, \downarrow\uparrow \middle| H^{(B)} \middle| \downarrow\uparrow, n_b \right\rangle \\
&= W + \frac{\varepsilon'}{2} \\
H_{24}^{(B)} &= \left\langle 0_a 0_b, \downarrow\uparrow \middle| H^{(B)} \middle| \downarrow\downarrow, 1_a 0_b \right\rangle = \left\langle n'_b, \downarrow\uparrow \middle| H^{(B)} \middle| \downarrow\downarrow, n_b \right\rangle \\
&= g \\
H_{33}^{(B)} &= \left\langle 1_a 0_b, \downarrow\downarrow \middle| H^{(B)} \middle| \downarrow\downarrow, 1_a 0_b \right\rangle = \left\langle n'_b, \downarrow\downarrow \middle| H^{(B)} \middle| \downarrow\downarrow, n_b \right\rangle \\
&= -\frac{\varepsilon'}{2} \\
H_{42}^{(B)} &= \left\langle 0_a 1_b, \downarrow\downarrow \middle| H^{(B)} \middle| \downarrow\downarrow, 0_a 0_b \right\rangle = \left\langle n'_b, \downarrow\downarrow \middle| H^{(B)} \middle| \downarrow\downarrow, n_b \right\rangle \\
&= -g \\
H_{44}^{(B)} &= \left\langle 0_a 1_b, \downarrow\downarrow \middle| H^{(B)} \middle| \downarrow\downarrow, 0_a 1_b \right\rangle = \left\langle n'_b, \downarrow\downarrow \middle| H^{(B)} \middle| \downarrow\downarrow, n_b \right\rangle \\
&= \omega - \frac{\varepsilon'}{2}
\end{aligned}
\tag{A.23}
$$

$$
H_{12}^{(B)} = H_{13}^{(B)} = H_{14}^{(B)} = H_{21}^{(B)} = H_{23}^{(B)} = H_{31}^{(B)} = H_{32}^{(B)} = H_{34}^{(B)} = H_{41}^{(B)} = H_{43}^{(B)} = 0.
$$

The matrix is,

$$
H^{(B)} = \begin{pmatrix}
-\frac{\varepsilon'}{2} & 0 & 0 & 0 \\
0 & W + \frac{\varepsilon'}{2} & 0 & g \\
0 & 0 & -\frac{\varepsilon'}{2} & 0 \\
0 & g & 0 & \omega - \frac{\varepsilon'}{2}
\end{pmatrix}
\tag{A.24}
$$

Therefore the add both matrices we finally get

$$H_{Total} = H^{(A)} + H^{(B)}$$

$$H_{Total} = \begin{pmatrix} W+\frac{\varepsilon'}{2} & 0 & g & 0 \\ 0 & -\frac{\varepsilon'}{2} & 0 & 0 \\ g & 0 & \omega-\frac{\varepsilon'}{2} & 0 \\ 0 & 0 & 0 & -\frac{\varepsilon'}{2} \end{pmatrix} + \begin{pmatrix} -\frac{\varepsilon'}{2} & 0 & 0 & 0 \\ 0 & W+\frac{\varepsilon'}{2} & 0 & g \\ 0 & 0 & -\frac{\varepsilon'}{2} & 0 \\ 0 & g & 0 & \omega-\frac{\varepsilon'}{2} \end{pmatrix}$$

$$H_{Total} = \begin{pmatrix} W & 0 & g & 0 \\ 0 & W & 0 & g \\ g & 0 & \omega-\varepsilon' & 0 \\ 0 & 0 & 0 & \omega-\varepsilon' \end{pmatrix} = \begin{pmatrix} W & 0 & g & 0 \\ 0 & W & 0 & g \\ g & 0 & \Delta' & 0 \\ 0 & g & 0 & \Delta' \end{pmatrix} \quad \text{(A.25)}$$

Where $\Delta' = \omega - \varepsilon' = \omega - (\varepsilon - W) = \Delta + W$ is the *Förster Detuning* of the Hamiltonian system of QDs. Also is very important note that operators for angular momentum change by operator of the spin $j = 1/2, \text{ and } m = -1/2, 1/2$, i.e $J_+ \to s_+, \ J_- \to s_-, \ \text{and} \ J_z \to 1, /2 s_z$. The matrix Hamiltonian correspond to the matrix (5.17), which we use in order to diagonalized the Hamiltonian for the two entangled QDs, that enabled us we found out their wave-function (5.21-22) $\left|\Psi(t)\right\rangle = \sum_{k=1}^{N=4} e^{(-i\lambda_{Ek}t)} \left\langle \lambda_{Ek} \middle| \Psi(0) \right\rangle \left| \lambda_{Ek} \right\rangle$, with this we calculate the Entanglement of Formation by means of Concurrence function.